The *miR-23-27-24* Clusters Drive Lipid-Associated Macrophage Proliferation in Obese Adipose Tissue

By

Neil T. Sprenkle

Dissertation (or Thesis) Submitted to

the Faculty of the

Graduate School of Vanderbilt University in

partial fulfillment of the requirements for

the degree of

DOCTOR OF PHILOSOPHY

In

Molecular Pathology & Immunology

December 16th, 2023

Nashville, Tennessee

Approved:

Dr. C. Henrique Serezani, Ph.D. (Committee Chair)

Dr. Manuel Ascano, Ph.D.

Dr. Mark Boothby, M.D. Ph.D.

Dr. Jeffery Rathmell, Ph.D.

Dr. Heather Pua, M.D. Ph.D. (Principal Investigator)

DEDICATION

To my amazing family for their continued support

and

To members of my M.S. laboratory Gordon Meares (PI), Savannah Sims, John Nowry, and Cristina Sanchez for cultivating a great experience at WVU that helped spark an interest in pursuing biomedical research.

ACKNOWLEDGEMENTS

I would like to thank Mr. Zachary Bressman, Ms. Katilyn Bunn, Dr. John Kariolich, Dr. Nathan Klopfenstien, Mr. Grant Nation, Ms. Cherie Saffold, and Dr. Yang Zhao for technical assistance and Dr. Heather Pua for her guidance throughout my time at Vanderbilt University. I am also happy to thank the following members of my thesis committee for their continued guidance and intellectual input: Dr.'s Manuel Ascano, Mark Boothby, Jeffery Rathmell, and C. Henrique Serezani. This study would not be possible without our collaborators Dr.'s Alyssa Hasty, C. Henrique Serezani, and Nathan Winn, who have all provided technical resources and intellectual input into the project from the very beginning.

TABLE OF CONTENTS

Page

DEDICATION……ii

ACKNOWLEDGEMENTS……...iii

LIST OF TABLES……vi

LIST OF FIGURES……..…..vii

LIST OF ABBREVIATIONS……..viii

CHAPTER

1. INTRODUCTION: MICRORNAS IN MACROPHAGES: REGULATORS OF ACTIVATION AND FUNCTION…….……..……....……1

    1.1. General Chapter Overview……..……1
    1.2. Introduction....……2
    1.3. Biogenesis and Processing of miRNAs……4
    1.4. Mechanism of Action of miRNAs……7
    1.5. Global miRNA Expression Restrains Classical Macrophage Activation.….9
    1.6. A Subset of miRNAs is Required for Macrophage Proinflammatory Activation.....10
    1.7. miRNAs Contribute to Feedback Inhibition of Classical Macrophage Activation……..……..15
    1.8. miRNAs Regulate Macrophage Alternative Activation Programs……...17
    1.9. miRNAs in Macrophage Priming, Tolerance, and Trained Immunity…….20
    1.10. miRNA Control of Macrophage Function in Obesity and Metabolic Diseases.....23
    1.11. Conclusions……26
    1.12. References……..29

2. MYELOID-SPECIFIC EXPRESSION OF THE MIR-23-27-24 CLUSTERS PROMOTES GLUCOSE METABOLISM AND LIPID-ASSCOIATED MACROPHAGE ACCRUAL IN OBESITY ……40

    2.1. General Chapter Overview…..……40
    2.2. Introduction……..42
    2.3. Materials & Methods……..44
    2.4. Results……48
    2.5. Discussion……58

2.6. Conclusions……………………………………………………………………….59
2.7. References……………………………………………………………………..60

3. MYELOID-SPECIFIC EXPRESSION OF THE *MIR-23-27-24* CLUSTERS PROMOTES LIPID-ASSOCIATED MACROPHAGE PROLIFERATION………….. 67

3.1. General Chapter Overview…..………………………………………………67
3.2. Introduction……………………………………………………………………..69
3.3. Materials & Methods…………………………………………………………..71
3.4. Results…………………………………………………………………………….75
3.5. Discussion……………………………………………………………………...79
3.6. Conclusions……………………………………………………………………….82
3.7. References…………………………………………………………………..….83

4. SUPPRESION OF *EIF4EBP2* BY MIR-23 PROMOTES MACROPHAGE PROLIFERATION……………………………………………………………………….86

4.1. General Chapter Overview…......……………………………………………86
4.2. Introduction……………………………………………………………………..88
4.3. Materials & Methods…………………………………………………………..90
4.4. Results…………………………………………………………………………….96
4.5. Discussion……………………………………………………………………109
4.6. Conclusions…………………………………………………………………...110
4.7. References……………………………………………………………………111

5. FUTURE DIRECTION AND OPPORTUNITIES………………………………………113

5.1. General Chapter Overview……..………………………………………...113
5.2. Test if Direct miR-23-*Eif4ebp2* mRNA Interactions are Required for Proliferation in Cultured Metabolically Activated Macrophages.……..…113
5.3. Investigate how Negative Regulation of *Eif4ebp2* Expression Promotes Macrophage Proliferation……………………………………………...…114
5.4. Determine if *miR-23-27-24* Cluster Suppression of *Eif4ebp2* Regulates LAM Accrual and Glucose Tolerance in Diet-Induced Obesity Murine Model……………………………………………………………………..121
5.5. Identification of Additional Targets Involved in Metabolically Activated Macrophage Proliferation and Function……………………………………123
5.6. Determine how Expression of the Clusters in Myeloid Cells Regulates Tissue-Specific Insulin Sensitivity in Diet-Induced Obesity model...……125
5.7. Relevance to Human Disease,,,,,,,,,,,,,,,,,,,,,,……………………………………..,,,,,,,,,,,,,,,,126
5.8. Author Summary……………………………………………………………..129
5.9. References……………………………………………………………………129

6. APPENDIX

A. RNA SEQUENCING ANALYSIS: OBESE ADIPOSE TISSUE MACROPHAGES..133
B. RNA SEQUENCING ANALYSIS: METABOLICALLY ACTIVATED MACROPHAGES……...134
C. CANDIDATE TARGET TRANSCRIPTS……135
D. RNA SEQUENCING ANALYSIS: NETRIN-1 PATHWAY IN OBESE ADIPOSE TISSUE MACROPHAGES……136

LIST OF TABLES

Table Page

1.1. Summary of miRNA action and targets in macrophage……29

A.1. Normalized gene counts from RNA-seq analysis of control (fl/fl) and *miR-23-27-24* cluster knockout (MyelΔ) obese ATMs……133

A.2. DESeq2 analysis of obese ATM (fl/fl vs MyelΔ) RNA-seq data set……133

B.1. Normalized gene counts from RNA-seq analysis of control (fl/fl) and *miR-23-27-24* cluster knockout (MyelΔ) MMe BMDMs……134

B.2. DESeq2 analysis of MMe BMDMs (fl/fl vs MyelΔ) RNA-seq data set ……...134

C.1. Candidate targets from fl/fl and MyelΔ obese ATMs and MMe BMDMs……135

LIST OF FIGURES

Figure Page

1.1. Select miRNAs Regulate Classical Activation Programs……..……...…13

1.2. Select miRNAs Regulate Alternative Activation Programs…….……..…19

1.3. miRNAs Regulate LPS Tolerization……..….23

1.4. miRNAs Regulate Atherogenic Macrophage Programming…….…26

2.1. Proposed Model of Chapter 2: Expression of the *miR-23-27-24* Clusters Confers Protection Against Obesity-Induced Glucose Intolerance and Promotes LAM Accrual in Obese Adipose Tissue.……..42

2.2. Myeloid-Specific Deletion of the *miR-23-27-24* Clusters Does Not Alter Systemic Glucose Tolerance in Male and Female Lean Mice……..……...49

2.3. Myeloid-Specific Expression of the *miR-23-27-24* Clusters Protects Against Obesity-Induced Glucose and Insulin Intolerance.…….……..……51

2.4. Myeloid-Specific Deletion of the *miR-23-27-24* Clusters Does Not Alter Systemic Glucose Tolerance Female Obese Mice…….……..……52

2.5. Expression of the *miR-23-27-24* Clusters Does Not Regulated Inflammatory ATM Accrual……..…...54

2.6. Deficiency of the *miR-23-27-24* Clusters Does Not Reduce mRNA Levels of M2-Like Macrophage-Associated Genes in Obese eWAT or Induce Marked Hepatic Dysfunction……..…55

2.7. Expression of the *miR-23-27-24* Clusters Promotes LAM Accumulation in Obese eWAT……56

2.8. Myeloid-Specific Deletion of the *miR-23-27-24* Clusters Reduces LAM Accrual in Visceral WAT of Female Mice……..…57

3.1. Proposed Model of Chapter 3: Expression of the miR-23-27-24 Clusters Promotes LAM Proliferation in Obese Adipose Tissue.……69

3.2. The *miR-23-27-24* Clusters Do Not Alter Blood or Adipose Tissue Monocyte Numbers……..……76

3.3. The *miR-23-27-24* Clusters Promote LAM Proliferation……..77

3.4. The *miR-23-27-24* Clusters Do Not Regulate Cell Death……78

4.1. Proposed Model for Chapter 3: miR-23 Suppresses *Eif4ebp2* to Promote Lipid-Associated Macrophage Proliferation in Obese Adipose Tissue……88

4.2. Myeloid-Specific Deletion of the *miR-23-27-24* Clusters Attenuates Expression of Genes Associated with Trem2^{+} LAMs and Proliferation in Obese ATMs ……..……99

4.3. The *miR-23-27-24* Clusters Transcriptionally Regulate Shared Pathways and Predicted Targets in Metabolically Activated Macrophages and Obese ATMs……101

4.4. Figure 4.4. The *miR-23-27-24* Clusters Negatively Regulate Multiple Genes Involved in Suppressing Cell Proliferation. ……..…104

4.5. *Eif4ebp2* is a Direct Target of miR-23 and Suppresses Macrophage Proliferation……..…108

5.1. Loss of the miR-23-27-24 Clusters or Individual Members of the Clusters Does Not Attenuate mTORC1 Signaling in Metabolically Activated Macrophages……117

5.2. Late-Stage mTOR Suppression Does Not Attenuate LAM Proliferation in Obese Adipose Tissue…..120

5.3. Levels of miR-23a, miR-23b, and miR-24 in Abdominal Subcutaneous Adipose Tissue are Inversely Correlated with Body Mass Index……..…128

D.1. RNA Sequencing Analysis: Netrin-1 Pathway in Obese Adipose Tissue Macrophages……136

LIST OF ABBREVIATIONS

APOE: apolipoprotein E; ATM: adipose tissue macrophage; BMDM: bone marrow-derived macrophage; C/EBP: CCAAT-enhancer-binding protein; DGCR8: Drosha in complex with the RNA-binding protein DiGeorge Critical Region 8; eWAT, epididymal white adipose tissue; HFD, high-fat diet; HITS-CLIP: high-throughput sequencing RNAs isolated by crosslinking immunoprecipitation; IFN-y: interferon-y; IL: interleukin; LAM: lipid-associated macrophage; LPS: lipopolysaccharide; miRNA: microRNA; MRE: miRNA response element; NASH: nonalcoholic steatohepatitis; PAMP: pathogen-associated molecular pattern; PAR-CLIP: photoactivatable ribonucleoside-enhanced crosslinking immunoprecipitation; PI3K: phosphatidylinositol 3-kinase; Pri-miRNA: primary miRNA; PRR: pattern recognition receptor; RIG1: retinoic acid-inducible gene I; RISC: RNA-induced silencing complex; SHIP1: SH2 containing inositol 5' polyphosphatase 1; SOCS: suppressor of cytokine signaling; TAM: tumor-associated macrophage; TLR: toll-like receptor; TRBP: transactivation response element RNA-binding protein; UTR: untranslated region; WAT, white adipose tissue.

CHAPTER 1

INTRODUCTION: MICRORNAS AND MACROPHAGES: REGULATORS OF ACTIVATION AND FUNCTION

Adapted from:

Neil T. Sprenkle, C. Henrique Serezani, & Heather H. Pua. 2023. MicroRNAs and macrophages: regulators of activation and function. J. Immunol. 210: 359-368.

1.1. General Chapter Overview

This chapter introduces what microRNAs (miRNA) are, canonical mechanisms involved in miRNA biogenesis and processing, and their role in governing networks of genes at the post-transcriptional level. Additionally, it provides a comprehensive summary of the reported roles of select miRNAs in programming effector macrophage function, how their dysregulation contributes to various disease outcomes, and the potential application of miRNA-based therapies to treat diseases containing an immunological component, such as metabolic diseases. Overall, initiatives integrating basic science immunology with bioinformatic and translational research have uncovered how dysregulation of functionally-relevant miRNAs and their downstream target genes aggravates macrophage-driven pathology and offers both clinical biomarkers and new therapeutic targets.

1.2. Introduction

Macrophages are a heterogeneous population of innate immune cells that serve pleiotropic roles in maintenance of tissue homeostasis and host defense. This heterogeneity begins with cellular origin during ontogeny and expands through the integration of signals from the local tissue environment (reviewed[1]). In response to pathogens or injury, macrophages promote immune cell recruitment, activate local immune cells, phagocytose pathogens, present antigens, participate in tissue remodeling, and contribute to resolution of inflammation. Historically, the activation of macrophages has been conceptualized as a dichotomy of classically and alternatively activated states (reviewed[2]). Classically activated proinflammatory M1-like macrophages are stimulated by pattern recognition receptors (PRRs) after detection of pathogen-associated molecular patterns (PAMPs) and inflammation-promoting cytokines such as interferon-γ (IFN-γ) to enhance anti-microbial effector functions and drive increased tissue inflammation through cytokine production. In contrast, alternatively activated M2-like macrophages respond to homeostatic cues and cytokines of type 2 inflammatory response including interleukin (IL)-4 and IL-13 to dampen type 1 inflammatory responses, clear cellular debris, and remodel the extracellular matrix. Yet these paradigms are only first principles, and it is becoming apparent that macrophage function is both intricate and complex.

Recently, the control of macrophage function through the post-transcriptional regulation of gene expression has been implicated in coordinating robust changes in global gene expression characteristic of macrophage activation and plasticity. Among these are finely tuned alterations imposed by short noncoding microRNAs (miRNAs).

miRNAs are post-transcriptional regulators of gene expression, which use nucleotide binding to target sequences in mRNAs to inhibit gene expression.

Coordinated changes in miRNA expression mediate macrophage development, quiescence, and commitment toward activation phenotypes in response to microbial motifs or intrinsic stresses. Microarray and RNA sequencing studies mapping miRNA expression patterns have identified more than 100 miRNAs differentially expressed during monocyte differentiation[3], and mature macrophages have a unique miRNAome when compared with other mature immune cells[4]. Furthermore, the induction of select miRNAs occurs within hours after macrophage activation by key instructing signals, and the response is dictated by both signals received and the cellular context. Global miRNA expression analysis of macrophages activated *in vitro* with the proinflammatory agonists lipopolysaccharide (LPS) and IFN-γ or the alternative activation signal IL-4 show selective and differential upregulation of miRNA expression. miRNAs preferentially expressed after LPS and IFN-γ stimulation include miR-9, miR-147, miR-155, and miR-181, while miRNAs preferentially expressed after IL-4 treatment included let-7 family members, miR-23, miR-27, and miR-223[5,6]. These alterations in select miRNA expression contribute to macrophage functional plasticity, which is guided by signals present within the local immunological milieu.

miRNAs selectively expressed in response to these signals following or during macrophage activation play an active role in controlling macrophage programing. Detection of bacterial or viral motifs induces the expression of miRNAs such as miR-125b, miR-127, and miR-155 to strengthen commitment toward a proinflammatory M1-like state. These activating miRNAs are balanced by expression of miR-21 and miR-146, which are

upregulated following PAMP exposure participate in feedback inhibition loops to limit aberrant inflammatory activity and reestablish homeostasis. Similar strategies are overseen by distinct miRNA molecules during alternative macrophage activation, with Let-7c, miR-124, miR-181, and miR-223 supporting and miR-23, miR-27, and miR-511 inhibiting alternative macrophage activation. Finally, while many of the most studied gene networks regulated by miRNAs center around signaling pathways that modulate immunological genes, recent progress in the miRNA field has uncovered previously unappreciated regulatory networks that result in metabolic and epigenetic changes which dictate immune cell function to modulate disease severity, which include miR-33 and miR-222.

Here, we will summarize evidence demonstrating that miRNAs are critical molecular effectors that control macrophage gene expression and function, regulating activation programs in response to extrinsic cues and intrinsic stresses. We chose to focus on mechanistic studies which leverage genetic and biochemical tools to demonstrate key miRNA-target interactions and the importance of these nodes in controlling downstream macrophage biology.

1.3. Biogenesis and Processing of miRNAs

Molecular mechanisms involved in the canonical miRNA biogenesis paradigm have been well characterized following decades of thorough investigation. Genes encoding miRNAs are dispersed across the genome, where many miRNA loci exist within intergenic or intronic regions[7]. Interestingly, many genomic regions are enriched with 2-7

miRNA loci, termed miRNA clusters, and are co-transcribed in polycistronic transcription units[7,8]. Gene duplication is thought to contribute to the formation of miRNA clusters, and miRNAs derived from a single transcript can cooperatively and/or redundantly target functionally-related genes[9]. Moreover, examples involving miRNA and protein-coding gene co-transcription highlight a potential feedback loop where miRNAs residing in introns of the transcript (i.e. mirtrons) regulate the translation of transcripts to complement the cellular functions of co-expressed host genes[10,11]. Therefore, the spatial distribution of miRNA loci likely supports the heterogenous regulatory mechanisms imposed on a particular process.

Transcription of isolated or clustered miRNA genes by RNA polymerase II or III, depending on their associated cis-elements[12], produces primary-miRNA (pri-miRNA) transcripts containing stem-loop motifs. After which, the Microprocessor complex converts pri-miRNA to a more mature intermediate called precursor miRNA (pre-miRNA). Composing the Microprocessor ensemble is the type III RNase enzyme Drosha and the RNA-binding protein DiGeorge Critical Region 8 (Dgcr8). Initial recognition of double-stranded RNA (dsRNA)-single-stranded RNA (ssRNA) junctions by Dgcr8 stabilizes the pri-miRNA for subsequent cleavage by Drosha, thereby releasing a 60-100 nt hairpin product (pre-miRNA). This step in the miRNA processing model appears to be tightly regulated by multiple pathways to encourage a miRNA milieu that reflects intrinsic conditions (reviewed extensively by Beezhold et al.[13] & Ha et al.[14]). Moreover, autoregulatory mechanisms are ingrained in the system to appropriately control the activity of the Microprocessor complex during normal states.

Nuclear exportation of pre-miRNA follows enzymatic processing and is considered the rate limiting step in miRNA biogenesis[15]. Exportin-5 mediates the mobilization of most pre-miRNAs from the nucleus to the cytoplasm via a sequence-independent mechanism[16]. Instead, recognition of dsRNA motifs presented by properly processed pre-miRNA seems to stimulate the activity of the export machinery[15,16]. Once localized in the cytoplasm, pre-miRNA undergoes additional maturation by the endoribonuclease Dicer. As proposed by Park and colleagues[17], human Dicer possesses binding pockets for the 3' and 5' ends of pre-miRNA that help position the substrate within the catalytic domain so site-specific cleavages occur ~22 nt from the 3' and 5' terminus of the hairpin, consequently producing a miRNA duplex containing 3'overhangs of 2 nt. Similar to how Dgcr8 facilitates Drosha-mediated processing, another protein called transactivation response element RNA-binding protein (Trbp) is involved in recruiting pre-miRNA to Dicer and stabilizing the interaction between the two[18].

Upon cleavage, the duplex is unwound, and one of the strands, referred to as the guide miRNA, is loaded onto Argonaute 2 (Ago2) within the RNA-induced silencing complex (RISC), an ensemble which also contains Dicer and Trbp[19]. The passenger strand – that is, the strand not incorporated onto Ago2 – is thought to be quickly degraded, though reports suggest that the passenger strand may have some underappreciated regulatory properties[20]. Of note, the mechanism deciding which strand is selected is not uniform across different miRNA-Ago isoform pairs, as either the sequence of the 5'terminus of miRNA or the thermostability of the miRNA-Ago interaction appear to contribute to strand selection[21]. Nevertheless, gene silencing is ready to commence once the guide strand is integrated into the RISC.

While most miRNAs are produced through the canonical biosynthetic pathway, there are examples that deviate from this paradigm. Differences between canonical and non-canonical miRNA biogenesis is largely based on the requirement of factors that contribute to the canonical pathway. For instance, since mirtrons reside in short introns of host genes and their ends resemble splice sites, excised introns containing mirtrons can bypass Drosha processing and serve as pre-miRNAs [22]. Furthermore, group II pre-miRNA contain a 1 nt 3'overhang as opposed to the typical 2 nt 3'overhang seen in group I pre-miRNAs and require 3'mono-uridylation in order to be processed by Dicer[23,24]. As it stands now, however, molecular characterizations into non-canonical pathways are not as extensive as compared to the classical miRNA biosynthetic process. Based on our understanding that both classical and atypical subgroups of miRNA have profound impacts on immune response, further insight into the details regulating abnormal miRNA transcription and processing could prove to be invaluable for therapeutic intervention.

1.4. Mechanism of Action of miRNAs

Following incorporation into the RISC, the selected miRNA "guides" the RISC to target mRNA by annealing to miRNA response elements (MRE) typically located within the 3' untranslated region (UTR). The 5' end of miRNA contains a 2-8 nt seed sequence that is critical for nucleating miRNAs to its cognate MRE on target mRNA[20]. The consequent messenger ribonucleoprotein (mRNP) complex formed concentrate to cytoplasmic foci called processing bodies (P bodies), which are considered membrane-less compartments consisting of translationally stalled mRNA[25]. These P bodies serve as

sites of translational repression or RNA degradation, where the majority of miRNAs promote mRNA deadenylation, decapping, and exonuclease-mediated degradation[26,27].

Imperfect binding of miRNA to its target can suppress mRNA translation by encouraging the sequestration of the mRNP within storage compartments of P bodies. Transcripts stored in this manner are capable of undergoing future translation under the appropriate conditions. While it still remains a topic of debate as to how stalled mRNAs become competent for translation, Bhattacharyya et al. proposed that the mechanism of starvation-induced de-repression requires an external factor for the localization of cationic amino acid transporter 1 (CAT1) mRNA out of P bodies[28]. Here, they found that by binding to AU-rich elements within CAT1 mRNA in P bodies, the RNA-binding protein human antigen R (HuR) could competitively antagonize the binding of miR-122 to the 3'UTR, consequently altering the fate of the miRNA-targeted transcript to encourage protein translation. Therefore, it appears that factors outside of the canonical miRNA regulatory components assist in making stored mRNA translationally active.

Uncommon to endogenous miRNAs, perfect binding of miRNA with its MRE triggers Ago-mediated cleavage of the transcript to permanently silence the message. This regulatory strategy is often manipulated experimentally through the administration of synthetic small-interfering RNA (siRNA) to produce successful gene knockdowns. Introduced RNA duplexes mimic the structure of pre-miRNA and enters the Dicer-mediated step in the miRNA biogenesis pathway to produce siRNA generally bearing a 2 nucleotide overhang on the 3′ end of each strand[29]. Because synthetic siRNA are engineered to base pair perfectly with MREs residing on mRNAs of interest, the endonuclease activity of Ago2 within the RISC goes on to facilitate mRNA cleavage[30].

1.5. Global miRNA Expression Restrains Classical Macrophage Activation

The expression and function of most mature miRNAs require well-conserved protein processing machinery. While the whole-body loss of this machinery results in embryonic lethality in mice[31–34], lineage-restricted deletion of these proteins has uncovered critical roles for miRNAs in regulating proinflammatory macrophage activation programs. In bone marrow-derived macrophages (BMDMs), genetic loss of the miRNA processing enzyme DICER1 results in cell-autonomous increases in classic proinflammatory gene expression including *Nos2*, *Tnf*, *Stat1*, *CD86*, and select chemokines[35,36]. *Dicer1* deletion also impairs the acquisition of alternative activation programs, with failed induction of oxidative metabolism and mitochondrial mass accumulation in response to IL-4[36]. Together, these results suggest that the dominant output of global miRNA expression is to restrict classic M1-like macrophage activation. Interestingly, these findings parallel observations made in *Dgcr8*-, *Drosha*-, or *Dicer1*-deficient $CD4^+$ T cells, which have enhanced proinflammatory T-helper type 1 cell differentiation and cytokine production[37–39].

These molecular changes in gene expression and cellular function are sufficient to alter disease processes. Myeloid-specific *Dicer1*-deficiency shifts M2-like tumor-associated macrophages (TAMs) to a proinflammatory program, increasing recruitment of tumor-infiltrating $CD8^+$ T cells, inhibiting tumor growth, and potentiating checkpoint blockade[35]. Deficiency of DICER1 in myeloid cells can also exacerbate atherosclerotic disease in *Apolipoprotein E* (*Apoe*)$^{-/-}$ mice, with increased foam cell formation and lesion

necrosis[36]. *Dicer1*-deficient adipose tissue macrophages also have increased inflammatory gene expression and reduced beige adipogenesis during adipose tissue remodeling[40]. Is regulation of global miRNA levels relevant to disease? Interestingly, reductions in DICER1 and mature miRNA levels in alveolar macrophages of smokers have been observed[41,42]. And activation of the phosphatase PTEN during sepsis induces nuclear relocalization of DROSHA-DGCR8 complexes and facilities processing of a group of miRNAs that dampen inflammatory responses that includes miR-125b[43].

Investigations into these models have uncovered some of the critical miRNAs including let-7 family and miR-10 miRNAs that inhibit proinflammatory macrophage programs. Reconstituting let-7d into *Dicer1*$^{-/-}$TAMs returns them to an M2-like phenotype, attenuates inflammatory gene expression, and lowers immune cell infiltration into tumors[35]. Exogenous expression of let-7b in *Dicer1*$^{-/-}$ BMDMs from *Apoe*$^{-/-}$ mice restores mitochondrial respiration acting in part by suppressing the expression of the direct target gene *Lcor*[36]*.* Let-7 family miRNAs inhibit both the NF-κB pathway and cytokine production[44,45] as well as the epigenetic regulator *Tet2*[46]*.* miR-10 mimics repress inflammatory gene expression in monocytes and macrophages[47], and *in vivo* treatment of miR-10a in *Dicer1*-deficient atherosclerotic and adipose therapeutic remodeling studies rescues their phenotype[36,40]. Together, these results point to defined molecular roles for miRNAs in restraining classic macrophage activation and the power of using globally miRNA deficient models to uncover critical functional miRNA and target gene interactions.

1.6. A Subset of miRNAs is Required for Macrophage Proinflammatory Activation

Although global miRNA expression restrains proinflammatory function in macrophages, a subset of miRNAs is essential for macrophage proinflammatory activation *in vitro* and *in vivo* (**Figure 1.1**). miR-155 is not only highly upregulated in response to proinflammatory cytokines and PAMPs[48], but it has emerged as a central hub for macrophage activation. Downstream of TLR4 activation by LPS, Akt2 programs macrophage activation in part through induction of miR-155 which directly represses the expression of CCAAT-enhancer-binding protein (C/EBP)β, a transcription factor that normally limits inflammation[49]. miR-155 induction by other endogenous danger signals such as the extracellular matrix glycoprotein Tenascin-C can potentiate TLR4-mediated proinflammatory cytokine production to further strengthen proinflammatory cell activation[50], while signals that restrict classic macrophage such as IL-10 and vitamin D reduce miR-155 expression[51,52]. Interestingly, emerging data suggest that this regulation may extend beyond transcriptional control, with IL-10 mediated inhibition of mature miR-155 production depending on the activity of the RNA binding protein CELF binding to the pre-miR-155 sequence[53].

An important molecular function of miR-155 is inhibiting mRNA targets that normally serve as breaks on macrophage activation. miR-155 targets the 3'UTR of SH-2 containing inositol 5' polyphosphatase 1 (SHIP1; encoded by *Inpp5d*) mRNA to reduce RNA and protein expression[51,54] of this lipid phosphatase that canonically inhibits PI3K signaling, mitogen-activated protein kinases, and NF-κB in immune cells[55,56]. Suppression of SHIP1 gives way to sustained cell cycle progression, allowing for robust proliferation during immunogenic challenges. The *suppressor of cytokine signaling 1*

(*Socs1*) 3'UTR is also directly regulated by miR-155[57], and acts as an inhibitor of activating JAK/STAT signaling downstream of engaged cytokine receptors and TLRs[58].

Given the importance of miRNAs in regulating networks of gene expression, additional mRNA targets of miR-155 are likely relevant to macrophage function. Transcriptome-wide mapping of miR-155 targets in wild type and miR-155 deficient cells has identified >300 direct mRNA targets in macrophages[59]. This analysis identified both shared and unique miR-155 target sites among immune cells, providing a foundation for cell-type-specific function for this miRNA. Intriguingly, even when identical 3'UTR sites were expressed, miR-155 binding was different among different immune cell subsets, suggesting cell-type specific complexities in the regulation of miRNA target selection. Determining the source of this differential binding will be critical to understanding the finely tuned activity of miRNAs in both macrophages and other immune cells.

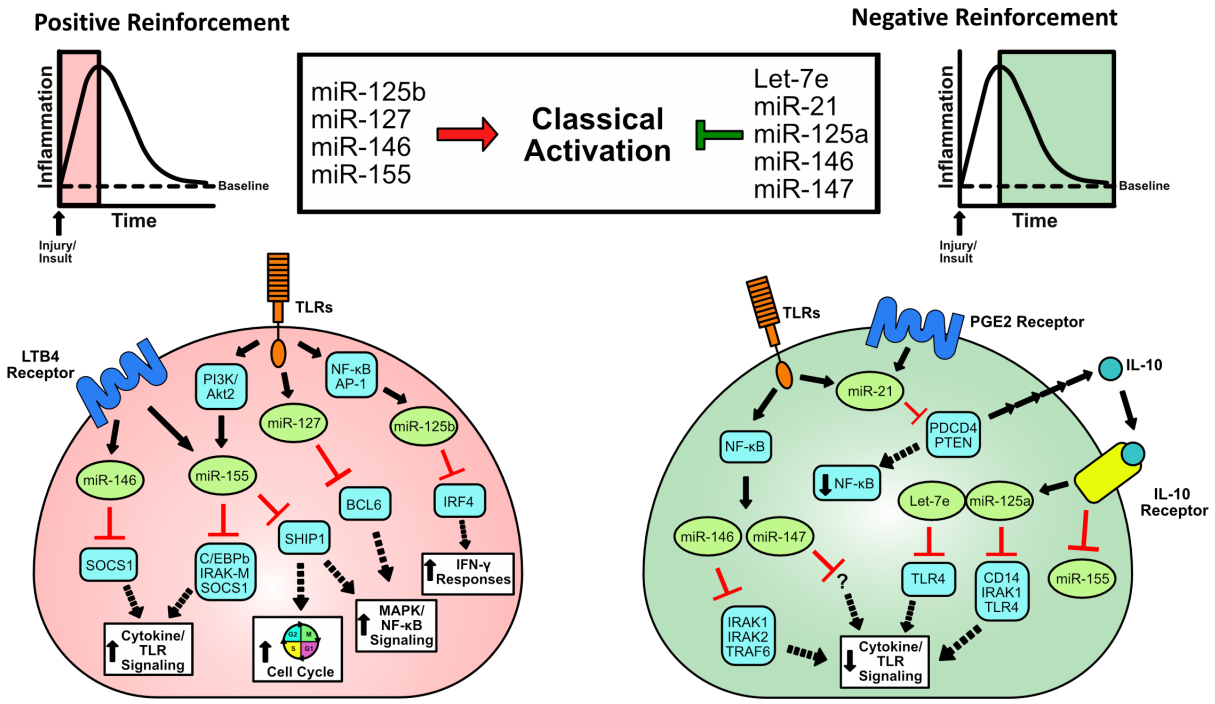

Figure 1.1. Select miRNAs Regulate Classical Activation Programs. Regulated expression of miRNAs controls positive and negative feedback loops in response to extracellular signals that drive "classically-activated" M1-like macrophage programming. Details in text.

Given its central role in promoting inflammation, miR-155 both drives protective and pathogenic macrophage-driven inflammatory responses. *mir155*$^{-/-}$ mice have reduced acute inflammatory responses to systemic bacterial infection, with decreased levels of serum IL-6 after injection of *Listeria monocytogenes*[60]. While miR-155 overexpression leads to enhanced NF-kB activation and increased systemic cytokine production after intraperitoneal injection of LPS in models of sepsis[60]. miR-155 is also essential for circadian regulation of macrophage proinflammatory function, with miR-155 targeting transcripts of the gene *Bmal1* required for diurnal regulation of macrophage TNF-α production in response to LPS[61].

This key driver of macrophage proinflammatory activation has also been implicated in disease processes, both in pre-clinical animal models and human disease. Kupffer cell proinflammatory responses to alcohol require miR-155, which reduces the expression of critical inhibitors of the proinflammatory responses, including SHIP1, SOCS1, IRAK-M, and C/EBPβ, and may help to drive alcoholic hepatitis[62]. Not only do synovial macrophages from patients with rheumatoid arthritis have increased miR-155 and decreased SHIP1 levels[63], but transfection of patient monocytes with miR-155 antagomirs is sufficient to reduce inflammatory activation in favor of an alternative activation program[64]. Finally, miR-155 is upregulated in alveolar macrophages of cigarette smoke-exposed mice[65], suggesting miR-155 regulation of this tissue-resident macrophage populations may contribute to lung disease.

Although miR-155 is the most well-studied proinflammatory activator, it is not the only miRNA that supports macrophage activation. Increased miR-125b expression in macrophages enhances co-stimulatory molecule expression and IFN-γ responsiveness, augmenting the capacity of macrophages to activate T cells and kill tumor cells *in vitro*[66]. This results through miRNA targeting the interferon responsive gene *Irf4,* a negative regulator of macrophage activation. miR-141/200c deficiency in BMDM reduces IL-6, IL-1β, and iNOS production by macrophages, and *miR-141/200c*$^{-/-}$ mice have reduced liver inflammation in models of nonalcoholic steatohepatitis (NASH)[67]. miR-127 is also upregulated in macrophages after PAMP stimulation or pathogen exposure, with pharmacologic manipulation of levels with mimics and inhibitors demonstrating that miR-127 can support a proinflammatory gene expression program in macrophages *in vitro* and exacerbate LPS-induced lung injury[68]. miR-127 targets the 3'UTR of the transcription

factor BCL6 to reduce *Dusp1* expression and increase JNK activation, demonstrating yet another critical role for miRNAs in removing the breaks on macrophage activation.

Finally, some miRNAs that have been shown to inhibit macrophage proinflammatory activation may also potentiate it in certain cellular contexts. Leukotriene LTB_4-mediated expression of miR-146 can potentiate TLR4 signaling by increasing MyD88 expression in macrophages through the inhibition of SOCS1[69]. In addition, the role of miR-27 in proinflammatory activation is complex, as this miRNA has been implicated in promoting, in addition to inhibiting, macrophage activation by reducing IL-10 levels[70]. Pharmacologic manipulation of other miRNAs *in vitro* has been used to explore the role of miRNAs in macrophage activation, including in human monocytes and monocyte-derived macrophages, and has been reviewed elsewhere (reviewed[71]).

1.7. miRNAs Contribute to Feedback Inhibition of Classic Macrophage Activation

Various miRNAs have been shown to antagonize canonical signaling pathways downstream of PAMP stimulation to limit proinflammatory macrophage responses *in vitro* and *in vivo* (**Figure 1.1**). miR-146 is upregulated in macrophages exposed to bacterial or viral products as well as cytokines, including TNF-α and IL-1β[72–74]. Its expression is driven by NF-κB[72,75], and it serves to negatively regulate macrophage proinflammatory pathways downstream of TLR4, TNF-α, IL-1β, and RIG-I pathways through directly suppressing protein expression of key signaling intermediates such as TRAF6, IRAK1, and IRAK2[72,73]. Loss of miR-146 expression results in enhanced proinflammatory cytokine production in response to PAMPs *in vitro* and endotoxin-induced sepsis *in vivo*[60]. It also regulates type

1 IFN responses after viral infection, participating in negative feedback loops that limit IFN-dependent antiviral immunity[73,76], as well as limiting proinflammatory activation of Kupffer cells in the liver to support hepatitis B viral infection[74]. miR-147 similarly serves in a negative feedback loop, which is induced by and then inhibits canonical signaling downstream of TLRs[77], though the molecular targets through which it acts remain undetermined. Additionally, TLR4-induced IL-10 induces the expression the of miR-125a~99b~let-7e cluster which suppresses late pro-inflammatory cytokine production through let-7e targeting of *Tlr4* and miR-125a targeting of *Tlr4*, *Cd14* and *Irak1*[78]. miR-146 is upregulated in monocyte-derived macrophages in patients with cystic fibrosis[79], and upregulation of miR-125a is observed in both Kupffer cells from ethanol-fed rats and monocytes from patients with alcoholic hepatitis[80], indicating that miRNAs maybe important in limiting inflammation in disease.

miR-21 also has a role in restricting macrophage responses to immunogenic signals. Similar to miR-146, levels of miR-21 rise during proinflammatory macrophage activation[81,82]. miR-21 restricts macrophage proinflammatory responses by suppressing NF-κB signaling and promoting the expression of the anti-inflammatory cytokine IL-10 through the regulation of direct target genes *Pten* and *Pdcd4*[82–84]. At sites of injury, clearance of apoptotic cells by macrophages through efferocytosis induces miR-21 expression to inhibit proinflammatory cell activation and promote resolution of wound inflammation[84]. This powerful anti-inflammatory role of miR-21 has important consequences on tissue inflammation. miR-21 expression can be beneficial by restricting pathogenic proinflammatory pathways, with loss of miR-21 worsening LPS-induced peritonitis[81] and atherosclerosis[85]. Alternatively, miR-21 expression can be detrimental by

limiting beneficial M1-like macrophage polarization in TAMs to promote anti-tumoral immune responses[86,87] as well as in *Mycobacterium tuberculosis* infections where robust inflammation is required to control infection[88].

Additional miRNAs also restrict proinflammatory macrophage activation. miR-27 regulates the target gene *Bag2*, a molecular co-chaperone protein involved in NF-kB signaling and apoptosis[89]. miR-127 inhibits the high-affinity FCGR1[90], miR-27 inhibits *Siglec1* and the E3 ubiquitin ligase *Trim27* downstream of type 1 IFN signaling[91], and miR-145 inhibits *Uvrag* to regulate autophagy[92], which together control inflammatory function of macrophages in viral and bacterial infections. And miR-145 suppresses the expression of the histone deacetylase HDAC11 to promote IL-10 production[93]. This work demonstrates that miRNAs regulate multiple facets of key biologic processes in macrophage activation.

1.8. miRNAs Regulate Macrophage Alternative Activation Programs

miRNAs do not exclusively regulate proinflammatory macrophage activation, and individual miRNAs also support alternative M2-like macrophage activation programs (**Figure 1.2**). Among miRNAs selectively expressed in M2-like macrophages with important functions in polarization is miR-223. Expression of miR-223 is driven by IL-4 through the activity of the nuclear receptor PPAR-y and supports alternative macrophage activation by suppressing the mRNA target genes, including *Rasa1* and *Nfat5*[94]. miR-223 simultaneously represses the expression of the gene *Pknox1* to limit proinflammatory activation[95]. *In vivo*, miR-223 expression protects against diet-induced obesity by

promoting alternative macrophage activation to alleviate nutrient-induced inflammation and systemic metabolic impairment[94,95]. Feedback inhibition of miR-223 expression by TLR-mediated IL-6 production during proinflammatory macrophage activation highlights the central role of miR-223 in regulating the M1-like and M2-like balance in macrophages[96].

Additional miRNAs support M2-like polarization in macrophages. miR-142 is induced by IL-4 and IL-13 and supports a pro-fibrogenic program in alternatively activated macrophages by inhibiting the negative regulator of STAT6 signaling SOCS1[97]. Pharmacologic inhibition of miR-142 *in vivo* is protective in mouse models of lung and liver fibrosis[97]. miR-182 is induced in macrophages within the breast tumor microenvironment to support an M2-like program, in part by limiting expression of TLR4 and proinflammatory pathway induction[98]. Finally, miR-181, miR-124, and let-7c are upregulated in M2-like macrophages and likely support alternative activation programs by inhibiting key transcription factors, including KLF6, C/EBPα, and C/EBPδ[99–101].

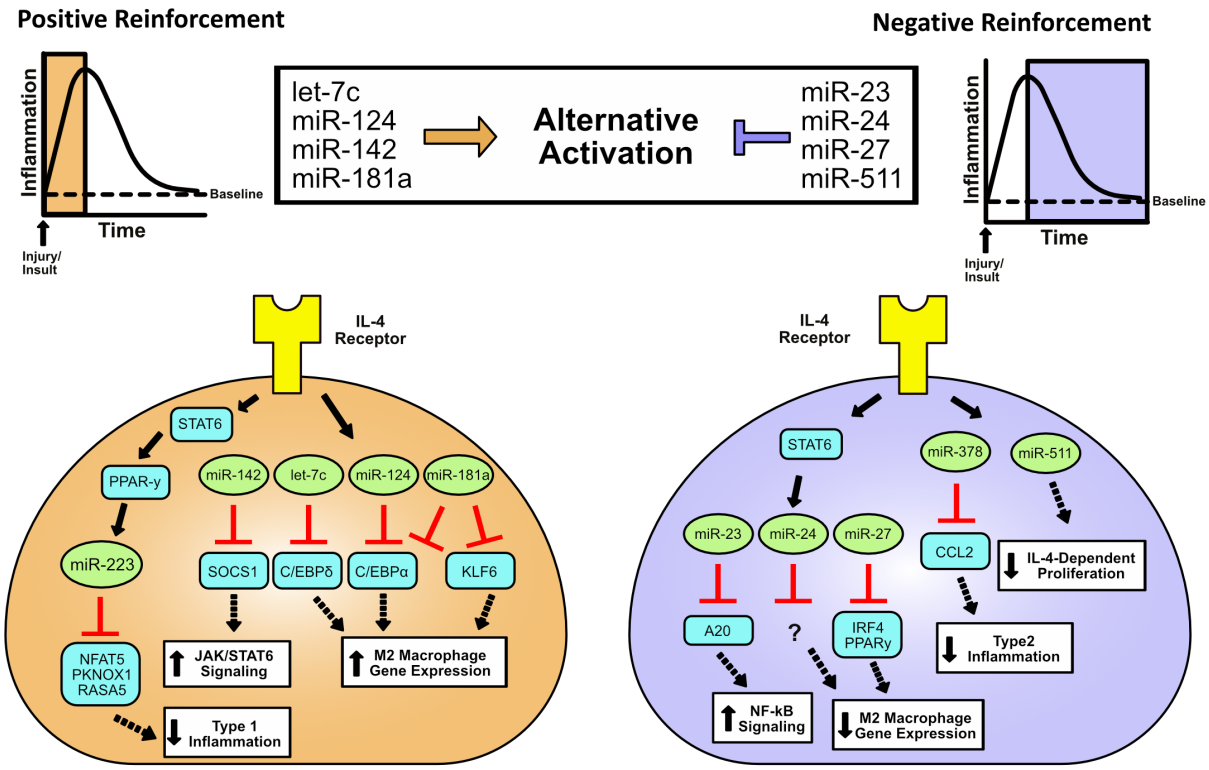

Figure 1.2. Select miRNAs Regulate Alternative Activation Programs. Regulated expression of miRNAs controls positive and negative feedback loops in response to extracellular signals that drive "alternatively-activated" M2-like macrophage programming. Details in text.

miRNAs also participate in inhibitory feedback loops to restrain alternative macrophage activation (**Figure 1.2**). miR-511 is expressed from an intron of the mannose receptor (CD206) locus, a gene whose expression is upregulated in alternatively activated macrophages[102]. miR-511 limits the pro-tumoral M2-like function of TAMs[102] and reduces *Ccl2* expression in M2-like macrophages in the lung to protect against allergic inflammation[103]. The clusters of miRNAs that encode miR-23, miR-24, and miR-27 are also upregulated in M2-like macrophages activated by IL-4 through STAT6 promoter binding[6,104,105]. The M2 macrophage-associated transcription factors IRF4 and PPAR-γ

are reported targets of miR-27, while miR-23 is predicted to repress expression of *A20*, which encodes a negative regulator of NF-κB signaling[104].

Pre-clinical models have demonstrated that regulation of alternative activation programs in macrophages may be critical in disease pathogenesis. Co-injection of RAW264.7 macrophages overexpressing miR-23, miR-24, or miR-27 with 4T1 mammary tumor cells reduces tumor growth *in vivo*[104]. Tumor growth is enhanced in mice lacking the miR-23a~miR-27a~miR-24-2 cluster or in tumors co-injected with BMDM deficient in these miRNAs[105]. miR-21 can restrict M2-like macrophage polarization in response to prostaglandin E2 stimulation by regulating *Stat3* and *Socs1*[106]. And in a cecal ligation and puncture model of sepsis, mice with a myeloid lineage-restricted deletion of miR-21 show enhanced survival with increased bacterial clearance and reduced inflammation[107,108]. M2-like macrophage proliferation and growth are also temporally controlled by miR-378, which is induced in the later stages of a *Brugai malayi* nematode infection model and proposed to limit type 2 inflammation through regulation of a IL-4/PI3K/Akt signaling axis[109]. Together, these findings highlight that miRNAs participate in regulatory feedback loops to both strengthen and dampen macrophage alternative activation pathways to control type 2 inflammation.

1.9. miRNAs in Macrophage Priming, Tolerance, and Trained Immunity

Although long considered a unique feature of the adaptive immune system, cells of the innate immune system can exhibit memory-like behaviors that lead to adaptations in their function. This can result in dampened or enhanced immune responses to

subsequent stimuli and depends critically on the type, dose, and duration of the inducing signal (reviewed in[110,111]). In both tolerance and trained immunity, macrophages receive a primary signal and then return to their basal state. Subsequently, on re-challenge they demonstrate either reduced (tolerance) or enhanced (trained immunity) molecular and cellular function. In priming, macrophages receive a second stimulus before returning to a basal activation state, and this results in additive or synergistic function. These activities variably rely on signaling, transcriptional, epigenetic and/or metabolic reprogramming of the cells, and the participation of miRNAs in this process is adding a layer of post-transcriptional regulation of gene expression to this critical macrophage function.

Recent work has demonstrated that miRNA regulation of epigenetics and signal transduction may play a critical role in immune tolerance, helping to program reduced responsiveness in tolerized macrophages (**Figure 1.3**). High dose LPS stimulation upregulates the expression of miR-222 in macrophages, which in turn impairs cytokine responses toward subsequent LPS treatment by repressing the target gene *Brg1*, encoding a central catalytic subunit of multiple chromatin-modifying enzymatic complexes[112]. In support of its role in LPS tolerance, genetic deletion of both miR-221 and miR-222, which are found on the same transcript and predicted to have overlapping targets, increases susceptibility to LPS-induced septic shock following pretreatment with LPS. Another miRNA critical for sustaining homeostatic immune tolerance is miR-146a. In Kupffer cells, physiologic induction of miR-146a through PPRs confers beneficial maintenance of liver homeostasis by attenuating secondary inflammatory responses[74]. In contrast, reduction of miR-146a can result in reduced tolerance and adverse *in vivo*

outcomes. Suppression of miR-146a expression through chronic morphine treatment disrupts endotoxin tolerance[113].

Indeed, miRNAs serve as essential downstream effectors of macrophage programming during immune tolerization. For example, *Akt1*$^{-/-}$ mice exhibit significant defects in LPS-induced tolerance due in part to the loss of inhibition of TLR4 expression by let-7e and elevated suppression of SOCS1 by miR-155[57]. Their ability to program this innate immunologic memory may reply on Ago-miRNA complexes which maintain their repressive capacity for up to 3 weeks following mitogenic stimulation[114], preconditioning late macrophage responsiveness. These findings demonstrate the importance of miRNAs in regulating immunological tolerance under homeostatic and inflammatory conditions.

Yet miRNAs are critical for more than immune tolerance and may be fundamental to regulating how macrophages respond to different doses and kinetics of signal exposure. Various secondary responses have been proposed to rely on the sustained expression of miRNAs[115]. For instance, low doses of LPS primes atherosclerotic inflammation by increasing levels of miR-24[116]. Upregulation of miR-24, in turn, suppresses SMAD4, which is required for the expression of the key negative-feedback regulator IRAK-M, resulting in the persistence of inflammatory monocytes. Reduction of miR-3473b suppression of PTEN contributes to the priming effects of IFN-γ on

macrophage activation[117]. Therefore, miRNAs serve as downstream effectors critical for the context-specific dynamics of immune tolerization and priming of macrophages.

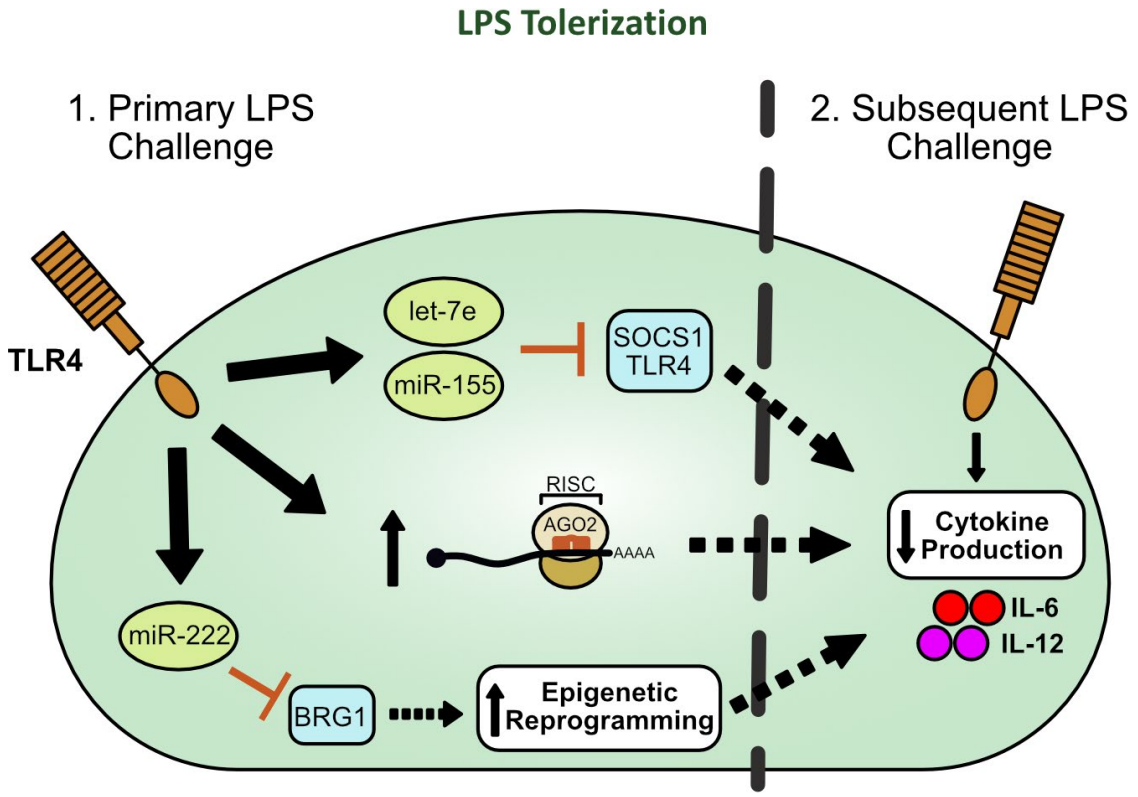

Figure 1.3. miRNAs Regulate LPS Tolerization. Expression of select miRNAs (e.g. let-7e, miR-155, and miR-222) and/or presence of mRNP complexes following initial LPS stimulation dampens inflammatory responses to subsequent LPS exposure. Details in text.

1.10. miRNA Control of Macrophage Function in Obesity and Metabolic Diseases

miRNAs are emerging as significant regulators of both homeostasis and disease in adipose tissue, liver, and the cardiovascular system. As discussed above, the global deletion of miRNA expression in macrophages changes their inflammatory function in atherosclerotic lesions[36] and adipose tissue[118], highlighting a critical role for miRNAs in

regulating inflammatory cell behavior in metabolic disease. miR-146 restrains macrophage proinflammatory programs in obese adipose tissue by inhibiting the direct target gene *Traf6*[119]. And loss of miR-17~92 cluster miRNAs in macrophages results in a dysregulation of pro and anti-inflammatory cytokine production through control of a YYF-Fos-IL-10 pathway which enhances weight gain and metabolic dysfunction[120]. Loss of miR-223 in bone marrow cells which normally restricts proinflammatory programs in macrophages enhances atherosclerotic disease in mice[121]. In contrast, miR-155 supports macrophage-driven inflammation in atherosclerotic lesions through repression of the transcription factor BCL6, inhibiting macrophage recruitment and activation by limiting CCL2 and TNF-α production[122]. However, the role of miRNAs in macrophages in metabolic diseases extends beyond the control of inflammatory programs (**Figure 1.4**).

The identification of critical roles for miR-33 in lipid handling in macrophages has demonstrated important direct links between lipid metabolism and disease-associated macrophage activity. miR-33 is an intronic miRNA encoded within the sterol-responsive transcription factor gene *Srebf2*, which regulates the expression of genes that control cholesterol uptake and metabolism. The gene and miRNA are co-transcriptionally regulated, and both *Srebf2* and miR-33 expression is upregulated after cholesterol depletion or in response to insulin[11]. Co-expression of miR-33 with *Srebf2* cooperatively drives changes in cholesterol homeostasis, with miR-33 preventing cholesterol efflux through the repression of the direct target genes including the cholesterol transporters *Abca1* and *Abcg1*[11,123]. Given the central role of macrophages in regulating cholesterol in atherosclerotic vascular disease, pharmacologic antagonism of miR-33 or selective genetic loss of miR-33 in hematopoietic cells induces regression of atherosclerotic

plaques in low-density lipoprotein receptor- or *Apoe*-deficient mice fed a high-fat diet[124–128]. These effects are associated with enhanced *Abca1* expression, decreased macrophage accumulation in plaques, and reduced proinflammatory macrophage accumulation in lipid-rich environments. Regulation of cholesterol handling by miR-33 in macrophages is also important in macular degeneration, where inhibition of miR-33 can also improve mouse models of disease[129].

Additional miRNAs such as miR-144, miR-204, miR-223, and miR-758 have evolved to directly target cholesterol transporters, including ABCA1 or scavenger receptors in macrophages, demonstrating that lipid transport is an essential molecular hub for miRNA-mediated regulation in metabolic disease[121,130–132]. Models demonstrating the efficacy of pharmacologic delivery of miRNAs such as miR-204 through adeno-associated virus[130] or inhibitors of miR-33[128,133] in ameliorating atherosclerotic disease and shifting the local immune infiltrate highlight the therapeutic potential of miRNAs in treating macrophage-associated cardiovascular pathology.

Consistent with the evolved function of miRNAs in regulating large networks of genes, miR-33 acts on additional target transcripts to control metabolic programming in macrophages. Pharmacologic or genetic inhibition of miR-33 in macrophages shifts cells away from aerobic glycolysis and toward mitochondrial fatty acid oxidation. This results from the inhibition of critical fatty acid oxidation enzymes, including carnitine palmitoyltransferase 1A and the inhibition of AMPK pathway activation[126,134]. This metabolic shift molecularly couples miR-33 with a glycolytic signature associated with proinflammatory macrophage activation and contributes to macrophage-driven inflammation in cardiovascular disease. miR-33 regulation of cellular metabolism also

impacts macrophage function in classic pathogen-associated responses. miR-33 induced in response to *Mycobacterium tuberculosis* infection contributes to pathogen survival by

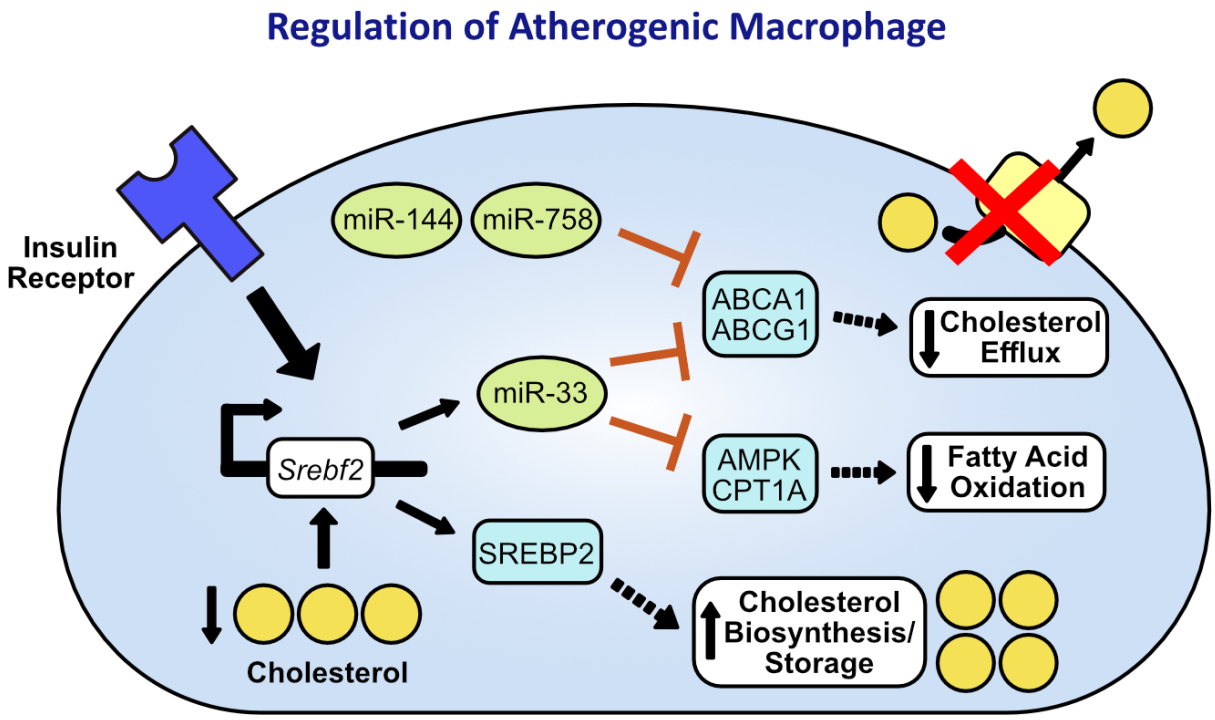

Figure 1.4. miRNAs Regulate Atherogenic Macrophage Programming. Details in text.

inhibiting AMPK pathway activation and downstream fatty acid oxidation and autophagy[135].

1.11. Conclusions

RNA-dependent post-transcriptional regulation is a critical component of gene circuits and networks that control immune cell behavior. In macrophages, miRNAs have been implicated in fundamental aspects of cell function, including classic proinflammatory activation, alternative activation, metabolism, and innate memory (**Table 1**). The study of

miRNA biology is helping to unlock a myriad of macrophage functions dictated by ontogeny, location, and environment that define these highly adaptable cells of the immune system. Yet the function of only a handful of the most abundantly expressed miRNAs in macrophages has been investigated. Future work will need to be guided by continued advances in genome-wide tools that identify key mRNA-miRNA-Argonaute interactions such as high-throughput sequencing RNAs isolated by crosslinking immunoprecipitation (HITS-CLIP) or photoactivatable ribonucleoside-enhanced CLIP (PAR-CLIP)[136,137]. It will also likely need to focus on the multi-layered control of miRNAs with other post transcriptional regulators of gene expression including long noncoding RNA (lncRNA)[138–140] and RNA binding proteins[141].

Finally, understanding the function of miRNAs not only can offer a window into key aspects of the cellular and molecular function of macrophages, but also holds promise for addressing human disease. Single nucleotide polymorphisms (SNPs) in miR-146 that reduce miRNA processing from the pre-miRNA to the mature miRNA form[142] have been linked with autoimmune disease[143] and sepsis[144], demonstrating that miRNAs important in controlling macrophage function may be disease-associated. Whether the activity of this and other miRNAs specifically in macrophages is relevant for disease remains an important area of future investigation. There have also been several human clinical trials for miRNA therapeutics in infectious or inflammatory diseases including miR-122 in hepatitis C virus infection, miR-103/107 in non-alcoholic steatohepatitis, and miR-124 in inflammatory bowel disease, demonstrating the potential of miRNAs mimics and inhibitors as novel therapeutics[145]. Overall, this demonstrates that miRNAs may both contribute

directly to disease pathogenesis as well as offer attractive therapeutic targets for modulating macrophage behavior.

miRNA	Upstream Inducer	Functions	Protein Products of Targets
Classical (M1-like) activation			
Let-7e	IL-10, LPS	Feedback inhibition of proinflammatory responses	TLR4
miR-21	TLR activation, apoptotic cells	Regulates the balance of proinflammatory and alternative macrophage activation, promotes efferocytosis	PDCD4, PTEN, PFK-M, SOCS1, STAT3
miR-125a	IL-10	Feedback inhibition of proinflammatory responses	CD14, IRAK1, TLR4
miR-125b	Leukotriene B4, TLR activation	Regulates the strength of proinflammatory macrophage activation	IRF4, MyD88
miR-127	TLR activation	Proinflammatory, strengthens TLR-induced responses	BCL6
miR-146	TLR activation, TNF-α, IL-1β	Feedback inhibition of proinflammatory responses	IRAK1, IRAK2, TRAF6
miR-155	TLR activation, leukotriene B4	Proinflammatory, strengthens TLR-induced responses	C/EBPβ, IRAK-M, SHIP1, SOCS1
Alternative (M2-like) activation			
Let-7c	IL-4	Alternative macrophage activation	C/EBPδ
miR-23	IL-4	Feedback inhibition of alternative macrophage activation	A20
miR-27	IL-4	Feedback inhibition of alternative macrophage activation, promotes proinflammatory gene expression	IL-10, IRF4, PPAR-γ
miR-124	IL-4, IL-13	Promotes alternatively activated macrophage-associated gene expression	C/EBPα
miR-223	IL-4	Alternative macrophage activation, attenuates obesity-associated inflammation	NFAT5, PKNOX1, RASA1
miR-511	IL-4	Supports feedback inhibition of alternative macrophage activation	CCL2
Other functions			
miR-33	Insulin/cholesterol depletion, coexpressed with SREBF1/2	Promotes atherogenic macrophage programming	ABCA1, ABCG1, AMPK, CPT1α
miR-222	LPS	LPS tolerization	BRG1
miR-24	LPS	LPS priming	SMAD4

Table 1. Summary of miRNA Action and Targets in Macrophage.

1.12. References

1. Lavin, Y., Mortha, A., Rahman, A. & Merad, M. Regulation of macrophage development and function in peripheral tissues. *Nature Reviews Immunology* **15**, 731–744 (2015).

2. Locati, M., Curtale, G. & Mantovani, A. Diversity, Mechanisms, and Significance of Macrophage Plasticity. *Annu. Rev. Pathol. Mech. Dis.* **15**, 123–147 (2020).

3. Zhou, H. *et al.* Identification of the microRNA networks contributing to macrophage differentiation and function. *Oncotarget* **7**, 28806–28820 (2016).

4. Kuchen, S. *et al.* Regulation of MicroRNA expression and abundance during lymphopoiesis. *Immunity* **32**, 828–839 (2010).

5. Zhang, Y., Zhang, M., Zhong, M., Suo, Q. & Lv, K. Expression profiles of miRNAs in polarized macrophages. *Int. J. Mol. Med.* (2013). doi:10.3892/ijmm.2013.1260

6. Lu, L. *et al.* Time Series miRNA-mRNA integrated analysis reveals critical miRNAs and targets in macrophage polarization. *Sci. Rep.* (2016). doi:10.1038/srep37446

7. Altuvia, Y. *et al.* Clustering and conservation patterns of human microRNAs. *Nucleic Acids Res.* **33**, 2697–2706 (2005).

8. Lee, Y., Jeon, K., Lee, J. T., Kim, S. & Kim, V. N. MicroRNA maturation: Stepwise processing and subcellular localization. *EMBO J.* **21**, 4663–4670 (2002).

9. Wang, Y., Luo, J., Zhang, H. & Lu, J. MicroRNAs in the Same Clusters Evolve to Coordinately Regulate Functionally Related Genes. *Mol. Biol. Evol.* **33**, 2232–2247 (2016).

10. Ono, K. MicroRNA-33 encoded by an intron of sterol regulatory element-binding protein 2 (Srebp2) regulates HDL in vivo. *Ther. Res.* **32**, 728–733 (2011).

11. Rayner, K. J. *et al.* MiR-33 contributes to the regulation of cholesterol homeostasis. *Science (80-.).* **328**, 1570–1573 (2010).

12. Borchert, G. M., Lanier, W. & Davidson, B. L. RNA polymerase III transcribes human microRNAs. *Nat. Struct. Mol. Biol.* **13**, 1097–1101 (2006).

13. Beezhold, K. J., Castranova, V. & Chen, F. Microprocessor of microRNAs: Regulation and potential for therapeutic intervention. *Molecular Cancer* **9**, (2010).

14. Ha, M. & Kim, V. N. Regulation of microRNA biogenesis. *Nature Reviews Molecular Cell Biology* **15**, 509–524 (2014).

15. Davis, B. N. & Hata, A. Regulation of MicroRNA Biogenesis: A miRiad of mechanisms. *Cell Communication and Signaling* **7**, (2009).

16. BOHNSACK, M. T. Exportin 5 is a RanGTP-dependent dsRNA-binding protein that mediates nuclear export of pre-miRNAs. *RNA* **10**, 185–191 (2004).

17. Park, J. E. *et al.* Dicer recognizes the 5′ end of RNA for efficient and accurate

processing. *Nature* **475**, 201–205 (2011).

18. Fareh, M. *et al.* TRBP ensures efficient Dicer processing of precursor microRNA in RNA-crowded environments. *Nat. Commun.* **7**, (2016).

19. Gregory, R. I., Chendrimada, T. P., Cooch, N. & Shiekhattar, R. Human RISC couples microRNA biogenesis and posttranscriptional gene silencing. *Cell* **123**, 631–640 (2005).

20. Kapinas, K. & Delany, A. M. MicroRNA biogenesis and regulation of bone remodeling. *Arthritis Res. Ther.* **13**, 220 (2011).

21. Takeda, A., Iwasaki, S., Watanabe, T., Utsumi, M. & Watanabe, Y. The mechanism selecting the guide strand from small RNA duplexes is different among Argonaute proteins. *Plant Cell Physiol.* **49**, 493–500 (2008).

22. Kim, Y.-K., Kim, B. & Kim, V. N. Re-evaluation of the roles of DROSHA, Exportin 5, and DICER in microRNA biogenesis. *Proc. Natl. Acad. Sci. U. S. A.* **113**, E1881-1889 (2016).

23. Heo, I. *et al.* Mono-uridylation of pre-microRNA as a key step in the biogenesis of group II let-7 microRNAs. *Cell* **151**, 521–532 (2012).

24. David, R. Small RNAs: Controlling maturity. *Nature Reviews Molecular Cell Biology* **13**, 752–753 (2012).

25. Liu, J., Valencia-Sanchez, M. A., Hannon, G. J. & Parker, R. MicroRNA-dependent localization of targeted mRNAs to mammalian P-bodies. *Nat. Cell Biol.* **7**, 719–723 (2005).

26. Lam, J. K. W., Chow, M. Y. T., Zhang, Y. & Leung, S. W. S. siRNA versus miRNA as therapeutics for gene silencing. *Molecular Therapy - Nucleic Acids* **4**, (2015).

27. Huntzinger, E. & Izaurralde, E. Gene silencing by microRNAs: Contributions of translational repression and mRNA decay. *Nature Reviews Genetics* **12**, 99–110 (2011).

28. Bhattacharyya, S. N., Habermacher, R., Martine, U., Closs, E. I. & Filipowicz, W. Relief of microRNA-Mediated Translational Repression in Human Cells Subjected to Stress. *Cell* **125**, 1111–1124 (2006).

29. Dana, H. *et al.* Molecular Mechanisms and Biological Functions of siRNA. *Int. J. Biomed. Sci.* **13**, 48–57 (2017).

30. Meister, G. *et al.* Human Argonaute2 mediates RNA cleavage targeted by miRNAs and siRNAs. *Mol. Cell* **15**, 185–197 (2004).

31. Bernstein, E. *et al.* Dicer is essential for mouse development. *Nat. Genet.* **35**, 215–217 (2003).

32. Alisch, R. S., Jin, P., Epstein, M., Caspary, T. & Warren, S. T. Argonaute2 is essential for mammalian gastrulation and proper mesoderm formation. *PLoS Genet.* **3**, 2565–2571 (2007).

33. Morita, S. *et al.* One Argonaute family member, Eif2c2 (Ago2), is essential for development and appears not to be involved in DNA methylation. *Genomics* **89**, 687–696 (2007).

34. Wang, Y., Medvid, R., Melton, C., Jaenisch, R. & Blelloch, R. DGCR8 is essential for microRNA biogenesis and silencing of embryonic stem cell self-renewal. *Nat. Genet.* **39**, 380–385 (2007).

35. Baer, C. *et al.* Suppression of microRNA activity amplifies IFN-γ-induced macrophage activation and promotes anti-tumour immunity. *Nat. Cell Biol.* (2016). doi:10.1038/ncb3371

36. Wei, Y. *et al.* Dicer in Macrophages Prevents Atherosclerosis by Promoting Mitochondrial Oxidative Metabolism. *Circulation* (2018). doi:10.1161/CIRCULATIONAHA.117.031589

37. Muljo, S. A. *et al.* Aberrant T cell differentiation in the absence of Dicer. *J. Exp. Med.* **202**, 261–269 (2005).

38. Chong, M. M. W., Rasmussen, J. P., Rudensky, A. Y. & Littman, D. R. The RNAseIII enzyme Drosha is critical in T cells for preventing lethal inflammatory disease. *J. Exp. Med.* **205**, 2005–2017 (2008).

39. Steiner, D. F. *et al.* MicroRNA-29 Regulates T-Box Transcription Factors and Interferon-γ Production in Helper T Cells. *Immunity* **35**, 169–181 (2011).

40. Cho, Y. K. *et al.* MicroRNA-10a-5p regulates macrophage polarization and promotes therapeutic adipose tissue remodeling. *Mol. Metab.* **29**, 86–98 (2019).

41. Gross, T. J. *et al.* A Microrna processing defect in smokers' macrophages is linked to sumoylation of the endonuclease DICER. *J. Biol. Chem.* **289**, 12823–12834 (2014).

42. Graff, J. W. *et al.* Cigarette Smoking Decreases Global MicroRNA Expression in Human Alveolar Macrophages. *PLoS One* **7**, (2012).

43. Sisti, F. *et al.* Nuclear PTEN enhances the maturation of a microRNA regulon to limit MyD88-dependent susceptibility to sepsis. *Sci. Signal.* (2018). doi:10.1126/scisignal.aai9085

44. Schulte, L. N., Eulalio, A., Mollenkopf, H. J., Reinhardt, R. & Vogel, J. Analysis of the host microRNA response to Salmonella uncovers the control of major cytokines by the let-7 family. *EMBO J.* **30**, 1977–1989 (2011).

45. Kumar, M. *et al.* MicroRNA let-7 modulates the immune response to mycobacterium tuberculosis infection via control of A20, an inhibitor of the NF-κB pathway. *Cell Host Microbe* **17**, 345–356 (2015).

46. Jiang, S., Yan, W., Wang, S. E. & Baltimore, D. Dual mechanisms of posttranscriptional regulation of Tet2 by Let-7 microRNA in macrophages. *Proc. Natl. Acad. Sci. U. S. A.* **116**, 12416–12421 (2019).

47. Njock, M. S. *et al.* Endothelial cells suppress monocyte activation through secretion of extracellular vesicles containing antiinflammatory microRNAs. *Blood* **125**, 3202–3212 (2015).

48. O'Connell, R. M., Taganov, K. D., Boldin, M. P., Cheng, G. & Baltimore, D. MicroRNA-155 is induced during the macrophage inflammatory response. *Proc. Natl. Acad. Sci. U. S. A.* **104**, 1604–1609 (2007).

49. Arranz, A. *et al.* Akt1 and Akt2 protein kinases differentially contribute to macrophage polarization. *Proc. Natl. Acad. Sci.* (2012). doi:10.1073/pnas.1119038109

50. Piccinini, A. M. & Midwood, K. S. Endogenous Control of Immunity against Infection: Tenascin-C Regulates TLR4-Mediated Inflammation via MicroRNA-155. *Cell Rep.* **2**, 914–926 (2012).

51. McCoy, C. E. *et al.* IL-10 inhibits miR-155 induction by toll-like receptors. *J. Biol. Chem.* (2010). doi:10.1074/jbc.M110.102111

52. Chen, Y. *et al.* 1,25-Dihydroxyvitamin D Promotes Negative Feedback Regulation of TLR Signaling via Targeting MicroRNA-155–SOCS1 in Macrophages. *J. Immunol.* **190**, 3687–3695 (2013).

53. Yoon, J. S. J. *et al.* Interleukin-10 control of pre-miR155 maturation involves CELF2. *PLoS One* **15**, e0231639 (2020).

54. O'Connell, R. M., Chaudhuri, A. A., Rao, D. S. & Baltimore, D. Inositol phosphatase SHIP1 is a primary target of miR-155. *Proc. Natl. Acad. Sci.* (2009). doi:10.1073/pnas.0902636106

55. Pauls, S. D. & Marshall, A. J. Regulation of immune cell signaling by SHIP1: A phosphatase, scaffold protein, and potential therapeutic target. *European Journal of Immunology* **47**, 932–945 (2017).

56. An, H. *et al.* Src homology 2 domain-containing inositol-5-phosphatase 1 (SHIP1) negatively regulates TLR4-mediated LPS response primarily through a phosphatase activity- and PI-3K-independent mechanism. *Blood* (2005). doi:10.1182/blood-2005-01-0191

57. Androulidaki, A. *et al.* The Kinase Akt1 Controls Macrophage Response to Lipopolysaccharide by Regulating MicroRNAs. *Immunity* (2009). doi:10.1016/j.immuni.2009.06.024

58. McCormick, S. M. & Heller, N. M. Regulation of macrophage, dendritic cell, and microglial phenotype and function by the SOCS proteins. *Frontiers in Immunology* **6**, (2015).

59. Hsin, J. P., Lu, Y., Loeb, G. B., Leslie, C. S. & Rudensky, A. Y. The effect of cellular context on miR-155-mediated gene regulation in four major immune cell types. *Nat. Immunol.* **19**, 1137–1145 (2018).

60. Mann, M. *et al.* An NF-κB-microRNA regulatory network tunes macrophage

inflammatory responses. *Nat. Commun.* (2017). doi:10.1038/s41467-017-00972-z

61. Curtis, A. M. *et al.* Circadian control of innate immunity in macrophages by miR-155 targeting Bmal1. *Proc. Natl. Acad. Sci. U. S. A.* **112**, 7231–7236 (2015).

62. Bala, S. *et al.* Alcohol-induced miR-155 and HDAC11 inhibit negative regulators of the TLR4 pathway and lead to increased LPS responsiveness of Kupffer cells in alcoholic liver disease. *J. Leukoc. Biol.* **102**, 487–498 (2017).

63. Kurowska-Stolarska, M. *et al.* MicroRNA-155 as a proinflammatory regulator in clinical and experimental arthritis. *Proc. Natl. Acad. Sci. U. S. A.* **108**, 11193–11198 (2011).

64. Paoletti, A. *et al.* Monocyte/Macrophage Abnormalities Specific to Rheumatoid Arthritis Are Linked to miR-155 and Are Differentially Modulated by Different TNF Inhibitors. *J. Immunol.* **203**, 1766–1775 (2019).

65. De Smet, E. G. *et al.* The role of miR-155 in cigarette smoke-induced pulmonary inflammation and COPD. *Mucosal Immunol.* **13**, 423–436 (2020).

66. Chaudhuri, A. A. *et al.* MicroRNA-125b Potentiates Macrophage Activation. *J. Immunol.* (2011). doi:10.4049/jimmunol.1102001

67. Tran, M., Lee, S.-M., Shin, D.-J. & Wang, L. Loss of miR-141/200c ameliorates hepatic steatosis and inflammation by reprogramming multiple signaling pathways in NASH. *JCI insight* (2017). doi:10.1172/jci.insight.96094

68. Ying, H. *et al.* MiR-127 Modulates Macrophage Polarization and Promotes Lung Inflammation and Injury by Activating the JNK Pathway. *J. Immunol.* **194**, 1239–1251 (2015).

69. Wang, Z. *et al.* Leukotriene B 4 Enhances the Generation of Proinflammatory MicroRNAs To Promote MyD88-Dependent Macrophage Activation . *J. Immunol.* (2014). doi:10.4049/jimmunol.1302982

70. Xie, N. *et al.* miR-27a Regulates Inflammatory Response of Macrophages by Targeting IL-10. *J. Immunol.* **193**, 327–334 (2014).

71. Self-Fordham, J. B., Naqvi, A. R., Uttamani, J. R., Kulkarni, V. & Nares, S. MicroRNA: Dynamic regulators of macrophage polarization and plasticity. *Frontiers in Immunology* **8**, 1062 (2017).

72. Taganov, K. D., Boldin, M. P., Chang, K. J. & Baltimore, D. NF-κB-dependent induction of microRNA miR-146, an inhibitor targeted to signaling proteins of innate immune responses. *Proc. Natl. Acad. Sci. U. S. A.* (2006). doi:10.1073/pnas.0605298103

73. Hou, J. *et al.* MicroRNA-146a Feedback Inhibits RIG-I-Dependent Type I IFN Production in Macrophages by Targeting TRAF6, IRAK1, and IRAK2. *J. Immunol.* (2009). doi:10.4049/jimmunol.0900707

74. Liu, Y. *et al.* miR-146a Maintains Immune Tolerance of Kupffer Cells and Facilitates

Hepatitis B Virus Persistence in Mice. *J. Immunol.* **208**, 2558–2572 (2022).

75. Doxaki, C., Kampranis, S. C., Eliopoulos, A. G., Spilianakis, C. & Tsatsanis, C. Coordinated Regulation of miR-155 and miR-146a Genes during Induction of Endotoxin Tolerance in Macrophages. *J. Immunol.* **195**, 5750–5761 (2015).

76. Liu, Z. *et al.* Downregulated NDR1 protein kinase inhibits innate immune response by initiating an miR146a-STAT1 feedback loop. *Nat. Commun.* **9**, (2018).

77. Liu, G. *et al.* miR-147, a microRNA that is induced upon toll-like receptor stimulation, regulates murine macrophage inflammatory responses. *Proc. Natl. Acad. Sci. U. S. A.* (2009). doi:10.1073/pnas.0901216106

78. Curtale, G. *et al.* Multi-step regulation of the TLR4 pathway by the miR-125a~99b~let-7e cluster. *Front. Immunol.* (2018). doi:10.3389/fimmu.2018.02037

79. Luly, F. R. *et al.* MiR-146a is over-expressed and controls IL-6 production in cystic fibrosis macrophages. *Sci. Rep.* **9**, (2019).

80. Kim, A., Saikia, P. & Nagy, L. E. MiRNAs involved in M1/M2 hyperpolarization are clustered and coordinately expressed in alcoholic hepatitis. *Front. Immunol.* **10**, (2019).

81. Barnett, R. E. *et al.* Anti-inflammatory effects of miR-21 in the macrophage response to peritonitis. *J. Leukoc. Biol.* (2016). doi:10.1189/jlb.4a1014-489r

82. Sheedy, F. J. *et al.* Negative regulation of TLR4 via targeting of the proinflammatory tumor suppressor PDCD4 by the microRNA miR-21. *Nat. Immunol.* (2010). doi:10.1038/ni.1828

83. Merline, R. *et al.* Signaling by the matrix proteoglycan decorin controls inflammation and cancer through PDCD4 and microRNA-21. *Sci. Signal.* **4**, ra75 (2011).

84. Das, A., Ganesh, K., Khanna, S., Sen, C. K. & Roy, S. Engulfment of Apoptotic Cells by Macrophages: A Role of MicroRNA-21 in the Resolution of Wound Inflammation. *J. Immunol.* **192**, 1120–1129 (2014).

85. Canfrán-Duque, A. *et al.* Macrophage deficiency of miR-21 promotes apoptosis, plaque necrosis, and vascular inflammation during atherogenesis. *EMBO Mol. Med.* **9**, 1244–1262 (2017).

86. Sahraei, M. *et al.* Suppressing miR-21 activity in tumor-associated macrophages promotes an antitumor immune response. *J. Clin. Invest.* **129**, 5518–5536 (2019).

87. Xi, J. *et al.* MiR-21 depletion in macrophages promotes tumoricidal polarization and enhances PD-1 immunotherapy. *Oncogene* **37**, 3151–3165 (2018).

88. Hackett, E. E. *et al.* Mycobacterium tuberculosis Limits Host Glycolysis and IL-1β by Restriction of PFK-M via MicroRNA-21. *Cell Rep.* **30**, 124-136.e4 (2020).

89. Liang, S. *et al.* MicroRNA-27b Modulates Inflammatory Response and Apoptosis during Mycobacterium tuberculosis Infection . *J. Immunol.* **200**, 3506–3518 (2018).

90. Xie, T. *et al.* MicroRNA-127 Inhibits Lung Inflammation by Targeting IgG Fcγ Receptor I. *J. Immunol.* **188**, 2437–2444 (2012).

91. Zheng, Q., Hou, J., Zhou, Y., Yang, Y. & Cao, X. Type I IFN–Inducible Downregulation of MicroRNA-27a Feedback Inhibits Antiviral Innate Response by Upregulating Siglec1/TRIM27. *J. Immunol.* **196**, 1317–1326 (2016).

92. Kim, J. K. *et al.* MicroRNA-125a Inhibits Autophagy Activation and Antimicrobial Responses during Mycobacterial Infection. *J. Immunol.* **194**, 5355–5365 (2015).

93. Lin, L. *et al.* Type I IFN Inhibits Innate IL-10 Production in Macrophages through Histone Deacetylase 11 by Downregulating MicroRNA-145. *J. Immunol.* **191**, 3896–3904 (2013).

94. Ying, W. *et al.* MicroRNA-223 is a crucial mediator of PPARγ-regulated alternative macrophage activation. *J. Clin. Invest.* (2015). doi:10.1172/JCI81656

95. Zhuang, G. *et al.* A novel regulator of macrophage activation: MiR-223 in obesity-associated adipose tissue inflammation. *Circulation* (2012). doi:10.1161/CIRCULATIONAHA.111.087817

96. Chen, Q. *et al.* Inducible microRNA-223 down-regulation promotes TLR-triggered IL-6 and IL-1β production in macrophages by targeting STAT3. *PLoS One* (2012). doi:10.1371/journal.pone.0042971

97. Su, S. *et al.* miR-142-5p and miR-130a-3p are regulated by IL-4 and IL-13 and control profibrogenic macrophage program. *Nat. Commun.* **6**, 1–19 (2015).

98. Ma, C. *et al.* miR-182 targeting reprograms tumor-associated macrophages and limits breast cancer progression. *Proc. Natl. Acad. Sci. U. S. A.* **119**, (2022).

99. Bi, J. *et al.* miR-181a Induces Macrophage Polarized to M2 Phenotype and Promotes M2 Macrophage-mediated Tumor Cell Metastasis by Targeting KLF6 and C/EBPα. *Mol. Ther. - Nucleic Acids* (2016). doi:10.1038/mtna.2016.71

100. Banerjee, S. *et al.* MicroRNA let-7c Regulates Macrophage Polarization. *J. Immunol.* (2013). doi:10.4049/jimmunol.1202496

101. Yu, A. *et al.* MiR-124 contributes to M2 polarization of microglia and confers brain inflammatory protection via the C/EBP-α pathway in intracerebral hemorrhage. *Immunol. Lett.* (2017). doi:10.1016/j.imlet.2016.12.003

102. Squadrito, M. L. *et al.* MiR-511-3p Modulates Genetic Programs of Tumor-Associated Macrophages. *Cell Rep.* **1**, 141–154 (2012).

103. Do, D. C. *et al.* MiR-511-3p protects against cockroach allergen-induced lung inflammation by antagonizing CCL2. *JCI Insight* **4**, (2019).

104. Ma, S. *et al.* A double feedback loop mediated by microRNA-23a/27a/24-2 regulates M1 versus M2 macrophage polarization and thus regulates cancer progression. *Oncotarget* **7**, 13502–13519 (2016).

105. Boucher, A. *et al.* The miR-23a∼27a∼24-2 microRNA Cluster Promotes

Inflammatory Polarization of Macrophages. *J. Immunol.* (2021). doi:10.4049/jimmunol.1901277

106. Wang, Z. *et al.* MicroRNA 21 Is a homeostatic regulator of macrophage polarization and prevents prostaglandin e2 -mediated M2 generation. *PLoS One* **10**, e0115855 (2015).

107. Melo, P. H., Alvarez, A. R. P. & Serezani, C. H. microRNA-21 controls inflammatory and metabolic program of macrophage and neutrophils during sepsis. *J. Immunol.* **202**, 185.14-185.14 (2019).

108. De Melo, P. *et al.* Macrophage-Derived MicroRNA-21 Drives Overwhelming Glycolytic and Inflammatory Response during Sepsis via Repression of the PGE2/IL-10 Axis. *J. Immunol.* **207**, 902–912 (2021).

109. Rückerl, D. *et al.* Induction of IL-4Rα-dependent microRNAs identifies PI3K/Akt signaling as essential for IL-4-driven murine macrophage proliferation in vivo. *Blood* (2012). doi:10.1182/blood-2012-02-408252

110. Netea, M. G. *et al.* Defining trained immunity and its role in health and disease. *Nature Reviews Immunology* **20**, 375–388 (2020).

111. Divangahi, M. *et al.* Trained immunity, tolerance, priming and differentiation: distinct immunological processes. *Nat. Immunol.* **22**, 2–6 (2021).

112. Seeley, J. J. *et al.* Induction of innate immune memory via microRNA targeting of chromatin remodelling factors. *Nature* **559**, 114–119 (2018).

113. Banerjee, S. *et al.* Morphine induced exacerbation of sepsis is mediated by tempering endotoxin tolerance through modulation of miR-146a. *Sci. Rep.* **3**, (2013).

114. Olejniczak, S. H., La Rocca, G., Gruber, J. J. & Thompson, C. B. Long-lived microRNA - Argonaute complexes in quiescent cells can be activated to regulate mitogenic responses. *Proc. Natl. Acad. Sci. U. S. A.* (2013). doi:10.1073/pnas.1219958110

115. Monticelli, S. & Natoli, G. Short-term memory of danger signals and environmental stimuli in immune cells. *Nature Immunology* **14**, 777–784 (2013).

116. Geng, S. *et al.* The persistence of low-grade inflammatory monocytes contributes to aggravated atherosclerosis. *Nat. Commun.* **7**, (2016).

117. Wu, C. *et al.* IFN-γ Primes Macrophage Activation by Increasing Phosphatase and Tensin Homolog via Downregulation of miR-3473b. *J. Immunol.* **193**, 3036–3044 (2014).

118. Cho, Y. K. *et al.* MicroRNA-10a-5p regulates macrophage polarization and promotes therapeutic adipose tissue remodeling. *Mol. Metab.* (2019). doi:10.1016/j.molmet.2019.08.015

119. Runtsch, M. C. *et al.* Anti-inflammatory microRNA-146a protects mice from diet-

induced metabolic disease. *PLoS Genet.* **15**, e1007970 (2019).

120. Zhang, X., Liu, J., Wu, L. & Hu, X. Micrornas of the mir-17 ~ 9 family maintain adipose tissue macrophage homeostasis by sustaining il-10 expression. *Elife* **9**, 1–19 (2020).

121. Nguyen, M. A. *et al.* miR-223 Exerts Translational Control of Proatherogenic Genes in Macrophages. *Circ. Res.* **131**, 42–58 (2022).

122. Nazari-Jahantigh, M. *et al.* MicroRNA-155 promotes atherosclerosis by repressing Bcl6 in macrophages. *J. Clin. Invest.* **122**, 4190–4202 (2012).

123. Najafi-Shoushtari, S. H. *et al.* MicroRNA-33 and the SREBP host genes cooperate to control cholesterol homeostasis. *Science (80-.).* (2010). doi:10.1126/science.1189123

124. Rayner, K. J. *et al.* Antagonism of miR-33 in mice promotes reverse cholesterol transport and regression of atherosclerosis. *J. Clin. Invest.* (2011). doi:10.1172/JCI57275

125. Price, N. L. *et al.* Genetic Dissection of the Impact of miR-33a and miR-33b during the Progression of Atherosclerosis. *Cell Rep.* **21**, 1317–1330 (2017).

126. Ouimet, M. *et al.* MicroRNA-33-dependent regulation of macrophage metabolism directs immune cell polarization in atherosclerosis. *J. Clin. Invest.* **125**, 4334–4348 (2015).

127. Karunakaran, D. *et al.* Macrophage Mitochondrial Energy Status Regulates Cholesterol Efflux and Is Enhanced by Anti-miR33 in Atherosclerosis. *Circ. Res.* (2015). doi:10.1161/CIRCRESAHA.117.305624

128. Zhang, X. *et al.* Targeted Suppression of miRNA-33 Using pHLIP Improves Atherosclerosis Regression. *Circ. Res.* **131**, 77–90 (2022).

129. Sene, A. *et al.* Impaired cholesterol efflux in senescent macrophages promotes age-related macular degeneration. *Cell Metab.* **17**, 549–561 (2013).

130. Liu, X. *et al.* Macrophage NFATc3 prevents foam cell formation and atherosclerosis: Evidence and mechanisms. *Eur. Heart J.* **42**, 4847–4861 (2021).

131. Ramírez, C. M. *et al.* Control of cholesterol metabolism and plasma high-density lipoprotein levels by microRNA-144. *Circ. Res.* (2013). doi:10.1161/CIRCRESAHA.112.300626

132. Ramirez, C. M. *et al.* MicroRNA-758 regulates cholesterol efflux through posttranscriptional repression of ATP-binding cassette transporter A1. *Arterioscler. Thromb. Vasc. Biol.* (2011). doi:10.1161/ATVBAHA.111.232066

133. Afonso, M. S. *et al.* MiR-33 Silencing Reprograms the Immune Cell Landscape in Atherosclerotic Plaques. *Circ. Res.* 1122–1138 (2021). doi:10.1161/CIRCRESAHA.120.317914

134. Davalos, A. *et al.* miR-33a/b contribute to the regulation of fatty acid metabolism

and insulin signaling. *Proc. Natl. Acad. Sci.* (2011). doi:10.1073/pnas.1102281108

135. Ouimet, M. *et al.* Mycobacterium tuberculosis induces the MIR-33 locus to reprogram autophagy and host lipid metabolism. *Nat. Immunol.* **17**, 677–686 (2016).

136. Hafner, M. *et al.* Transcriptome-wide Identification of RNA-Binding Protein and MicroRNA Target Sites by PAR-CLIP. *Cell* (2010). doi:10.1016/j.cell.2010.03.009

137. Chi, S. W., Zang, J. B., Mele, A. & Darnell, R. B. Argonaute HITS-CLIP decodes microRNA-mRNA interaction maps. *Nature* (2009). doi:10.1038/nature08170

138. Xu, H. *et al.* Inducible degradation of lncRNA Sros1 promotes IFN-γ-mediated activation of innate immune responses by stabilizing Stat1 mRNA. *Nat. Immunol.* **20**, 1621–1630 (2019).

139. Bai, X. Z. *et al.* MicroRNA-138 Aggravates Inflammatory Responses of Macrophages by Targeting SIRT1 and Regulating the NF-κB and AKT Pathways. *Cell. Physiol. Biochem.* (2018). doi:10.1159/000492988

140. Hennessy, E. J. *et al.* The long noncoding RNA CHROME regulates cholesterol homeostasis in primates. *Nat. Metab.* **1**, 98–110 (2019).

141. Lu, Y. C. *et al.* ELAVL1 Modulates Transcriptome-wide miRNA Binding in Murine Macrophages. *Cell Rep.* (2014). doi:10.1016/j.celrep.2014.11.030

142. Jazdzewski, K. *et al.* Common SNP in pre-miR-146a decreases mature miR expression and predisposes to papillary thyroid carcinoma. *Proc. Natl. Acad. Sci. U. S. A.* **105**, 7269–7274 (2008).

143. Li, C. *et al.* Meta-analysis of microRNA-146a rs2910164 G>C polymorphism association with autoimmune diseases susceptibility, an update based on 24 studies. *PLoS One* **10**, (2015).

144. Shao, Y. *et al.* The Functional Polymorphisms of miR-146a Are Associated with Susceptibility to Severe Sepsis in the Chinese Population. *Mediators Inflamm.* **2014**, (2014).

145. Bonneau, E., Neveu, B., Kostantin, E., Tsongalis, G. J. & De Guire, V. How close are miRNAs from clinical practice? A perspective on the diagnostic and therapeutic market. *Electron. J. Int. Fed. Clin. Chem. Lab. Med.* **30**, 114–127 (2019).

CHAPTER 2

MYELOID-SPECIFIC EXPRESSION OF THE *MIR-23-27-24* CLUSTERS PROMOTES GLUCOSE METABOLISM AND LIPID-ASSCOIATED MACROPHAGE ACCRUAL IN OBESITY

Adapted from:

Neil T. Sprenkle, Nathan C. Winn, Kaitlyn E Bunn, Yang Zhao, Deborah J. Park, Brenna G Giese, John J. Karijolich, K Mark Ansel, C. Henrique Serezani, Alyssa H. Hasty, & Heather H. Pua. 2023. Cell Rep. 42.

2.1. General Chapter Overview

Studies from this chapter provide novel insights into how expression of miR-23, miR-24, and miR-27 in macrophages regulates systemic glucose-handling and reprograms the innate immune cell compartment of adipose tissue during chronic obesity. Male mice containing a genetic deletion of the *miR-23a-27a-24-2* and *miR-23b-27b-24-1* miRNA clusters– herein referred to together as the *miR-23-27-24* clusters - in myeloid cells exhibited greater glucose and insulin intolerance in a diet-induced model of murine obesity (20 weeks high-fat diet feeding). This regulation on systemic glucose metabolism is not influenced by baseline differences in glucose tolerance and is sex-dependent, as no differences in glucose-handling were observed in *miR-23-27-24*-deficient female mice

following dietary intervention. Additionally, worsened glucose-handling was uncoupled to enhanced weight gain and increases in 1) inflammatory adipose tissue macrophage (ATM) accumulation, 2) inflammatory gene expression in purified ATMs and whole adipose tissue, and 3) systemic inflammatory signatures in obese *miR-23-27-24*-deficient mice. Further immunophenotyping via flow cytometry revealed a selective reduction in protective $CD9^{+}$ lipid-associated macrophages (LAMs) in obese perigonadal white adipose tissue (WAT) of knockout male and female mice. This was accompanied by a reduction in crown-like structures in obese WAT, histological structures where ATMs surround dying or dead adipocytes. Overall, these studies demonstrate that expression of the *miR-23-27-24* clusters in macrophages confers protection against obesity-induced dysfunction in nutrient metabolism in male mice, a phenomenon linked to the reduction in a protective subset of ATM reported to mediate tissue-level lipid homeostasis in obese adipose tissue.

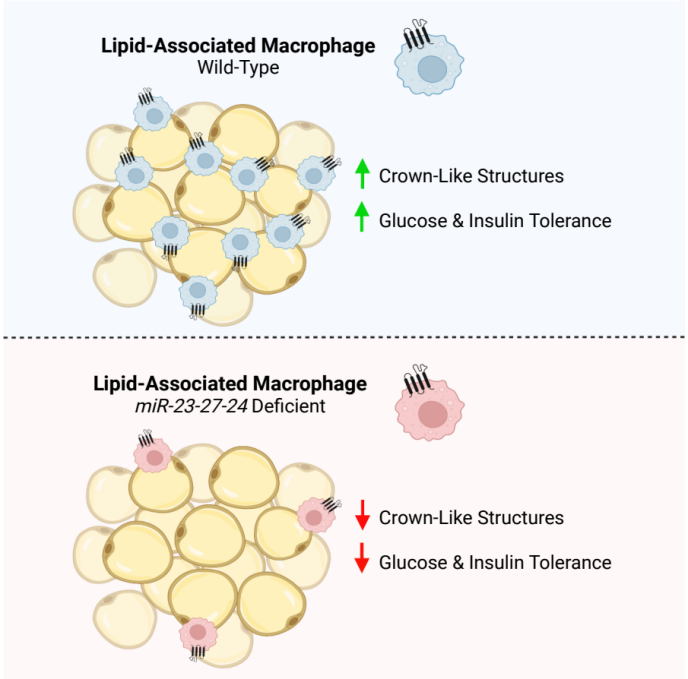

Figure 2.1. Proposed Model of Chapter 2: Expression of the *miR-23-27-24* Clusters Confers Protection Against Obesity-Induced Glucose Intolerance and Promotes LAM Accrual in Obese Adipose Tissue.

2.2. Introduction

Obesity is a risk factor for metabolic diseases, including type 2 diabetes and cardiovascular disease, by promoting peripheral insulin resistance (IR)[1]. Visceral white adipose tissue (WAT) IR is a crucial contributor to obesity-induced metabolic impairments due to its roles as a primary lipid storage depot and dynamic endocrine organ[2]. Accompanying WAT dysfunction in obesity is dramatic cellular and physiological remodeling within the myeloid cell compartment[3,4]. A critical event contributing to WAT IR is macrophage accumulation and sterile activation. In lean WAT, adipose tissue macrophages (ATMs) maintain tissue integrity by fostering an immunosuppressive

microenvironment and regulating tissue iron and lipid homeostasis[5–8]. In contrast, chronic overnutrition and increased visceral adiposity incite local proliferation of tissue-resident macrophages and recruitment of monocyte-derived macrophages into WAT, where they acquire a unique activation program that promotes aberrant production of pro-inflammatory factors that disrupt adipocyte function[9–14].

While early studies assigned ATMs as key drivers of WAT dysfunction by propagating low-grade tissue inflammation, recent evidence indicates that the lipid-handling and phagocytic capabilities of monocyte-derived $CD9^{+}Trem2^{+}$ ATMs can confer protection against adipocyte hypertrophy and systemic metabolic dysregulation in obesity[4]. Mechanistically, it has been proposed that these lipid-associated macrophages (LAMs) accrue within crown-like structures and phagocytize dying lipid-laden adipocytes from the microenvironment to prevent lipid spillover that results in pathology[4]. Importantly, the regulation of LAMs is poorly defined. While most work has focused on Trem2 as a major driver of the transcriptional and functional profile of LAMs, reports on the metabolic consequences of Trem2 ablation are mixed[4,15,16]. This suggests that other key regulators could be involved in LAM function and highlight a complex interaction between innate immunity and WAT physiology. Mechanisms driving macrophage accumulation in obese WAT and their physiologic functions remain incompletely understood. Determining the molecular regulation and function of macrophage subpopulations in obesity is essential for understanding the pathophysiology of obesity-associated metabolic diseases.

Observations from our group and other laboratories indicate that the cooperative regulation of gene expression by the paralogous *miR-23a-27a-24-2* (*Mirc11*) and *miR-23b-27b-24-1* (*Mirc22*) clusters – together referred to as the *miR-23-27-24* clusters here-

controls effector immune cell responses[23,25–27]. In macrophages, expression of miR-23a or miR-27a has been reported to restrain interleukin-4 (IL-4)-induced alternative “M2-like” macrophage activation, a functional state associated with homeostasis, tissue repair, and wound healing[18,27]. Nevertheless, how the *miR-23-27-24* clusters regulate ATM programming in obesity and the physiologic outcomes of these interactions remains unknown due to the heterogeneous nature of ATMs *in vivo* and the lack of published studies utilizing macrophage-specific methods to investigate the biology of the clusters in models of obesity. In this study, we used a myeloid-specific deletion of the *miR-23-27-24* clusters to test the function of these miRNAs in ATMs, identify genes regulated by these clusters, and define a role for these miRNAs in obesity-associated metabolic function.

2.3. Materials & Methods

Animals and Diets

All animal studies were performed after obtaining approval from the Vanderbilt Institutional Animal Care and Use Committee. C57BL/6 ES cells were targeted using constructs generated as a resource for the conditional deletion of miRNA clusters as described[28] to produce chimeric mice with a conditionally mutant allele of the miRNA cluster containing miR-23a, miR-27a, and miR-24-2 (the *Mirc11* cluster). These chimeras were crossed to *Rosa26-Flp* mice (*Gt(ROSA)26Sortm1(FLP1)Dym*; 009086, the Jackson Laboratory) to delete the selection cassette. Mice previously generated with a

conditionally mutant allele containing miR-23b, miR-27b and miR-24-1 (the *Mirc22* cluster)[25] were backcrossed for 10 generations to C57BL/6J mice (000664, the Jackson Laboratory). These two lines were intercrossed, and the progeny crossed to *Lyz2*^{Cre} mice (*B6.129P2-Lyz2*$^{tm1(cre)Ifo}$*/J*; 004781, the Jackson Laboratory) to generate mice with myeloid cells lacking expression of *Mirc11* and *Mirc22* clusters in myeloid cells (MyelΔ). For the diet-induced obesity model, 7–9-week-old male or female *Mirc11*$^{fl/fl}$*Mirc22*$^{fl/fl}$ and *Mirc11*$^{fl/fl}$*Mirc22*$^{fl/fl}$*Lyz2*^{Cre} mice were fed a high-fat diet (HFD, 60% kcal fat; Research Diets) for 20+ weeks. Body weight and food intake were recorded weekly. Body composition measurements, collection of fasting blood samples, and intraperitoneal glucose and insulin tolerance tests were performed before or during HFD feeding. All other analyses were performed after the mice were euthanized.

Body Composition

Fat and lean mass were quantified at the Vanderbilt University Mouse Metabolic Phenotyping Center via nuclear magnetic resonance (Bruker Minispec, Woodlands, TX).

Bone Marrow-Derived Macrophage Cultures

Primary bone marrow-derived macrophages (BMDMs) were prepared by culturing bone marrow of mice in RPMI-1640 media supplemented with 20% L929-conditioned medium, 10% FBS, gentamicin, glutamine, HEPES, non-essential amino acids, and penicillin-streptomycin for 7+ days. Media was changed on Day 1, then every three days of culture. To plate for experiments, BMDMs were detached from the flask using cold PBS containing 0.5 - 5 mM EDTA and plated into tissue culture plates at a concentration of 1 x 10^6 cells/mL.

To metabolically activate BMDMs, BMDMs were cultured in supplemented DMEM media containing 25 mM glucose, 10 nM insulin (Novolin), and 150-250 μM palmitic acid (MP Biomedicals) conjugated to BSA (Research Products International) for 24 h – 48 h. BMDMs in the control group were cultured in supplemented RPMI-1640 medium (11 mM glucose) containing BSA alone. Conditions were adapted from Kratz et al.[12].

Fasting Glucose, Insulin, and Glucose/Insulin Tolerance Tests

Fasting blood samples were collected from the tail vein following a 5-6 h fast. After collecting baseline blood samples, mice underwent an intraperitoneal glucose or insulin tolerance test. In brief, blood samples were collected by massaging the tail at the indicated time points after receiving an intraperitoneal injection of glucose (1 g/kg lean body mass) or insulin (0.5 U/kg lean body mass), respectively. Blood glucose levels were measured using a CONTOUR®NEXT glucometer. Fasting plasma insulin concentrations were determined using a radioimmunoassay; insulin measurements were carried out by the Hormone Assay & Analytical Services Core at Vanderbilt University.

Luminex Analysis

Serum samples from mice fed an HFD were sent to Vanderbilt Hormone Assay & Analytical Services Core for Luminex analysis. Analytes examined in this study were chosen from their “Mouse Metabolic Hormone Panel”.

miRNA and mRNA Quantification via RT-qPCR

TRIzol® Reagent (Life Technologies) was used to extract and purify RNA from tissues and cultured cells. Small RNA (< 200 nt) of F4/80-selected adipose tissue macrophages from perigonadal fat pads was isolated using the RNeasy Mini Kit (Qiagen). For miRNA

quantitation, the Mir-X miRNA First-Strand Synthesis Kit (Takara) was used for cDNA synthesis. For mRNA quantitation, the SuperScript™ IV First-Strand Synthesis System Kit (Invitrogen) was used for cDNA synthesis. Real-time PCR of cDNA was performed on a CFX96 Real-Time PCR Detection System (BioRad) located at the Vanderbilt Cell & Developmental Biology Equipment Resource Core using FastStart Universal SYBR Green master mix (Roche). Expression of the indicated genes was normalized to β-actin (*Actb*) using the $2^{-\Delta\Delta Ct}$ method.

Stromal Vascular Fraction Isolation and Flow Cytometric Analysis

The stromal vascular fraction (SVF) from perigonadal fat pads were isolated following collagenase digestion and differential centrifugation as previously described[30]. Adipose tissue (AT) myeloid cells were characterized via flow cytometry using the following anti-mouse antibodies [BioLegend, eBioscience, BD Pharmingen, Tonbo]: PE-Cy7 F4/80; FITC Ly6G; PE Siglec F; APC and V450 CD9; V450 CD9; APC CD64; FITC and PerCP-Cy5.5 CD64; FITC CD11c; PE CD163; PE-Cy7 CD206; BV421 CCR2; FITC Ly6C; PE-Cy7 TCRβ. Dead cells were identified with e780 viability dye (ThermoFisher).

Statistical Analyses

Statistics were done on experiments with 3+ biological replicates or independent experiments as outlined in figure legends. Analyses were performed using R (www.r-project.org) and GraphPad Prism8 (GraphPad Software, Version 8.02). *P* values of less than 0.05 were considered significant.

2.4. Results

Expression of the miR-23-27-24 Clusters in Myeloid Cells Protects Against Obesity-Induced Glucose and Insulin Intolerance

Given the important role of macrophages on obesity-induced metabolic outcomes[4,9–12] and studies demonstrating the ability of the *miR-23-27-24* clusters to regulate macrophage function[18,23,27], we sought to study how loss of expression of these miRNAs in macrophages regulates metabolic function in an *in vivo* murine model of obesity. We generated mice from embryonic stem cells with a targeted allele for *Mirc11* (the *miR-23a-27a-24-2* cluster)[28] and crossed them to mice with a targeted allele for *Mirc22* (the *miR-23b-27b-24-1* cluster)[25] and mice with *Lyz2*^{Cre} to generate *Mirc11*$^{fl/fl}$*Mirc22*$^{fl/fl}$ (fl/fl) control and *Mirc11*$^{fl/fl}$*Mirc22*$^{fl/fl}$*Lyz2*^{Cre} (MyelΔ) mice. In bone marrow-derived macrophages (BMDMs) (**Figure 2.2A**), peritoneal macrophages (**Figure 2.2B**), and bead-selected F4/80^{+} ATMs from mice fed a high-fat diet (HFD, 60% kcal of fat) (**Figure 2.2C**), miR-23, miR-24 and miR-27 expression was reduced by ≥ 70-95% in

MyelΔ compared to fl/fl controls. These results indicate that the clusters are effectively deleted in bone marrow-derived and tissue-resident macrophage populations.

To determine how expression of the *miR-23-27-24* clusters in myeloid cells regulates systemic metabolic function, we first examined metabolic parameters in young lean mice. Neither male nor female MyelΔ mice exhibited altered body weights (**Figure**

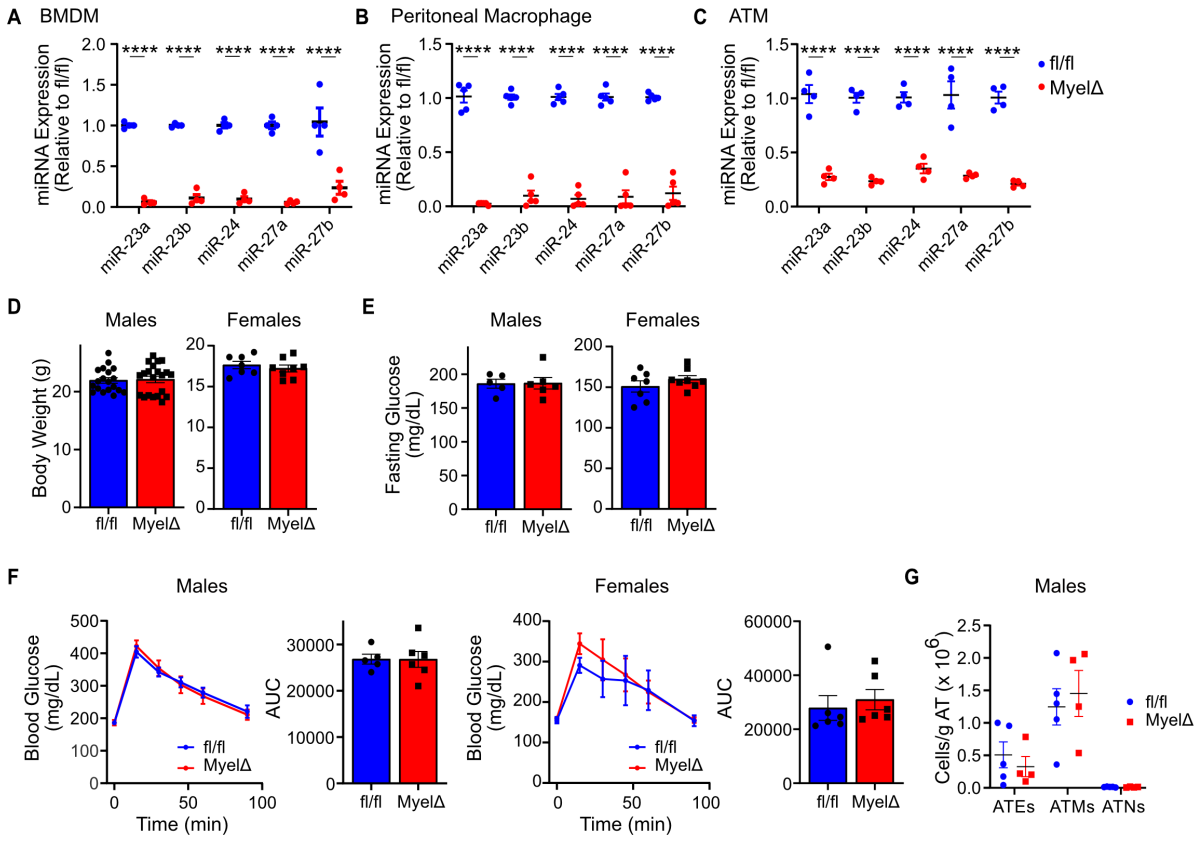

Figure 2.2. Myeloid-Specific Deletion of the *miR-23-27-24* Clusters Does Not Alter Systemic Glucose Tolerance in Male and Female Lean Mice. Relative levels of the indicated miRNAs in (**A**) bone marrow-derived macrophages (BMDMs), (**B**) peritoneal macrophages from lean fl/fl or MyelΔ mice, or (**C**) F4/80-selected ATMs from obese fl/fl or MyelΔ mice (two-way ANOVA with Sidák's multiple comparison test). (**D**) Total bodyweight or (**E**) fasting glucose levels were recorded in lean male or female fl/fl or MyelΔ mice (two-tailed t-test). (**F**) Intraperitoneal glucose tolerance test was performed on lean male or female fl/fl or MyelΔ mice 1 wk before HFD feeding (two-way ANOVA for curves; two-tailed t-test for AUC). (**G**) Myeloid cell numbers were quantified in the epididymal WAT of lean fl/fl or MyelΔ mice (one-way ANOVA with Sidák's multiple comparison test). (**D-G**) All lean mice were 7-9 weeks old. ± S.E.M. ****, p<0.0001.

2.2D), fasting glucose levels (**Figure 2.2E**), or glucose tolerance (**Figure 2.2F**). Additionally, myeloid cell numbers in visceral-like epididymal WAT (eWAT) were not different between genotypes (**Figure 2.2G**). These findings demonstrate that lean fl/fl and MyelΔ mice display similar immunometabolic characteristics.

To test how expression of these clusters in myeloid cells regulates systemic metabolic function in obesity, male fl/fl and MyelΔ mice were fed a high-fat diet (HFD, 60% kcal of fat) for 20 weeks to induce obesity (**Figure 2.3A**). Male MyelΔ mice gained less body weight over 20 wks of HFD feeding (**Figure 2.3B-C**). Fat mass was ~3g lower in obese MyelΔ mice, while lean mass remained unchanged (**Figure 2.3D**). Slopes for cumulative energy intake curves differed significantly between fl/fl and MyelΔ mice (98.58 vs 92.93 kcal/mouse/week, respectively) over the dietary intervention (**Figure 2.3E**), suggesting reduced energy consumption may have contributed to reduced fat accumulation.

The rate of weight gain was also lower in MyelΔ versus fl/fl female mice on HFD for 20 wks (**Figure 2.4A-B**). Like males, MyelΔ female mice accrued less fat mass (~5g) following dietary intervention (**Figure 2.4C**). We then assessed glucose tolerance between both genotypes following HFD feeding. While no differences in fasting blood glucose or insulin levels were observed (**Figure 2.3F**), obese male MyelΔ mice exhibited a significant delay in glucose clearance during an intraperitoneal glucose tolerance test (IP-GTT; **Figure 2.3G**).

To determine if insulin responsiveness was impaired in MyelΔ mice, an IP-insulin tolerance test was performed. Obese male MyelΔ mice exhibited blunted insulin-induced glucose clearance compared to obese control mice (**Figure 2.3H**). Myeloid-specific deletion of the *miR-23-27-24* clusters did not impair glucose tolerance in HFD-fed female mice (**Figure 2.4D-E**). Studies testing sex-specific responses toward HFD feeding show that female mice are protected against obesity-driven impairments in glucose metabolism compared to their male counterparts[31–33]. This protective response has been proposed to

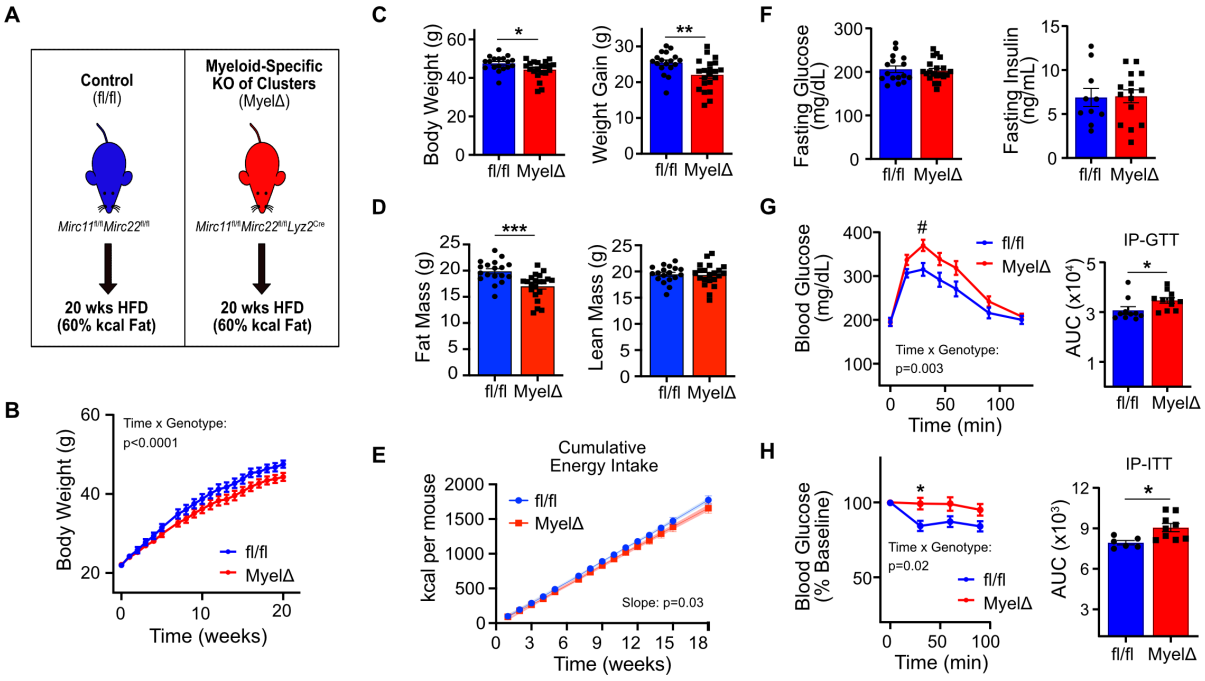

Figure 2.3. Myeloid-Specific Expression of the *miR-23-27-24* Clusters Protects Against Obesity-Induced Glucose and Insulin Intolerance. (**A**) Schematic of dietary interventions. *Mirc11*$^{fl/fl}$*Mirc22*$^{fl/fl}$ (fl/fl) and *Mirc11*$^{fl/fl}$*Mirc22*$^{fl/fl}$*Lyz2*^{Cre} (MyelΔ) mice were fed a high-fat diet (HFD) for 20 wks. (**B**) Body weight curves (two-way ANOVA with Sidák's multiple comparison test), (**C**) final body weights and weight gain (two-tailed t-test), (**D**) final body composition measurements by NMR (two-tailed t-test), or (**E**) cumulative energy intake (simple linear regression). (**F**) Fasting glucose and insulin levels were recorded following HFD feeding (two-tailed t-test). Intraperitoneal (**G**) glucose (1g/kg lean mass) or (**H**) insulin tolerance tests (0.5 U/kg lean mass) were performed on fl/fl and MyelΔ mice after dietary intervention (two-way ANOVA with Sidák's multiple comparison test for curves; two-tailed t-test for area under curve (AUC) comparisons). Male mice 8-10 weeks old at beginning of dietary intervention. Each dot in bar graphs represents one mouse after HFD feeding. **B**&**E**: 18-21 mice per genotype. ± S.E.M. #, p=0.07; *, p≤0.05; **, p<0.01; ***, p<0.001.

be mediated, in part, by sex-dependent suppression of low-grade tissue inflammation, reduction in ATM accrual, and increased WAT vascularization, leading to improved WAT function. These findings indicate that the myeloid cell-specific expression of the *miR-23-27-24* clusters in male mice protects against obesity-induced impairments in glucose regulation.

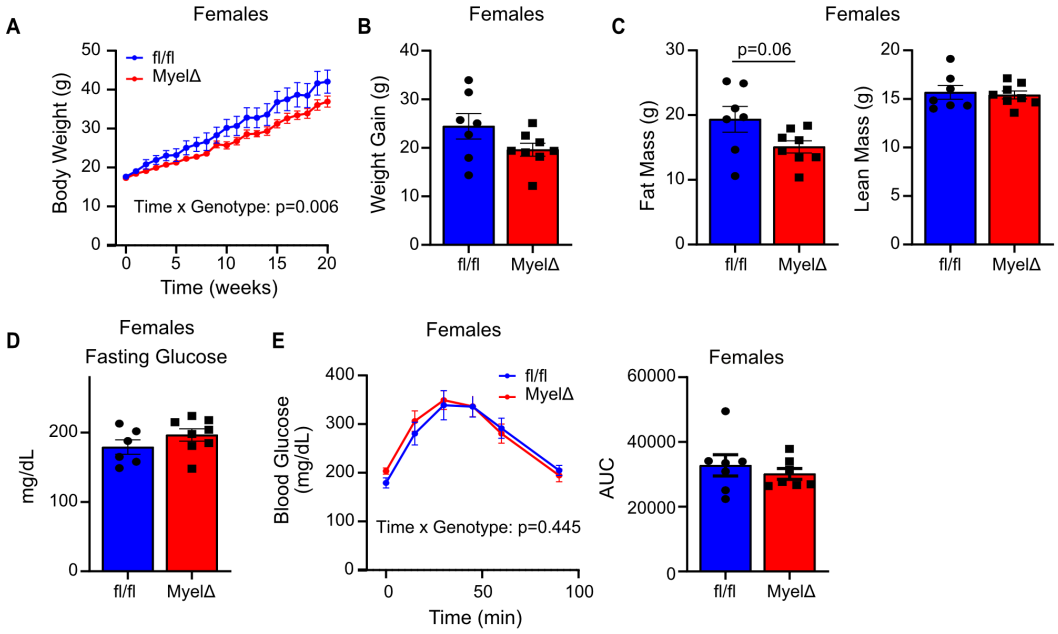

Figure 2.4. Myeloid-Specific Deletion of the *miR-23-27-24* Clusters Does Not Alter Systemic Glucose Tolerance in Female Obese Mice. Female fl/fl or MyelΔ mice were fed a HFD for 20 weeks followed by measurement of (**A**) body weight curves (two-way ANOVA with Sidák's multiple comparison test), (**B**) weight gain (two-tailed t-test), and (**C**) body composition measurements by NMR (two-tailed t-test). (**D**) Fasting glucose levels were recorded following HFD feeding (two-tailed t-test). (**E**) Intraperitoneal glucose tolerance tests (1g/kg lean mass) were performed on female fl/fl and MyelΔ mice following dietary intervention (two-way ANOVA with Sidák's multiple comparison test for curves; two-tailed t-test for area under curve AUC comparisons). Each dot in bar graphs represents one mouse. (**A-E**) Female mice were 8-10 weeks old at beginning of dietary intervention. **A**: 7-8 mice per genotype. ± S.E.M.

miR-23-27-24 Cluster Expression Promotes LAM Accumulation in Obese Adipose Tissue

Because obese male MyelΔ mice are more glucose and insulin intolerant, we hypothesized that deleting the clusters in myeloid cells would exacerbate obesity-induced inflammatory ATM accumulation. To examine if myeloid-specific expression of the *miR-23-27-24* clusters remodels the myeloid cell compartment of obese eWAT, we immunophenotyped the stromal vascular fraction (SVF) of eWAT from male obese fl/fl and MyelΔ mice by flow cytometry. We defined ATMs based on their expression of the surface antigens F4/80 and CD64 and lack of expression of the neutrophil marker Ly6G and the eosinophil marker Siglec F (**Figure 2.5A**)[34]. Contrary to our initial hypothesis, we observed a selective decrease in ATMs in MyelΔ compared to control mice by flow cytometry (**Figure 2.5B**).

Next, we sought to determine whether deletion of the *miR-23-27-24* clusters in myeloid cells alters the function or polarization of ATMs to enhance tissue inflammation, despite reducing total ATM numbers. However, no differences in levels of mRNA encoding the pro-inflammatory cytokines IL-6 and TNF-α in whole eWAT (**Figure 2.5C**) or serum levels of IL-6 and TNF-α (**Figure 2.5D**) were observed. In addition, flow cytometric analysis revealed a significant decrease in surface levels of CD11c on macrophages in the obese adipose tissue of MyelΔ mice, an integrin molecule often expressed by inflammatory ATMs (**Figure 2.5E**)[35–37].

We also examined the expression of markers associated with an insulin-sensitizing M2-like macrophage phenotype on ATMs. However, we did not detect differences in the numbers of $CD163^+$ ATMs or surface levels of the M2-like markers CD71 and CD206 between genotypes (**Figure 2.5F-G**). Levels of the M2-like macrophage-associated

genes *Cd38, Chil3, Egr2, Irf4, Mrc1, Retnla,* and *Lyve1* were also unchanged in eWAT from obese MyelΔ compared to control fl/fl mice (**Figure 2.6A**). Together, these findings demonstrate that overall adipose tissue inflammation is not increased after miR-23, miR-24, and miR-27 deletion in myeloid cells. To test for tissue inflammation in another insulin-sensitive site, we examined the liver in male mice.

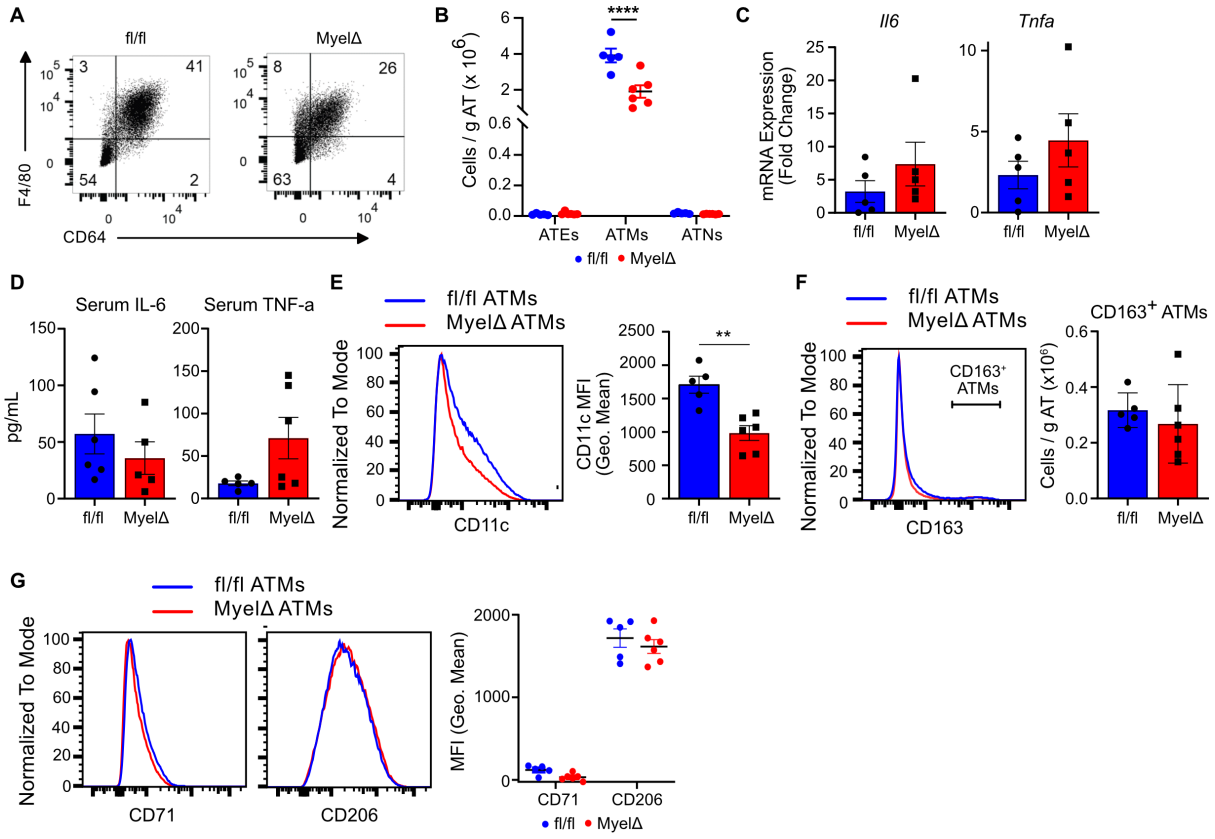

Figure 2.5. Expression of the *miR-23-27-24* Clusters Does Not Regulate Inflammatory ATM Accrual. (**A**) Representative flow panels identifying ATMs from obese fl/fl and MyelΔ mice. (**B**) Myeloid cell numbers were compared between obese fl/fl and MyelΔ mice (two-way ANOVA with Sidák's multiple comparison test). ATE, adipose tissue eosinophil; ATM, adipose tissue macrophage; ATN, adipose tissue neutrophil. (**C**) mRNA levels in whole epididymal WAT (eWAT) or (**D**) serum levels of IL-6 and TNF-α were compared between obese fl/fl and MyelΔ mice (two-tailed t-test). (**E-G**) Quantification of M1-like and M2-like markers on ATMs via flow cytometry (two-tailed t-test for comparison of **E & F**, two-way ANOVA with Sidák's multiple comparison test for **G**). Each dot represents one male mouse after HFD feeding. ± S.E.M. ****, p<0.0001.

While we observed significantly elevated *Il6* mRNA levels in whole MyelΔ hepatic tissue, we did not detect differences in mRNA expression levels of other pro-inflammatory

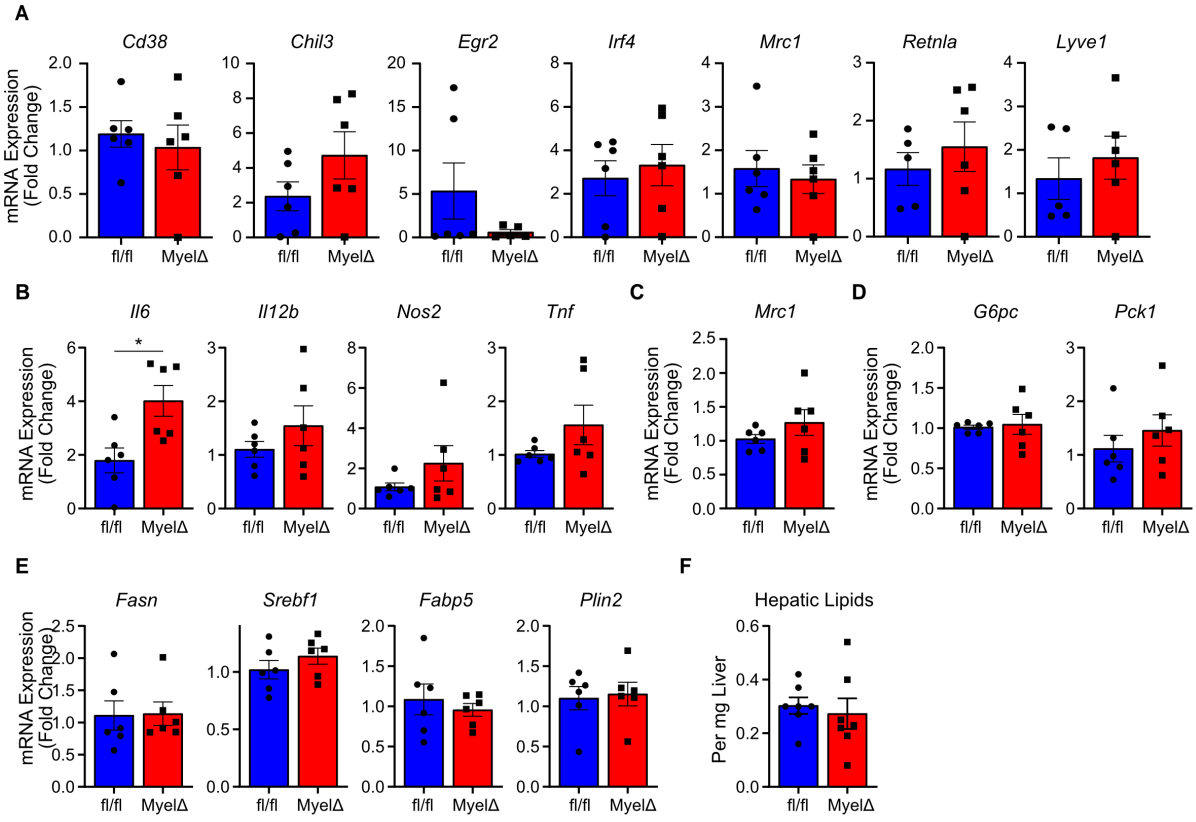

Figure 2.6. Deficiency of the *miR-23-27-24* Clusters Does Not Reduce mRNA Levels of M2-like Macrophage-Associated Genes in Obese eWAT or Induce Marked Hepatic Dysfunction. (**A**) Levels of M2-like macrophage-associated genes were quantified from eWAT via RT-qPCR (two-tailed t-test). Hepatic mRNA levels of (**B**) pro-inflammatory factors, (**C**) *Mrc1*/CD206, (**D**) gluconeogenic enzymes, or (**E**) lipid metabolism enzymes were compared between obese fl/fl or MyelΔ mice (two-tailed t-test). (**F**) Neutral lipid content was quantified from hepatic tissue from obese fl/fl or MyelΔ mice (two-tailed t-test). Each dot represents one male mouse after HFD feeding. ± S.E.M. *, p≤0.05.

factors, M2-like macrophage markers, rate-limiting gluconeogenic enzymes (i.e., *G6pc* and *Pck1*), or enzymes involved in lipid biosynthesis or storage (**Figure 2.6B-E**).

Furthermore, quantification of neutral lipids in the livers of obese fl/fl and MyelΔ mice revealed no differences in pathologic lipid deposition (**Figure 2.6F**). These findings suggest that the systemic impairment in glucose metabolism found in obese MyelΔ mice

is not correlated with changes in metabolism and inflammation in other insulin-sensitive tissues.

Because we found no evidence to suggest that MyelΔ ATMs exacerbated pathologic inflammation, we sought to determine if deleting the clusters in myeloid cells alters LAM accumulation. CD9^{+}Trem2^{+} LAMs are a lipid-laden subset of ATMs that accumulate in crown-like structures within obese WAT and confer protection against obesity-induced pathology in some[4,38], but not all[15,16], studies. Flow cytometric analysis for the LAM marker CD9 revealed a significant reduction in surface levels of CD9 on

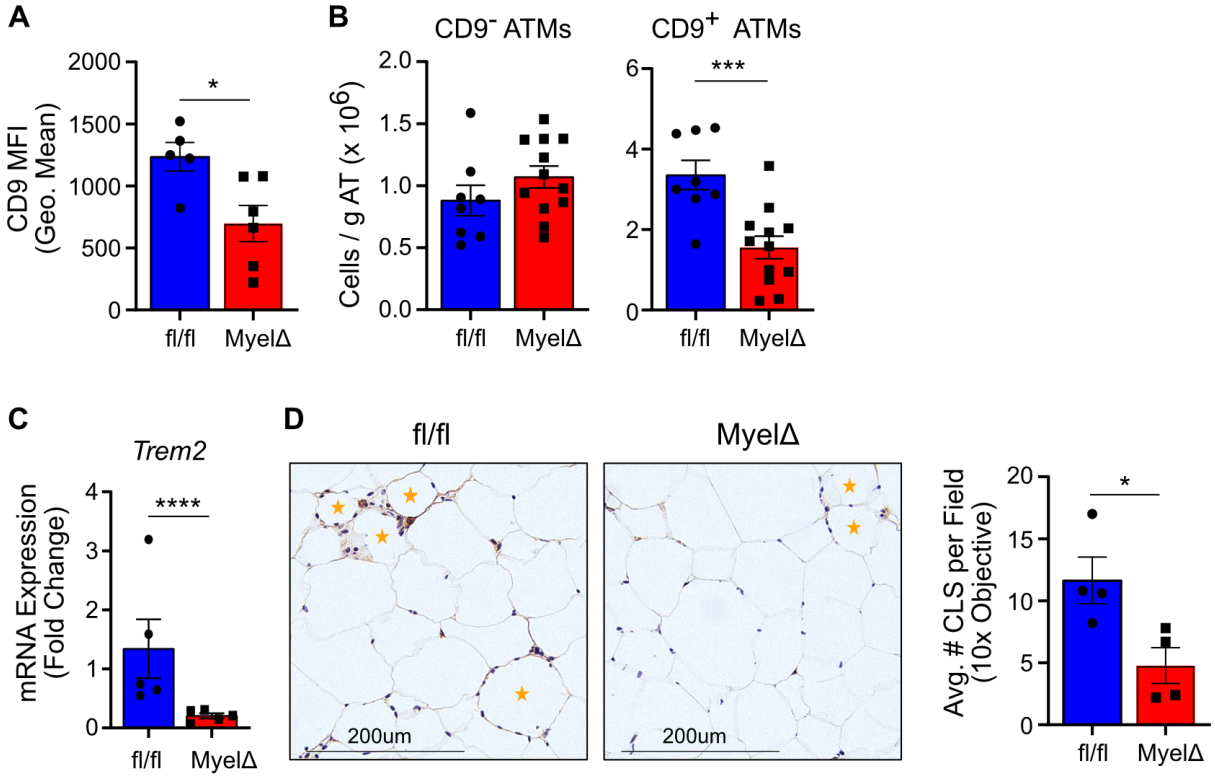

Figure 2.7. Expression of the *miR-23-27-24* Clusters Promotes LAM Accumulation in Obese eWAT (**A-B**) Expression of CD9 and number of CD9^{+} ATMs by flow cytometry (two-tailed t-test). (**C**) *Trem2* mRNA levels from whole fl/fl and MyelΔ eWAT compared via RT-qPCR (one sample t-test). (**D**) Representative image of eWAT sections stained with anti-F4/80 to visualize crown-like structures (orange star) with quantitation (one-tailed t-test). Each dot represents one male mouse after HFD feeding. ± S.E.M. *, p≤0.05; ***, p<0.001; ****, p<0.0001.

obese MyelΔ ATMs in male mice (**Figure 2.7A**). This was accompanied by a selective decrease in the absolute counts of $CD9^+$ ATMs from obese MyelΔ eWAT (**Figure 2.7B)** and *Trem2* mRNA levels in whole MyelΔ eWAT (**Figure 2.7C**).

As in males, total ATM and LAM numbers were significantly reduced in female MyelΔ perigonadal WAT (**Figure 2.8A-B**). We also observed a decrease in crown-like structures in the obese adipose tissue of MyelΔ mice (**Figure 2.7D**). Overall, our findings identify a role for *miR-23-27-24* cluster expression in LAMs and link a reduction in the number of protective LAMs in eWAT with worsened systemic glucose regulation in obese MyelΔ mice.

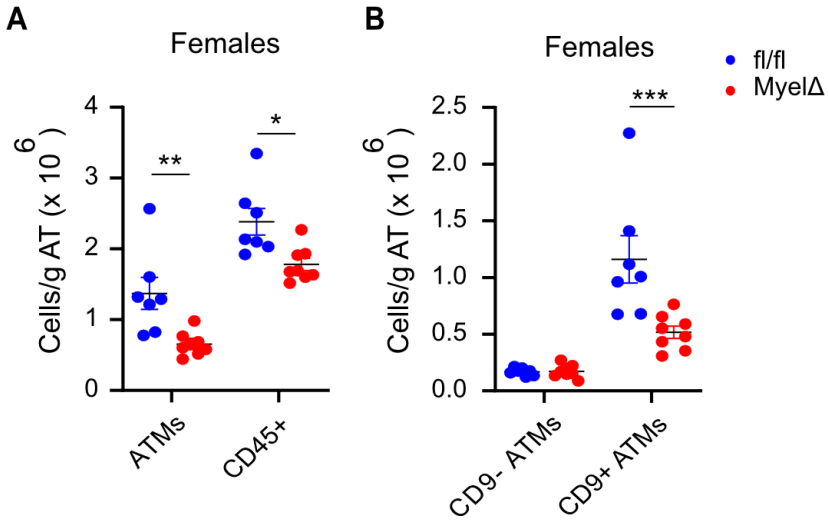

Figure 2.8. Myeloid-Specific Deletion of the *miR-23-27-24* Clusters Reduces LAM Accrual in Visceral WAT of Female Mice. (**A**) Total ATMs and $CD45^+$ immune cells and (**B**) $CD9^-$ and $CD9^+$ ATMs were quantified from fl/fl and MyelΔ perigonadal WAT of female mice (two-way ANOVA with Sidák's multiple comparison test). Each dot represents one female mouse after HFD feeding. ± S.E.M. *, $p \leq 0.05$; **, $p < 0.01$; ***, $p < 0.001$.

2.5. Discussion

Accumulation of macrophages in adipose tissue is a hallmark of obesity, a condition with growing worldwide prevalence that can significantly increase the risk of type 2 diabetes, cardiovascular disease, and cancer[48–50]. Cells of the innate immune system play a complex role in the regulation of obesity-induced insulin resistance. While the accumulation of inflammatory ATMs has been linked to metabolic outcomes associated with chronic obesity[9–14], recent evidence demonstrates that ATMs can also protect against the metabolic complications of obesity through proposed lipid-handling and phagocytic capabilities[4]. Because the key molecular mechanisms driving ATM adaptations in obesity and their influence on systemic insulin resistance remain incompletely understood, we hypothesized that miRNAs might both serve as important molecular regulators of this critical cell population and provide unique insight into the gene networks and pathways that control these cells.

miRNAs control macrophage-driven inflammation in obesity and obesity-associated metabolic diseases. miR-155 promotes macrophage-driven inflammation in atherosclerotic plaques, while miR-146a and miR-223 restrain aberrant inflammatory activation in obese adipose tissue[51–53]. And the regulation of lipid metabolism by miR-33 promotes development of atherogenic macrophages and progression of artherosclerosis[54,55]. Although published data demonstrate that miRNAs of the *miR-23-27-24* clusters can limit M2-like macrophage differentiation and function[18,27], we did not observe an increase in M2-like macrophages in obese adipose tissue. Furthermore, male mice with a myeloid-specific deletion of these clusters showed worsened glucose and

insulin tolerance, rather than protection from obesity-associated metabolic dysfunction. This finding is consistent with a recent study showing that global deletion of the miR-23b-27b-24-1 (*Mirc22*) cluster aggravated glucose intolerance in mice fed a HFD[56]. Of note, we did not observe differences in systemic glucose handling in female mice with a myeloid-specific deletion of the *miR-23-27-24* clusters, which adds to literature showing discordant regulation of obesity and metabolism in females and males[31–33]. However, we identified that the *miR-23-27-24* clusters support LAM accrual in WAT during chronic obesity in both males and females, a unique subset of $Trem2^{+}CD9^{+}$ macrophages that accumulate late in obesity and may play a role in improving systemic glucose tolerance[4]. Importantly, this impairment of systemic metabolic function occurred in the absence of increased weight gain, uncoupling the degree of adiposity from metabolic function through the selective regulation of these noncoding RNAs in myeloid cells.

We cannot exclude that loss of the *miR-23-27-24* clusters in macrophages outside eWAT contributes to the observed metabolic phenotype. For example, loss of this cluster's expression in liver macrophages may also be important, as liver macrophages have been intimately linked to obesity-induced defects in systemic glucose regulation, and LAM signatures have been reported in hepatic tissue in murine obesity[4,63,64]. It will be important in the future to determine if the *miR-23-27-24* clusters contribute to the function of other macrophage populations found in metabolic and other diseases, including in atherosclerosis[65,66], liver dysfunction during obesity[4], within the tumor microenvironment[67,68] and in Alzheimer's disease[69].

2.6. Conclusions

Findings from Chapter 2 indicate that myeloid-specific expression of the *miR-23-27-24* clusters confers protection against obesity-induced defects in systemic glucose regulation in male mice. Because female mice are intrinsically more protected from obesity-associated metabolic dysfunction, modest differences in glucose tolerance between genotypes may not be discernable without more extensive testing. The metabolic phenotype observed in male MyelΔ mice on HFD appears to be uncoupled to enhanced weight gain and differential inflammatory ATM accrual. Instead, our findings indicate that *miR-23-27-24* deficiency results in selective reduction of $CD9^+$ LAMs and crown-like structures in obese eWAT, potentially disrupting adipose tissue function and encouraging systemic defects in glucose regulation. These findings highlight opportunities for investigations of the layered complexity of post-transcriptional regulation at the intersection of immunometabolism, cellular immunology, and RNA biology.

2.7. References

1. Haffner, S.M. (1990). Cardiovascular Risk Factors in Confirmed Prediabetic Individuals. Jama *263*, 2893. 10.1001/jama.1990.03440210043030.
2. Rosen, E.D., and Spiegelman, B.M. (2006). Adipocytes as regulators of energy balance and glucose homeostasis. Nature *444*, 847–853. 10.1038/nature05483.
3. Surmi, B.K., and Hasty, A.H. (2008). Macrophage infiltration into adipose tissue: Initiation, propagation and remodeling. Future Lipidol. *3*, 545-556. 10.2217/17460875.3.5.545.
4. Jaitin, D.A., Adlung, L., Thaiss, C.A., Weiner, A., Li, B., Descamps, H., Lundgren, P., Bleriot, C., Liu, Z., Deczkowska, A., et al. (2019). Lipid-Associated Macrophages Control Metabolic Homeostasis in a Trem2-Dependent Manner. Cell. *178*, 686-698.

10.1016/j.cell.2019.05.054.

5. Hubler, M.J., Peterson, K.R., and Hasty, A.H. (2015). Iron homeostasis: A new job for macrophages in adipose tissue? Trends Endocrinol. Metab. *26*, 101-109. 10.1016/j.tem.2014.12.005.

6. Flaherty, S.E., Grijalva, A., Xu, X., Ables, E., Nomani, A., and Ferrante, A.W. (2019). A lipase-independent pathway of lipid release and immune modulation by adipocytes. Science. *363*, 989-993. 10.1126/science.aaw2586.

7. Hubler, M.J., Erikson, K.M., Kennedy, A.J., and Hasty, A.H. (2018). MFe hi adipose tissue macrophages compensate for tissue iron perturbations in mice. Am. J. Physiol. Physiol. *315*, 319-319. 10.1152/ajpcell.00103.2018.

8. Lumeng, C.N., Delproposto, J.B., Westcott, D.J., and Saltiel, A.R. (2008). Phenotypic switching of adipose tissue macrophages with obesity is generated by spatiotemporal differences in macrophage subtypes. Diabetes. *57*, 3239-3246. 10.2337/db08-0872.

9. Weisberg, S.P., Hunter, D., Huber, R., Lemieux, J., Slaymaker, S., Vaddi, K., Charo, I., Leibel, R.L., and Ferrante, A.W. (2006). CCR2 modulates inflammatory and metabolic effects of high-fat feeding. J. Clin. Invest. *116*, 115-124. 10.1172/JCI24335.

10. Kanda, H., Tateya, S., Tamori, Y., Kotani, K., Hiasa, K.I., Kitazawa, R., Kitazawa, S., Miyachi, H., Maeda, S., Egashira, K., et al. (2006). MCP-1 contributes to macrophage infiltration into adipose tissue, insulin resistance, and hepatic steatosis in obesity. J. Clin. Invest. *116*, 1494-1505. 10.1172/JCI26498.

11. Zheng, C., Yang, Q., Cao, J., Xie, N., Liu, K., Shou, P., Qian, F., Wang, Y., and Shi, Y. (2016). Local proliferation initiates macrophage accumulation in adipose tissue during obesity. Cell Death Dis. *7*, 1-9. 10.1038/cddis.2016.54.

12. Kratz, M., Coats, B.R., Hisert, K.B., Hagman, D., Mutskov, V., Peris, E., Schoenfelt, K.Q., Kuzma, J.N., Larson, I., Billing, P.S., et al. (2014). Metabolic dysfunction drives a mechanistically distinct proinflammatory phenotype in adipose tissue macrophages. Cell Metab. *20*, 614-625. 10.1016/j.cmet.2014.08.010.

13. Christ, A., Lauterbach, M., and Latz, E. (2019). Western Diet and the Immune System: An Inflammatory Connection. Immunity. *51*, 794-811. 10.1016/j.immuni.2019.09.020.

14. Hotamisligil, G.S. (2017). Inflammation, metaflammation and immunometabolic disorders. Nature. *542*, 177-185. 10.1038/nature21363.

15. Winn, N.C., Wolf, E.M., Garcia, J.N., and Hasty, A.H. (2022). Exon 2-mediated deletion of Trem2 does not worsen metabolic function in diet-induced obese mice. J. Physiol. *600*, 4485–4501. 10.1113/JP283684.

16. Sharif, O., Brunner, J.S., Korosec, A., Martins, R., Jais, A., Snijder, B., Vogel, A., Caldera, M., Hladik, A., Lakovits, K., et al. (2021). Beneficial Metabolic Effects of TREM2 in Obesity Are Uncoupled From Its Expression on Macrophages. Diabetes

70, 2042–2057. 10.2337/DB20-0572.

17. Wu, X.Q., Dai, Y., Yang, Y., Huang, C., Meng, X.M., Wu, B.M., and Li, J. (2016). Emerging role of microRNAs in regulating macrophage activation and polarization in immune response and inflammation. Immunology. 148, 237-248. 10.1111/imm.12608.

18. Boucher, A., Klopfenstein, N., Hallas, W.M., Skibbe, J., Appert, A., Jang, S.H., Pulakanti, K., Rao, S., Cowden Dahl, K.D., and Dahl, R. (2021). The miR-23a∼27a∼24-2 microRNA Cluster Promotes Inflammatory Polarization of Macrophages. J. Immunol. *206*, 540-553. 10.4049/jimmunol.1901277.

19. Androulidaki, A., Iliopoulos, D., Arranz, A., Doxaki, C., Schworer, S., Zacharioudaki, V., Margioris, A.N., Tsichlis, P.N., and Tsatsanis, C. (2009). The Kinase Akt1 Controls Macrophage Response to Lipopolysaccharide by Regulating MicroRNAs. Immunity. *31*, 220-231. 10.1016/j.immuni.2009.06.024.

20. Ebert, M.S., and Sharp, P.A. (2012). Roles for MicroRNAs in conferring robustness to biological processes. Cell. 149, 515-524. 10.1016/j.cell.2012.04.005.

21. Farh, K.K.H., Grimson, A., Jan, C., Lewis, B.P., Johnston, W.K., Lim, L.P., Burge, C.B., and Bartel, D.P. (2005). The widespread impact of mammalian microRNAs on mRNA repression and evolution. Science *310*, 1817-1821. 10.1126/science.1121158.

22. Kabekkodu, S.P., Shukla, V., Varghese, V.K., D'Souza, J., Chakrabarty, S., and Satyamoorthy, K. (2018). Clustered miRNAs and their role in biological functions and diseases. Biol. Rev. *93*, 1955-1986. 10.1111/brv.12428.

23. Cho, S., Wu, C.-J., Yasuda, T., Cruz, L.O., Khan, A.A., Lin, L.-L., Nguyen, D.T., Miller, M., Lee, H.-M., Kuo, M.-L., et al. (2016). miR-23~27~24 clusters control effector T cell differentiation and function. J. Exp. Med. *213*. 235-249. 10.1084/jem.20150990.

24. Wang, Y., Luo, J., Zhang, H., and Lu, J. (2016). MicroRNAs in the Same Clusters Evolve to Coordinately Regulate Functionally Related Genes. Mol. Biol. Evol. *33*, 2232–2247. 10.1093/molbev/msw089.

25. Pua, H.H., Steiner, D.F., Patel, S., Gonzalez, J.R., Ortiz-Carpena, J.F., Kageyama, R., Chiou, N.T., Gallman, A., de Kouchkovsky, D., Jeker, L.T., et al. (2016). MicroRNAs 24 and 27 Suppress Allergic Inflammation and Target a Network of Regulators of T Helper 2 Cell-Associated Cytokine Production. Immunity *44*, 821–832. 10.1016/j.immuni.2016.01.003.

26. Cho, S., Wu, C.-J., Nguyen, D.T., Lin, L.-L., Chen, M.-C., Khan, A.A., Yang, B.-H., Fu, W., and Lu, L.-F. (2017). A Novel miR-24–TCF1 Axis in Modulating Effector T Cell Responses. J. Immunol. *198*, 3919–3926. 10.4049/jimmunol.1601404.

27. Ma, S., Liu, M., Xu, Z., Li, Y., Guo, H., Ge, Y., Liu, Y., Zheng, D., and Shi, J. (2016). A double feedback loop mediated by microRNA-23a/27a/24-2 regulates M1 versus M2 macrophage polarization and thus regulates cancer progression. Oncotarget *7*,

13502–13519. 10.18632/oncotarget.6284.

28. Park, C.Y., Jeker, L.T., Carver-Moore, K., Oh, A., Liu, H.J., Cameron, R., Richards, H., Li, Z., Adler, D., Yoshinaga, Y., et al. (2012). A Resource for the Conditional Ablation of microRNAs in the Mouse. Cell Rep. *1*, 385–391. 10.1016/j.celrep.2012.02.008.

29. Kiritsy, M.C., Ankley, L.M., Trombley, J., Huizinga, G.P., Lord, A.E., Orning, P., Elling, R., Fitzgerald, K.A., and Olive, A.J. (2021). A genetic screen in macrophages identifies new regulators of ifnγ-inducible mhcii that contribute to t cell activation. Elife *10,* 1-30. 10.7554/eLife.65110.

30. Orr, J.S., Kennedy, A.J., and Hasty, A.H. (2013). Isolation of Adipose Tissue Immune Cells. J. Vis. Exp. 10.3791/50707.

31. Pettersson, U.S., Waldén, T.B., Carlsson, P.O., Jansson, L., and Phillipson, M. (2012). Female Mice are Protected against High-Fat Diet Induced Metabolic Syndrome and Increase the Regulatory T Cell Population in Adipose Tissue. PLoS One *7*, 1-10. 10.1371/journal.pone.0046057.

32. Ingvorsen, C., Karp, N.A., and Lelliott, C.J. (2017). The role of sex and body weight on the metabolic effects of high-fat diet in C57BL/6N mice. Nutr. Diabetes *7*, 1-7. 10.1038/nutd.2017.6.

33. Rudnicki, M., Abdifarkosh, G., Rezvan, O., Nwadozi, E., Roudier, E., and Haas, T.L. (2018). Female mice have higher angiogenesis in perigonadal adipose tissue than males in response to high-fat diet. Front. Physiol. *9*. 10.3389/fphys.2018.01452.

34. Cho, K.W., Zamarron, B.F., Muir, L.A., Singer, K., Porsche, C.E., DelProposto, J.B., Geletka, L., Meyer, K.A., O'Rourke, R.W., and Lumeng, C.N. (2016). Adipose Tissue Dendritic Cells Are Independent Contributors to Obesity-Induced Inflammation and Insulin Resistance. J. Immunol. *197*, 3650-3661. 10.4049/jimmunol.1600820.

35. Wu, J., Wu, H., An, J., Ballantyne, C.M., and Cyster, J.G. (2018). Critical role of integrin CD11c in splenic dendritic cell capture of missing-self CD47 cells to induce adaptive immunity. Proc. Natl. Acad. Sci. U. S. A. *115*, 6786-6791. 10.1073/pnas.1805542115.

36. Lukácsi, S., Nagy-Baló, Z., Erdei, A., Sándor, N., and Bajtay, Z. (2017). The role of CR3 (CD11b/CD18) and CR4 (CD11c/CD18) in complement-mediated phagocytosis and podosome formation by human phagocytes. Immunol. Lett. *189*, 64-72. 10.1016/j.imlet.2017.05.014.

37. Lumeng, C.N., Bodzin, J.L., and Saltiel, A.R. (2007). Obesity induces a phenotypic switch in adipose tissue macrophage polarization. J. Clin. Invest. *117*, 175-184. 10.1172/JCI29881.

38. Hill, D.A., Lim, H.W., Kim, Y.H., Ho, W.Y., Foong, Y.H., Nelson, V.L., Nguyen, H.C.B., Chegireddy, K., Kim, J., Habertheuer, A., et al. (2018). Distinct macrophage

populations direct inflammatory versus physiological changes in adipose tissue. Proc. Natl. Acad. Sci. U. S. A. *115*, 5096-5105. 10.1073/pnas.1802611115.

39. Amano, S.U., Cohen, J.L., Vangala, P., Tencerova, M., Nicoloro, S.M., Yawe, J.C., Shen, Y., Czech, M.P., and Aouadi, M. (2014). Local proliferation of macrophages contributes to obesity-associated adipose tissue inflammation. Cell Metab. *19*, 162-171.10.1016/j.cmet.2013.11.017.

40. Ponomarev, E.D., Veremeyko, T., Barteneva, N., Krichevsky, A.M., and Weiner, H.L. (2011). MicroRNA-124 promotes microglia quiescence and suppresses EAE by deactivating macrophages via the C/EBP-α-PU.1 pathway. Nat. Med. *17*, 64-70. 10.1038/nm.2266.

41. Sprenkle, N.T., Serezani, C.H., and Pua, H.H. (2023). MicroRNAs in Macrophages: Regulators of Activation and Function. J. Immunol. *210*, 359–368. 10.4049/jimmunol.2200467.

42. Lewis, B.P., Burge, C.B., and Bartel, D.P. (2005). Conserved Seed Pairing , Often Flanked by Adenosines , Indicates that Thousands of Human Genes are MicroRNA Targets We predict regulatory targets of vertebrate microRNAs. Cell.*120*, 15-20. 10.1016/j.cell.2004.12.035.

43. Gebert, L.F.R., and MacRae, I.J. (2019). Regulation of microRNA function in animals. Nat. Rev. Mol. Cell Biol. *20*, 21-37. 10.1038/s41580-018-0045-7.

44. Richter, J.D., and Sonenberg, N. (2005). Regulation of cap-dependent translation by eIF4E inhibitory proteins. Nature 433, 477-480. 10.1038/nature03205.

45. Matsuo, H., Li, H., McGuire, A.M., Fletcher, C.M., Gingras, A.-C., Sonenberg, N., and Wagner, G. (1997). Structure of translation factor eIF4E bound to m7GDP and interaction with 4E-binding protein. Nat. Struct. Biol. *4*. 10.1038/nsb0997-717.

46. Jarjour, N.N., Schwarzkopf, E.A., Bradstreet, T.R., Shchukina, I., Lin, C.C., Huang, S.C.C., Lai, C.W., Cook, M.E., Taneja, R., Stappenbeck, T.S., et al. (2019). Bhlhe40 mediates tissue-specific control of macrophage proliferation in homeostasis and type 2 immunity. Nat. Immunol. *20*, 687–700. 10.1038/s41590-019-0382-5.

47. Colina, R., Costa-Mattioli, M., Dowling, R.J.O., Jaramillo, M., Tai, L.H., Breitbach, C.J., Martineau, Y., Larsson, O., Rong, L., Svitkin, Y. V., et al. (2008). Translational control of the innate immune response through IRF-7. Nature *452*, 323–328. 10.1038/nature06730.

48. Sanders, J.W., Fuhrer, G.S., Johnson, M.D., and Riddle, M.S. (2008). The epidemiological transition: The current status of infectious diseases in the developed world versus the developing world. Sci. Prog. *91*, 1–38. 10.3184/003685008X284628.

49. Cao, Z., Zheng, X., Yang, H., Li, S., Xu, F., Yang, X., and Wang, Y. (2020). Association of obesity status and metabolic syndrome with site-specific cancers: a population-based cohort study. Br. J. Cancer *123*, 1336–1344. 10.1038/s41416-

020-1012-6.

50. A.C., S., E.M., P., L.A., M., and J.A., S. (2015). Cardiometabolic risks and severity of obesity in children and young adults. N. Engl. J. Med. *373*, 1307–1317. 10.1056/NEJMoa1502821.

51. Nazari-Jahantigh, M., Wei, Y., Noels, H., Akhtar, S., Zhou, Z., Koenen, R.R., Heyll, K., Gremse, F., Kiessling, F., Grommes, J., et al. (2012). MicroRNA-155 promotes atherosclerosis by repressing Bcl6 in macrophages. J. Clin. Invest. *122*, 4190–4202. 10.1172/JCI61716.

52. Ying, W., Tseng, A., Chang, R.C.A., Morin, A., Brehm, T., Triff, K., Nair, V., Zhuang, G., Song, H., Kanameni, S., et al. (2015). MicroRNA-223 is a crucial mediator of PPARγ-regulated alternative macrophage activation. J. Clin. Invest. *125*, 4149-4159. 10.1172/JCI81656.

53. Runtsch, M.C., Nelson, M.C., Lee, S.H., Voth, W., Alexander, M., Hu, R., Wallace, J., Petersen, C., Panic, V., Villanueva, C.J., et al. (2019). Anti-inflammatory microRNA-146a protects mice from diet-induced metabolic disease. PLoS Genet. *15*, e1007970. 10.1371/journal.pgen.1007970.

54. Ouimet, M., Ediriweera, H.N., Mahesh Gundra, U., Sheedy, F.J., Ramkhelawon, B., Hutchison, S.B., Rinehold, K., Van Solingen, C., Fullerton, M.D., Cecchini, K., et al. (2015). MicroRNA-33-dependent regulation of macrophage metabolism directs immune cell polarization in atherosclerosis. J. Clin. Invest. *125*, 4334–4348. 10.1172/JCI81676.

55. Rayner, K.J., Suárez, Y., Dávalos, A., Parathath, S., Fitzgerald, M.L., Tamehiro, N., Fisher, E.A., Moore, K.J., and Fernández-Hernando, C. (2010). MiR-33 contributes to the regulation of cholesterol homeostasis. Science *328*, 1570–1573. 10.1126/science.1189862.

56. Jiang, Y.H., Man, Y.Y., Liu, Y., Yin, C.J., Li, J.L., Shi, H.C., Zhao, H., and Zhao, S.G. (2021). Loss of mir-23b/27b/24-1 cluster impairs glucose tolerance via glycolysis pathway in mice. Int. J. Mol. Sci. *22*, 1–13. 10.3390/ijms22020550.

57. Carlyle, W.C., Mcclain, J.B., Tzafriri, A.R., Bailey, L., Brett, G., Markham, P.M., Stanley, J.R.L., Edelman, E.R., Sciences, C.B., Technologies, E., et al. (2015). TREM2 maintains microglial metabolic fitness in Alzheimer's disease. Cell *162*, 561–567.

58. Grasset, M.-F., Gobert-Gosse, S., Mouchiroud, G., and Bourette, R.P. (2010). Macrophage differentiation of myeloid progenitor cells in response to M-CSF is regulated by the dual-specificity phosphatase DUSP5. J. Leukoc. Biol. *87*, 127–135. 10.1189/jlb.0309151.

59. Lee, J.H., Budanov, A. V., Talukdar, S., Park, E.J., Park, H.L., Park, H.W., Bandyopadhyay, G., Li, N., Aghajan, M., Jang, I., et al. (2012). Maintenance of metabolic homeostasis by Sestrin2 and Sestrin3. Cell Metab. *16*, 311–321. 10.1016/j.cmet.2012.08.004.

60. Bayle, J., Letard, S., Frank, R., Dubreuil, P., and De Sepulveda, P. (2004). Suppressor of Cytokine Signaling 6 Associates with KIT and Regulates KIT Receptor Signaling. J. Biol. Chem. *279*, 12249–12259. 10.1074/jbc.M313381200.

61. Hanafusa, H., Torii, S., Yasunaga, T., and Nishida, E. (2002). Sprouty1 and Sprouty2 provide a control mechanism for the Ras/MAPK signalling pathway. Nat. Cell Biol. *4*, 850–858. 10.1038/ncb867.

62. Kim, E., Ilagan, J.O., Liang, Y., Daubner, G.M., Stanley, C., Ramakrishnan, A., Li, Y., Chung, Y.R., Micol, J., Murphy, M., et al. (2010). Germline mutations in TMEM127 confer susceptibility to pheochromocytoma. Nat. Genet. *42*, 229–233. 10.1038/ng.533.

63. Morgantini, C., Jager, J., Li, X., Levi, L., Azzimato, V., Sulen, A., Barreby, E., Xu, C., Tencerova, M., Näslund, E., et al. (2019). Liver macrophages regulate systemic metabolism through non-inflammatory factors. Nat. Metab. *1*, 445-459. 10.1038/s42255-019-0044-9.

64. Tencerova, M., Aouadi, M., Vangala, P., Nicoloro, S.M., Yawe, J.C., Cohen, J.L., Shen, Y., Garcia-Menendez, L., Pedersen, D.J., Gallagher-Dorval, K., et al. (2015). Activated Kupffer cells inhibit insulin sensitivity in obese mice. FASEB J. *29*, 2959-2969. 10.1096/fj.15-270496.

65. Cochain, C., Vafadarnejad, E., Arampatzi, P., Pelisek, J., Winkels, H., Ley, K., Wolf, D., Saliba, A.E., and Zernecke, A. (2018). Single-cell RNA-seq reveals the transcriptional landscape and heterogeneity of aortic macrophages in murine atherosclerosis. Circ. Res. *122*, 1661–1674. 10.1161/CIRCRESAHA.117.312509.

66. Willemsen, L., and de Winther, M.P.J. (2020). Macrophage subsets in atherosclerosis as defined by single-cell technologies. J. Pathol. *250*, 705–714. 10.1002/path.5392.

67. Song, Q., Hawkins, G.A., Wudel, L., Chou, P.C., Forbes, E., Pullikuth, A.K., Liu, L., Jin, G., Craddock, L., Topaloglu, U., et al. (2019). Dissecting intratumoral myeloid cell plasticity by single cell RNA-seq. Cancer Med. *8*, 3072–3085. 10.1002/cam4.2113.

68. M, M., E, E., W, V., J, H., Y, C., J, L., S, B., M, B., AS, O., B, R., et al. (2020). TREM2 Modulation Remodels the Tumor Myeloid Landscape Enhancing Anti-PD-1 Immunotherapy. Cell *182*, 886-900.e17.

69. Y., W., M., C., K., M., J.D., U., K.L., Y., M.L., R., S., G., G.M., K., S., S., B.H., Z., et al. (2015). TREM2 lipid sensing sustains the microglial response in an Alzheimer's disease model. Cell *160*, 1061–1071.

CHAPTER 3

MYELOID-SPECIFIC EXPRESSION OF THE *MIR-23-27-24* CLUSTERS PROMOTES LIPID-ASSOCIATED MACROPHAGE PROLIFERATION IN OBESE ADIPOSE TISSUE

Adapted from:

Neil T. Sprenkle, Nathan C. Winn, Kaitlyn E Bunn, Yang Zhao, Deborah J. Park, Brenna G Giese, John J. Karijolich, K Mark Ansel, C. Henrique Serezani, Alyssa H. Hasty, & Heather H. Pua. 2023. Cell Rep. 42.

3.1 General Chapter Overview

This chapter focuses on the cellular mechanism by which myeloid-specific expression of the *miR-23-27-24* clusters supports lipid-associated macrophage (LAM) accumulation in obese adipose tissue. Monocyte recruitment, proliferation, prolonged survival, and reduced egress have all been linked to inflammatory ATM accrual and are implicated in promoting obesity-associated abnormalities. Immunophenotyping of blood and visceral white adipose tissue (WAT) of male mice showed no significant differences in the number of blood or tissue monocytes, respectively, arguing against an impairment in monocyte production or infiltration. Staining for the proliferation marker Ki67 in cells from the stromal vascular fraction (SVF) of WAT from mice containing a myeloid-specific knockout of the clusters (MyelΔ) revealed a selective reduction in proliferative $Ki67^{+}$ $CD9^{+}$

LAMs relative to control. Consistently, defects in proliferation as assayed through Ki67 staining and BrdU labeling were also observed in obese-like metabolically activated bone marrow-derived macrophages (MMe BMDMs) deficient of the *miR-23-27-24* clusters in culture. Loss of the *miR-23-27-24* clusters did not influence cell death in $CD9^{+}$ LAMs or MMe BMDMs, suggesting that defective proliferation was a driver reducing LAM counts. To elucidate which products of the clusters promote macrophage proliferation, we selectively depleted individual members of the clusters using locked nucleic acid inhibitors in MMe BMDMs. Here, we discovered that depletion of miR-23 or miR-24 impaired macrophage proliferation during metabolic activation. Altogether, data from these studies indicates the expression of the *miR-23-27-24* clusters, specifically miR-23 and miR-24, promotes LAM proliferation in obese adipose tissue and that this event is associated with improved metabolic function.

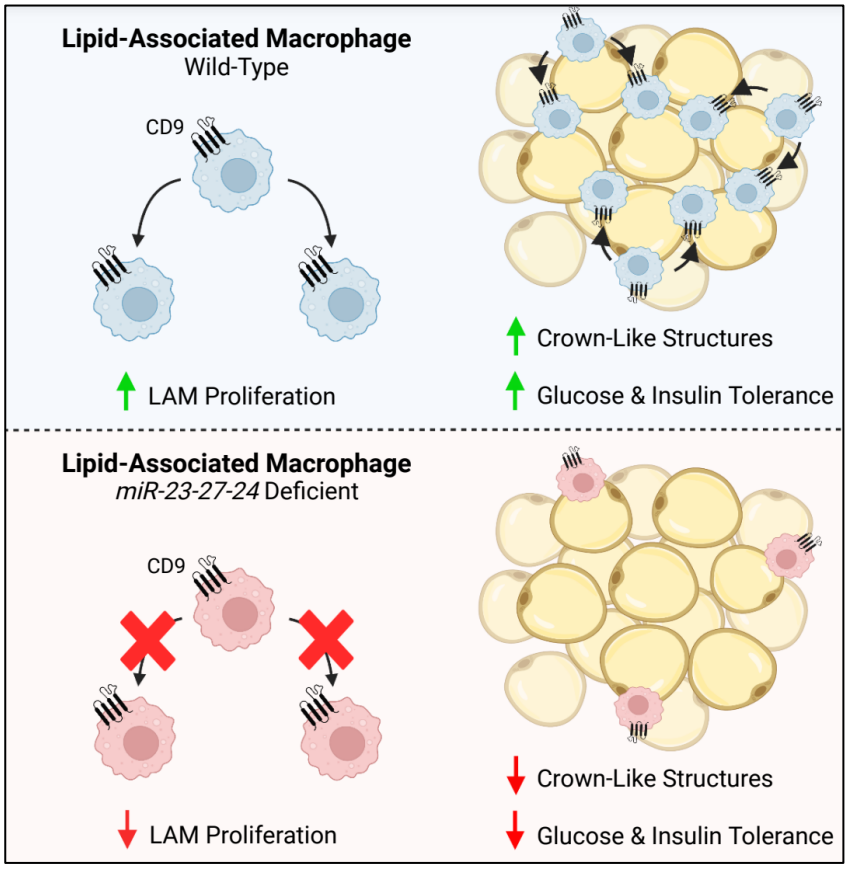

Figure 3.1. Proposed model of Chapter 3: Expression of the miR-23-27-24 clusters promotes LAM proliferation in obese adipose tissue.

3.2. Introduction

Adipose tissue macrophages (ATMs) represent critical regulators of obesity-induced metabolic outcomes. Historically, temporal accumulation of inflammatory macrophages in obese visceral adipose tissue was shown to aggravate systemic defects in glucose regulation[1–3]. Mechanisms proposed to underscore pathological inflammatory ATM accrual in murine obesity include monocyte recruitment[4], enhanced ATM

proliferation in tissue[2,3], prolonged inflammatory ATM survival[6], and impaired ATM egress from inflamed tissue[7]. However, recent investigation employing single cell transcriptomics uncovered a conserved population of macrophage called $CD9^{+}Trem2^{+}$ lipid-associated macrophages (LAMs) present in crown-like structures in obese visceral adipose tissue[8,9]. Contrary to paradigm, recent evidence indicates that the lipid-handling and phagocytic functions of LAMs confers protection against systemic glucose intolerance by supporting tissue-level lipid homeostasis, though the molecular drivers of this program remain controversial[9,10]. Lineage tracing studies indicate LAMs are monocytic in origin and the temporal accrual of LAMs in obese adipose tissue over the course of high-fat diet (HFD) feeding is a product of monocyte recruitment into inflamed tissue late in obesity[9]. Nevertheless, complementary mechanisms driving LAM accrual in obese adipose tissue and how they overlap with those that promote pathological ATM accumulation remains unknown.

Findings from Chapter 2 demonstrated that myeloid-specific expression of the *miR-23-27-24* clusters confers protection against obesity-induced glucose and insulin intolerance in male mice (**Chapter 2**). Contrary to our initial hypothesis, the worsened metabolic phenotype observed in MyelΔ mice on HFD was not associated with augmented adipose tissue inflammation and inflammatory ATM accumulation (**Chapter 2**). Instead, we found a selective reduction in total numbers of $CD9^{+}$ LAMs in obese MyelΔ adipose tissue (**Chapter 2**). Due to the reported protective functions of $CD9^{+}Trem2^{+}$ LAMs, we linked the loss of this subpopulation of macrophage to worsened glucose regulation observed in obese male MyelΔ mice. The focus of the following studies in

Chapter 3 will interrogate the cellular mechanism underlying how myeloid-specific deletion of the *miR-23-27-24* clusters impairs LAM accrual in obese adipose tissue.

3.3. Materials & Methods

Animals and Diets

All animal studies were performed after obtaining approval from the Vanderbilt Institutional Animal Care and Use Committee. C57BL/6 ES cells were targeted using constructs generated as a resource for the conditional deletion of miRNA clusters as described[11] to produce chimeric mice with a conditionally mutant allele of the miRNA cluster containing miR-23a, miR-27a, and miR-24-2 (the *Mirc11* cluster). These chimeras were crossed to *Rosa26-Flp* mice (*Gt(ROSA)26Sortm1(FLP1)Dym*; 009086, the Jackson Laboratory) to delete the selection cassette. Mice previously generated with a conditionally mutant allele containing miR-23b, miR-27b and miR-24-1 (the *Mirc22* cluster)[12] were backcrossed for 10 generations to C57BL/6J mice (000664, the Jackson Laboratory). These two lines were intercrossed, and the progeny crossed to *Lyz2*^{Cre} mice (*B6.129P2-Lyz2*$^{tm1(cre)Ifo}$*/J*; 004781, the Jackson Laboratory) to generate mice with myeloid cells lacking expression of *Mirc11* and *Mirc22* clusters in myeloid cells (MyelΔ). For the diet-induced obesity model, 7–9-week-old male or female *Mirc11*$^{fl/fl}$*Mirc22*$^{fl/fl}$ and *Mirc11*$^{fl/fl}$*Mirc22*$^{fl/fl}$*Lyz2*^{Cre} mice were fed a high-fat diet (HFD, 60% kcal fat; Research Diets) for 20+ weeks. Body weight and food intake were recorded weekly. Body composition measurements, collection of fasting blood samples, and intraperitoneal

glucose and insulin tolerance tests were performed before or during HFD feeding. All other analyses were performed after the mice were euthanized.

Bone Marrow-Derived Macrophage Cultures

Primary bone marrow-derived macrophages (BMDMs) were prepared by culturing bone marrow of mice in RPMI-1640 media supplemented with 20% L929-conditioned medium, 10% FBS, gentamicin, glutamine, HEPES, non-essential amino acids, and penicillin-streptomycin for 7+ days. Media was changed on Day 1, then every three days of culture. To plate for experiments, BMDMs were detached from the flask using cold PBS containing 0.5 - 5 mM EDTA and plated into tissue culture plates at a concentration of 1 x 10^6 cells/mL.

To metabolically activate BMDMs, BMDMs were cultured in supplemented DMEM media containing 25 mM glucose, 10 nM insulin (Novolin), and 150-250 μM palmitic acid (MP Biomedicals) conjugated to BSA (Research Products International) for 24 h – 48 h. BMDMs in the control group were cultured in supplemented RPMI-1640 medium (11 mM glucose) containing BSA alone. Conditions were adapted from Kratz et al.[13].

Caspase 3 Activity Assay

BMDMs were plated into tissue culture plates (1 x 10^6 cells/mL) and allowed to rest overnight. Media was replaced the next day, and cells were subjected to metabolic activation for ~24h. Afterward, cleaved caspase 3 assay was carried out using EnzChek Caspase 3 Assay Kit (Molecular Probes) according to the manufacturer's instructions.

Locked Nucleic Acid Treatments

BMDMs were plated into tissue culture plates (1 x 10^6 cells/mL) and allowed to rest overnight. Media was replaced the next day, and cells were treated with 50 nM of the indicated locked nucleic acid inhibitor (miRCURY LNA miRNA Power Inhibitors). Cells incubated with inhibitors for 24h, then subjected to metabolic activation.

Luminex Analysis

Serum samples from mice fed an HFD were sent to Vanderbilt Hormone Assay & Analytical Services Core for Luminex analysis. Analytes examined in this study were chosen from their "Mouse Metabolic Hormone Panel".

Palmitic Acid-BSA Preparation

Palmitic acid (MP Biomedical) was dissolved in Molecular Biology Grade Ethanol (Fisher BioReagents) by alternating between heating at 70^{o}C and vortexing to produce a 1M palmitic acid solution. Immediately afterward, the dissolved palmitic acid was conjugated to BSA by gently mixing and heating (70^{o}C) 40 uL of the 1 M palmitic acid solution with 960 uL of a 10% BSA in HEPES (Gibco) solution for 20 – 30 min, creating a 40 mM palmitic acid-BSA solution. Before cell culture treatment, the 40 mM palmitic acid-BSA solution was shaken at 50^{o}C for 20 min prior to dispensing into a tube containing supplemented DMEM media which was then incubated with cells. 10% BSA in HEPES solution was used as the vehicle control.

Stromal Vascular Fraction Isolation and Flow Cytometric Analysis

The stromal vascular fraction (SVF) from perigonadal fat pads were isolated following collagenase digestion and differential centrifugation as previously described[14]. Adipose tissue (AT) myeloid cells were characterized via flow cytometry using the following anti-

mouse antibodies [BioLegend, eBioscience, BD Pharmingen, Tonbo]: PE-Cy7 F4/80; FITC Ly6G; PE Siglec F; APC and V450 CD9; V450 CD9; APC CD64; FITC and PerCP-Cy5.5 CD64; FITC CD11c; PE CD163; PE-Cy7 CD206; BV421 CCR2; FITC Ly6C; PE-Cy7 TCRβ. Dead cells were identified with e780 viability dye (ThermoFisher).

For Ki67 staining, cells were first stained with surface antigen fluorescent antibodies, then were fixed and permeabilized using the Foxp3 / Transcription Factor Staining Buffer Set (ThermoFisher). Afterward, intracellular staining was performed using either PE anti-Ki67 or PE IgG1, κ isotype control from the PE Mouse Anti-Ki67 Set (BD Biosciences) according to the manufacturer's instructions. % $Ki67^+$ cells were calculated by subtracting % PE^+ cells stained with isotype control from % PE^+ cells stained with anti-Ki67 [% PE^+ (anti-Ki67) - % PE^+ (isotype)]. For Annexin V and 7-AAD staining, SVF cells were stained using reagents from the FITC Annexin V Apoptosis Detection Kit with 7-AAD (TONBO) as described by manufacturers. For BrdU staining, BMDMs were metabolically activated for 24 hours then labeled with 10 μM BrdU overnight with the eBioscience BrdU Staining Kit (Invitrogen). Afterward, cells were harvested, stained with e780 viability dye, fixed, subjected to DNase I digestion, then intracellularly stained with APC anti-BrdU as described by manufacturers. All flow cytometry was performed on an 8-color FACSCANTO II flow cytometer (BD Biosciences) provided by the Division of Molecular Pathogenesis. FlowJo was used to process data.

Statistical Analyses

Statistics were done on experiments with 3+ biological replicates or independent experiments as outlined in figure legends. Analyses were performed using R (www.r-

project.org) and GraphPad Prism8 (GraphPad Software, Version 8.02). *P* values of less than 0.05 were considered significant.

3.4. Results

The miR-23-27-24 Clusters Support LAM Proliferation in Obesity

Since LAMs may provide a protective adaptation in expanding adipose tissue, we investigated the cellular mechanisms by which loss of expression of the *miR-23-27-24* clusters in myeloid cells decreased LAM accumulation. LAMs are derived from monocytes[9], thus we began by comparing numbers of circulating and eWAT-resident monocytes between fl/fl and MyelΔ mice after HFD feeding. We did not detect any differences in blood monocytes by complete blood count (**Figure 3.2A**), arguing against a defect in the production or survival of monocytes in circulation. Total SSC-A^{lo}Ly6C^{+} monocytes within eWAT were also equivalent in fl/fl and MyelΔ mice (**Figure 3.2B**). We then characterized monocytes and ATMs based on the receptor for CCL2, a chemotactic factor important for monocyte infiltration into obese eWAT[4]. Although we did not find differences in CCR2^{+} monocytes in obese mice among both genotypes (**Figure 3.2B**), we found significant reductions in both CCR2^{-} and CCR2^{+} ATMs in MyelΔ eWAT compared to control (**Figure 3.2C**). These findings indicate that loss of the *miR-23-27-24*

clusters in myeloid cells diminishes absolute ATM numbers in this visceral fat depot through a mechanism downstream of monocyte recruitment.

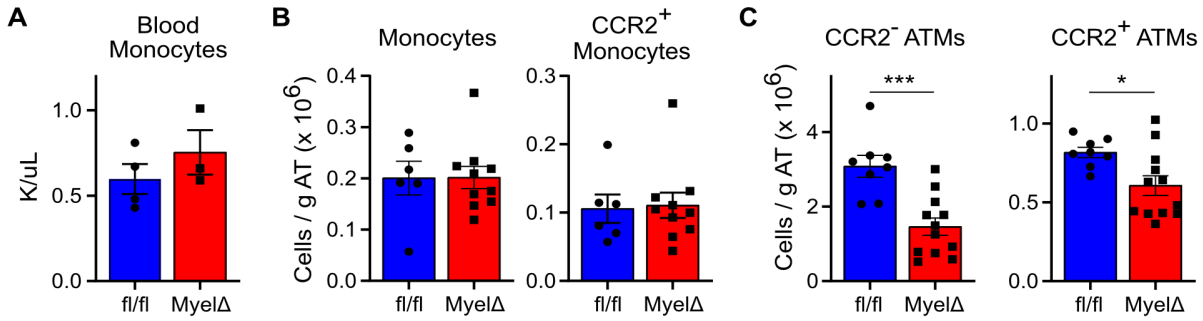

Figure 3.2. The *miR-23-27-24* Clusters Do Not Alter Blood or Adipose Tissue Monocyte Numbers. (**A**) Circulating monocyte numbers, (**B**) total monocytes and CCR2$^+$ monocytes in eWAT, or (**C**) CCR2$^-$ or CCR2$^+$ ATMs were compared between obese fl/fl and MyelΔ mice (two-tailed t-test. (**A-C**) one male mouse after HFD feeding. ±S.E.M. *, p≤0.05; ***, p<0.001.

Because ATM proliferation represents a key event contributing to ATM accumulation in obese eWAT[5], we next investigated if loss of the clusters in myeloid cells impaired LAM proliferation by staining for Ki67, a nuclear antigen expressed by cells undergoing proliferation. Consistent with a proliferation defect, we observed a significant reduction in Ki67$^+$ CD9$^+$ LAMs, but not Ki67$^+$ CD9$^-$ ATMs, in MyelΔ eWAT (**Figure 3.3A-C**). This included both an ~50% reduction in the total number of Ki67$^+$ cells per gram of adipose tissue (**Figure 3.3B**), as well as a relative reduction in the percent of Ki67$^+$ CD9$^+$ LAMs among CD9$^+$ LAMs in MyelΔ compared to fl/fl controls (**Figure 3.3C**). Furthermore, MyelΔ BMDMs cultured under metabolically activating conditions (MMe BMDMs) to promote an obese-like ATM phenotype[13] exhibited a significant defect in proliferation compared to fl/fl MMe BMDMs (**Figure 3.3D-E**). To determine which miRNAs of the cluster were capable of regulating proliferation, we treated wild-type (WT) MMe BMDMs

with locked nucleic acids (LNAs) to selectively deplete miR-23, miR-24, or miR-27. We found that acute inhibition of miR-23 or miR-24, but not miR-27, expression in WT BMDMs was sufficient to reduce the number of Ki67$^+$ cells in MMe conditions (**Figure 3.3F**). These findings indicate that expression of the *miR-23-27-24* clusters supports LAM proliferation in obese eWAT and in MMe macrophages.

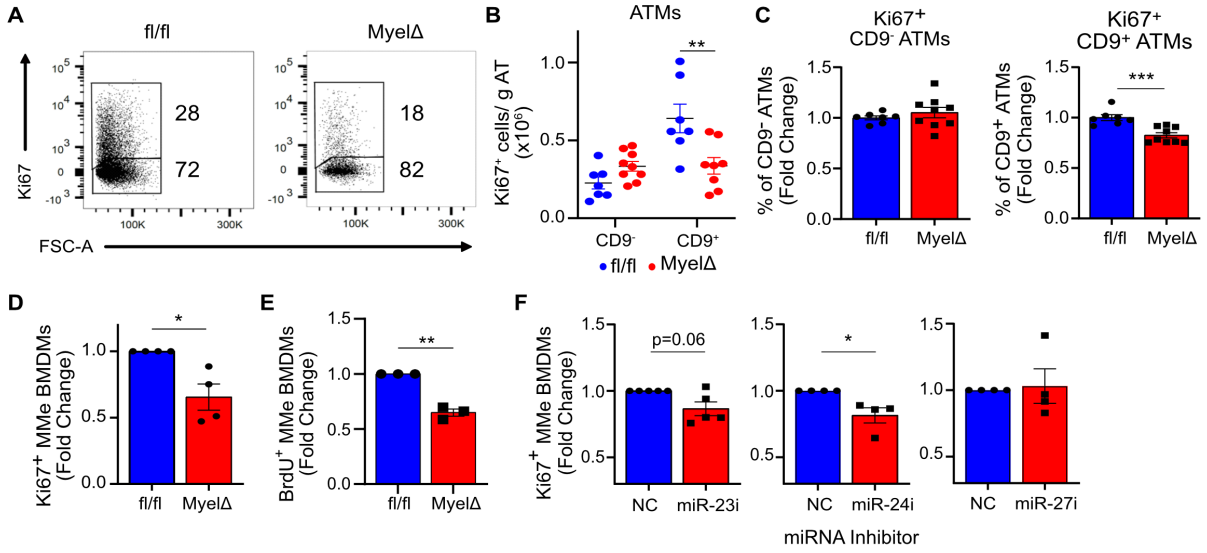

Figure 3.3. The *miR-23-27-24* Clusters Promote LAM Proliferation. (**A**) Representative flow panel of Ki67 proliferation index of CD9$^+$ ATMs from obese fl/fl and MyelΔ mice with (**B**) quantitation of number of Ki67$^+$ ATMs (two-way ANOVA with Sidák's multiple comparison test) and (**C**) percentage of proliferating cells (one sample t-test). (**D**) Ki67 and (**E**) BrdU staining of BMDM from fl/fl and MyelΔ mice cultured under metabolically activating conditions (MMe) (one sample t-test). (**F**) Relative changes in Ki67$^+$ wild type MMe BMDMs treated with the indicated miRNA locked nucleic acid (LNA) inhibitor (one sample t-test). Each dot represents (**A-C**) one male mouse after HFD feeding or (**D-F**) one biological replicate. ±S.E.M. *, p≤0.05; **, p<0.01.

Finally, we performed assays to determine whether augmented cell death contributed to reduced LAM accumulation in obese MyelΔ eWAT. We detected no differences in apoptotic (AnnexinV$^+$7-AAD$^-$) or late apoptotic/necrotic (AnnexinV$^+$7-AAD$^+$) LAMs between genotypes (**Figure 3.4A-B**). Furthermore, Caspase-3 activity was similar between fl/fl or MyelΔ BMDMs cultured under MMe conditions (**Figure 3.4C**). These

findings argue against elevated cell death being responsible for the observed defect in LAM numbers. Overall, our data demonstrate that expression of the *miR-23-27-24* clusters supports LAM accrual in obese eWAT by promoting proliferation.

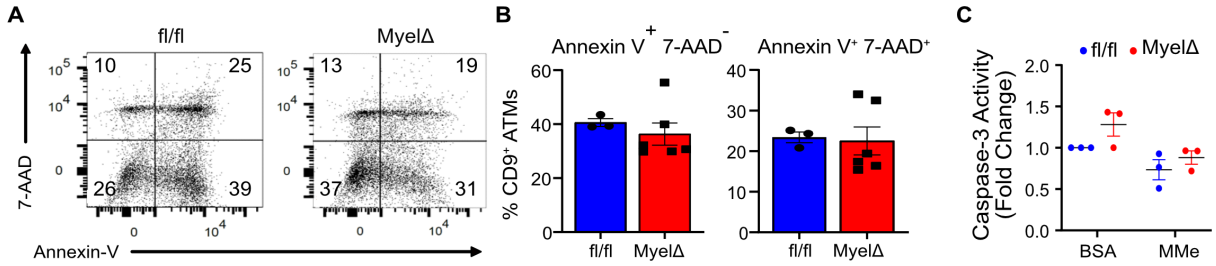

Figure 3.4. The *miR-23-27-24* Clusters Do Not Regulate Cell Death. (**A**) Representative Annexin V and 7-AAD cell death staining gated on CD9$^+$ ATMs in the SVF from obese fl/fl and MyelΔ mice with (**B**) quantitation (two-tailed t-test). (**C**) Caspase 3 activity was quantified in fl/fl and MyelΔ MMe BMDMs (two-way ANOVA with Šídák's multiple comparisons test). Each dot represents (**A**-**B**) one male mouse after HFD feeding or (**C**) one biological replicate. ±S.E.M.

3.5. Discussion

Mechanisms underlying ATM accumulation have been thoroughly investigated over the past two decades. This is due to the potential application of therapeutics to limit entry or buildup of pathological ATMs that drives adipose tissue dysfunction[3,15,16]. Monocyte recruitment, proliferation, prolonged survival, and reduced egress have all been linked to inflammatory ATM accrual and are implicated in promoting obesity-associated abnormalities[3,4,6,17]. Paradoxically, while myeloid-specific deletion of the *miR-23-27-24* clusters disrupted glucose tolerance in male mice on HFD (**Chapter 2**), we observed a selective reduction in total numbers of ATMs and no indication of elevated tissue or systemic inflammation (**Chapter 2**). These findings shifted our attention to the prospect that loss of miRNA products resulted in the reduction of protective LAMs. Immunophenotyping studies uncovered a corresponding impairment in $CD9^+$ LAM accumulation in perigonadal WAT of obese MyelΔ female and male mice (**Chapter 2**), linking the observed changes in the immune cell compartment of adipose tissue to worsened glucose tolerance.

Work in Chapter 3 investigates cellular mechanisms underlying how the *miR-23-27-24* clusters promote LAM accrual in obese adipose tissue. Because LAMs are derived from monocytes[9], we began by comparing numbers of blood and adipose tissue monocytes between control and MyelΔ to determine if *miR-23-27-24* deficiency impaired monocyte production or entry into adipose tissue. Our findings did not uncover any differences in monocyte numbers from either tissue between genotypes (**Figure 3.2**). Together with the observation that counts of both $CCR2^-$ and $CCR2^+$ ATMs were reduced,

we reasoned that faulty monocyte recruitment did not drive the reduction of LAMs in MyelΔ obese adipose tissue and that an event downstream of monocyte infiltration may be involved.

Because we found no evidence to implicate differential regulation monocyte migration, we turned our attention to investigating mechanism that could impact macrophage accretion in obese adipose tissue. As discussed, miRNAs represent key governors of macrophage function by negatively regulating the expression of tens to hundreds of target transcripts at the post-transcriptional level[18]. Products from both *miR-23-27-24* clusters have been reported to directly target genes involved in cell proliferation and cell death in other cellular and disease contexts[19–24]. Since local proliferation and prolonged survival of ATMs contribute to pathological ATM accrual[3,6], we investigated if the *miR-23-27-24* clusters impaired one or both of these to reduce LAM accumulation in obese adipose tissue.

To this end, we found that loss of the clusters selectively compromised CD9+ LAM, but not CD9- ATM, proliferation in a visceral fat depot (**Figure 3.3A-C**) while no difference in apoptotic or late-apoptotic/necrotic LAMs were observed (**Figure 3.4A-B**). Use of a previously established cell culture system used to induce an obese-like phenotype in cultured BMDMs[13] supported our *in vivo* observations, as metabolically activated *miR-23-27-24*-deficient BMDMs exhibited a similar defect in proliferation (**Figure 3.3D-E**) with no accompanying changes in apoptosis (**Figure 3.4C**). Experiments depleting individual members of the *miR-23-27-24* clusters in MMe BMDMs implicate miR-23 and miR-24 as the critical determinants of the clusters that promote proliferation of cultured macrophages (**Figure 3.3F**). Altogether, our findings indicate that impaired proliferation of LAMs

represents the key cellular mechanism underlying their reduced presence in visceral adipose tissue of MyelΔ mice on HFD for 20 wks.

While we employed multiple studies to interrogate the cellular mechanism regulating LAM accrual, the contribution of enhanced LAM egress from adipose tissue was not thoroughly explored in our investigation. ATM retention constitutes a major contributor to ATM accumulation in obese adipose tissue and is regulated by activation of cell-autonomous netrin-1 signaling[17,25]. Netrin-1 is a secreted laminin-like protein that directs both chemoattractive and -repulsive signaling to control leukocyte trafficking. Chemorepulsion in myeloid cells is mediated by netrin-1 engaging UNC5-family receptors and/or ADORA2B[25–29]. Regarding ATMs, upregulation of netrin-1 production by ATMs in obesity disrupts macrophage egress from inflamed WAT in a feed-forward loop by binding to UNC5B residing on ATMs, consequently impairing responses to chemokines directing egress from tissues (e.g. CCL19) to discourage inflammatory resolution[7,17].

Though our study does not extensively investigate the contribution of netrin-1 signaling in LAM retention, our preliminary gene set enrichment analysis of our RNA sequencing data comparing transcriptomic differences between F4/80-selected fl/fl and MyelΔ ATMs reveals an enrichment of genes involved in the netrin-1/UNC5B signaling pathway within differentially upregulated transcripts in MyelΔ ATMs (**ADDENDIX D.1A**). Furthermore, there was an increase in mRNA levels of notable mediators (i.e. *Adroa2b*, *Ntn1*, *Ntn4, Unc5a, and Unc5b* mRNA*)* involved in the netrin-1 signaling pathway in MyelΔ obese ATMs (**APPENDIX D.1B**). These findings argue against the contribution of reduced netrin-1 signaling in impairing LAM accretion in obese MyelΔ eWAT. Nevertheless, additional chemotactic, monocyte/macrophage-tracing, and cell signaling experiments

will be required to define the role of differential ATM retention over the course of obesity *in vivo*.

Importantly, findings from this study provide mechanistic insights into molecular entities driving the accrual of this novel subset of ATM. LAM signatures are observed 12 weeks after the start of HFD feeding and increase in distribution as obesity persists[9]. Our data supports a model where expression of the clusters promotes proliferation of differentiated LAMs once in tissue. Because our studies utilize a murine system modeling chronic obesity, future studies investigating the spatiotemporal kinetics of this regulation on ATM behavior at different stages of obesity and its relevance to the regulation on systemic and tissue-specific metabolic function are required to provide a detailed illustration into the role of the clusters in immune cell reprogramming of adipose tissue. Furthermore, whether regulation imposed by the clusters is unique to LAMs or also contributes to pathological ATM accumulation earlier in obesity represents an outstanding question, where the answer could lead to the identification molecular nodes that could selectively be targeted to promote beneficial macrophage populations in obese adipose tissue.

3.6. Conclusions

Findings from Chapter 3 indicate that myeloid-specific expression of the *miR-23-27-24* clusters supports $CD9^+$ LAM proliferation in obese adipose tissue after 20 weeks on HFD, with no accompanying influence on blood monocyte production, adipose tissue

monocyte counts, or LAM apoptosis/necrosis. Furthermore, we demonstrate that miR-23 and miR-24 are the critical regulators of macrophage proliferation during metabolic activation. Follow up studies will be required to elucidate downstream target genes and gene networks regulated by miR-23 and miR-24 to promote macrophage proliferation.

3.7. References

1. Lumeng, C.N., Bodzin, J.L., and Saltiel, A.R. (2007). Obesity induces a phenotypic switch in adipose tissue macrophage polarization. J. Clin. Invest. 10.1172/JCI29881.
2. Zheng, C., Yang, Q., Cao, J., Xie, N., Liu, K., Shou, P., Qian, F., Wang, Y., and Shi, Y. (2016). Local proliferation initiates macrophage accumulation in adipose tissue during obesity. Cell Death Dis. 10.1038/cddis.2016.54.
3. Amano, S.U., Cohen, J.L., Vangala, P., Tencerova, M., Nicoloro, S.M., Yawe, J.C., Shen, Y., Czech, M.P., and Aouadi, M. (2014). Local proliferation of macrophages contributes to obesity-associated adipose tissue inflammation. Cell Metab. 10.1016/j.cmet.2013.11.017.
4. Weisberg, S.P., Hunter, D., Huber, R., Lemieux, J., Slaymaker, S., Vaddi, K., Charo, I., Leibel, R.L., and Ferrante, A.W. (2006). CCR2 modulates inflammatory and metabolic effects of high-fat feeding. J. Clin. Invest. 10.1172/JCI24335.
5. Amano, S.U., Cohen, J.L., Vangala, P., Tencerova, M., Nicoloro, S.M., Yawe, J.C., Shen, Y., Czech, M.P., and Aouadi, M. (2014). Local proliferation of macrophages contributes to obesity-associated adipose tissue inflammation. Cell Metab. *19*, 162–171. 10.1016/j.cmet.2013.11.017.
6. Hill, A.A., Anderson-Baucum, E.K., Kennedy, A.J., Webb, C.D., Yull, F.E., and Hasty, A.H. (2015). Activation of NF-κB drives the enhanced survival of adipose tissue macrophages in an obesogenic environment. Mol. Metab. 10.1016/j.molmet.2015.07.005.
7. Sharma, M., Schlegel, M., Brown, E.J., Sansbury, B.E., Weinstock, A., Afonso, M.S., Corr, E.M., van Solingen, C., Shanley, L.C., Peled, D., et al. (2019). Netrin-1 Alters Adipose Tissue Macrophage Fate and Function in Obesity. Immunometabolism *1*. 10.20900/immunometab20190010.
8. Hill, D.A., Lim, H.W., Kim, Y.H., Ho, W.Y., Foong, Y.H., Nelson, V.L., Nguyen, H.C.B., Chegireddy, K., Kim, J., Habertheuer, A., et al. (2018). Distinct macrophage

populations direct inflammatory versus physiological changes in adipose tissue. Proc. Natl. Acad. Sci. U. S. A. *115*, E5096–E5105. 10.1073/pnas.1802611115.

9. Jaitin, D.A., Adlung, L., Thaiss, C.A., Weiner, A., Li, B., Descamps, H., Lundgren, P., Bleriot, C., Liu, Z., Deczkowska, A., et al. (2019). Lipid-Associated Macrophages Control Metabolic Homeostasis in a Trem2-Dependent Manner. Cell. 10.1016/j.cell.2019.05.054.

10. Sharif, O., Brunner, J.S., Korosec, A., Martins, R., Jais, A., Snijder, B., Vogel, A., Caldera, M., Hladik, A., Lakovits, K., et al. (2021). Beneficial Metabolic Effects of TREM2 in Obesity Are Uncoupled From Its Expression on Macrophages. Diabetes *70*, 2042–2057. 10.2337/DB20-0572.

11. Park, C.Y., Jeker, L.T., Carver-Moore, K., Oh, A., Liu, H.J., Cameron, R., Richards, H., Li, Z., Adler, D., Yoshinaga, Y., et al. (2012). A Resource for the Conditional Ablation of microRNAs in the Mouse. Cell Rep. *1*, 385–391. 10.1016/j.celrep.2012.02.008.

12. Pua, H.H., Steiner, D.F., Patel, S., Gonzalez, J.R., Ortiz-Carpena, J.F., Kageyama, R., Chiou, N.T., Gallman, A., de Kouchkovsky, D., Jeker, L.T., et al. (2016). MicroRNAs 24 and 27 Suppress Allergic Inflammation and Target a Network of Regulators of T Helper 2 Cell-Associated Cytokine Production. Immunity *44*, 821–832. 10.1016/j.immuni.2016.01.003.

13. Kratz, M., Coats, B.R., Hisert, K.B., Hagman, D., Mutskov, V., Peris, E., Schoenfelt, K.Q., Kuzma, J.N., Larson, I., Billing, P.S., et al. (2014). Metabolic dysfunction drives a mechanistically distinct proinflammatory phenotype in adipose tissue macrophages. Cell Metab. 10.1016/j.cmet.2014.08.010.

14. Orr, J.S., Kennedy, A.J., and Hasty, A.H. (2013). Isolation of Adipose Tissue Immune Cells. J. Vis. Exp. 10.3791/50707.

15. Weisberg, S.P., McCann, D., Desai, M., Rosenbaum, M., Leibel, R.L., and Ferrante, A.W. (2003). Obesity is associated with macrophage accumulation in adipose tissue. J. Clin. Invest. 10.1172/JCI200319246.

16. Kim, J., Chung, K., Choi, C., Beloor, J., Ullah, I., Kim, N., Lee, K.Y., Lee, S.K., and Kumar, P. (2016). Silencing CCR2 in Macrophages Alleviates Adipose Tissue Inflammation and the Associated Metabolic Syndrome in Dietary Obese Mice. Mol. Ther. - Nucleic Acids. 10.1038/mtna.2015.51.

17. Ramkhelawon, B., Hennessy, E.J., Ménager, M., Ray, T.D., Sheedy, F.J., Hutchison, S., Wanschel, A., Oldebeken, S., Geoffrion, M., Spiro, W., et al. (2014). Netrin-1 promotes adipose tissue macrophage retention and insulin resistance in obesity. Nat. Med. *20*, 377–384. 10.1038/nm.3467.

18. Sprenkle, N.T., Serezani, C.H., and Pua, H.H. (2023). MicroRNAs in Macrophages: Regulators of Activation and Function. J. Immunol. *210*, 359–368. 10.4049/jimmunol.2200467.

19. Du, W.W., Fang, L., Li, M., Yang, X., Liang, Y., Peng, C., Qian, W., O'Malley, Y.Q.,

Askeland, R.W., Sugg, S.L., et al. (2013). Microrna mir-24 enhances tumor invasion and metastasis by targeting PTPN9 and PTPRF to promote EGF signaling. J. Cell Sci. *126*, 1440–1453. 10.1242/jcs.118299.

20. Zhu, R., Li, X., and Ma, Y. (2019). miR-23b-3p suppressing PGC1α promotes proliferation through reprogramming metabolism in osteosarcoma. Cell Death Dis. *10*. 10.1038/s41419-019-1614-1.

21. Chhabra, R., Dubey, R., and Saini, N. (2010). Cooperative and individualistic functions of the microRNAs in the miR-23a~27a~24-2 cluster and its implication in human diseases. Mol. Cancer *9*. 10.1186/1476-4598-9-232.

22. Ji, J., Zhang, J., Huang, G., Qian, J., Wang, X., and Mei, S. (2009). Over-expressed microRNA-27a and 27b influence fat accumulation and cell proliferation during rat hepatic stellate cell activation. FEBS Lett. *583*, 759–766. 10.1016/j.febslet.2009.01.034.

23. Lal, A., Navarro, F., Maher, C.A., Maliszewski, L.E., Yan, N., O'Day, E., Chowdhury, D., Dykxhoorn, D.M., Tsai, P., Hofmann, O., et al. (2009). miR-24 Inhibits Cell Proliferation by Targeting E2F2, MYC, and Other Cell-Cycle Genes via Binding to "Seedless" 3′UTR MicroRNA Recognition Elements. Mol. Cell *35*, 610–625. 10.1016/j.molcel.2009.08.020.

24. Chhabra, R., Adlakha, Y.K., Hariharan, M., Scaría, V., and Saini, N. (2009). Upregulation of miR-23a∼27a∼24-2 cluster induces caspase-dependent and -independent apoptosis in human embryonic kidney cells. PLoS One *4*. 10.1371/journal.pone.0005848.

25. Netrin-1 Alters Adipose Tissue Macrophage Fate and Function in Obesity (2019). Immunometabolism. 10.20900/immunometab20190010.

26. Ramkhelawon, B., Hennessy, E.J., Ménager, M., Ray, T.D., Sheedy, F.J., Hutchison, S., Wanschel, A., Oldebeken, S., Geoffrion, M., Spiro, W., et al. (2014). Netrin-1 promotes adipose tissue macrophage retention and insulin resistance in obesity. Nat. Med. 10.1038/nm.3467.

27. Cirulli, V., and Yebra, M. (2007). Netrins: Beyond the brain. Nat. Rev. Mol. Cell Biol. 10.1038/nrm2142.

28. Aherne, C.M., Collins, C.B., Masterson, J.C., Tizzano, M., Boyle, T.A., Westrich, J.A., Parnes, J.A., Furuta, G.T., Rivera-Nieves, J., and Eltzschig, H.K. (2012). Neuronal guidance molecule netrin-1 attenuates inflammatory cell trafficking during acute experimental colitis. Gut. 10.1136/gutjnl-2011-300012.

29. Rosenberger, P., Schwab, J.M., Mirakaj, V., Masekowsky, E., Mager, A., Morote-Garcia, J.C., Unertl, K., and Eltzschig, H.K. (2009). Hypoxia-inducible factor-dependent induction of netrin-1 dampens inflammation caused by hypoxia. Nat. Immunol. 10.1038/ni.1683.

CHAPTER 4

SUPPRESION OF *EIF4EBP2* BY MIR-23 PROMOTES MACROPHAGE PROLIFERATION

Adapted from:

Neil T. Sprenkle, Nathan C. Winn, Kaitlyn E Bunn, Yang Zhao, Deborah J. Park, Brenna G Giese, John J. Karijolich, K Mark Ansel, C. Henrique Serezani, Alyssa H. Hasty, & Heather H. Pua. 2023. Cell Rep. 42.

4.1 General Chapter Overview

This chapter describes a novel microRNA (miRNA)-dependent mechanism promoting lipid-associated macrophage (LAM) proliferation in obese adipose tissue, an event associated with improved glucose regulation in murine obesity (**Figure 4.1**). Leveraging our understanding of miRNA biology, we utilized bulk RNA sequencing to identify 1) differentially regulated transcripts in key biological pathways relative to respective controls and 2) shared candidate target genes for each member of the cluster in *miR-23-27-24*-deficient macrophages from visceral white adipose tissue (WAT) of mice on high-fat diet for 20 wks and cultured metabolically activated bone marrow derived macrophages (MMe BMDMs). Deletion of the *miR-23-27-24* clusters (MyelΔ) resulted in concordant changes in many differentially expressed genes between both cell types. These findings support the use of MMe BMDMs as a model to study *miR-23-27-24*-based

regulation of obese ATM biology in culture. Moreover, candidate target genes identified in obese adipose tissue macrophages (ATMs) were largely upregulated in MyelΔ MMe BMDMs.

Cross-referencing our list of candidate target genes found in obese ATMs to GSEA gene sets harboring genes involved in negatively regulating proliferation, proliferative signaling pathways, or anabolic metabolism led to the identification of 6 candidate target genes whose suppression by the *miR-23-27-24* clusters could promote macrophage proliferation: *Eif4ebp2*, *Dusp5*, *Sesn2*, *Socs6*, *Spry1*, and *Tmem127*. Consistently, mRNA levels of each candidate target gene were elevated in knockout MMe macrophages in culture. A functional siRNA screen against candidate targets using MyelΔ MMe BMDMs determined that only knockdown of the translational inhibitor *Eif4ebp2* enhanced proliferation. Importantly, *Eif4ebp2* knockdown in MyelΔ obese ATMs also augmented proliferation *ex vivo*. *Eif4ebp2* is a predicted target of miR-23 and overexpression of miR-23 reduced *Eif4ebp2* mRNA levels in knockout MMe BMDMs. Consistent with these findings, Argonaute 2 (AGO2) immunoprecipitation assays demonstrated that miR-23 directly interacts with *Eif4ebp2* mRNA during metabolic activation. Overall, our findings indicate that the miR-23-*Eif4ebp2* signaling axis is critical in promoting macrophage proliferation in culture and *ex vivo*.

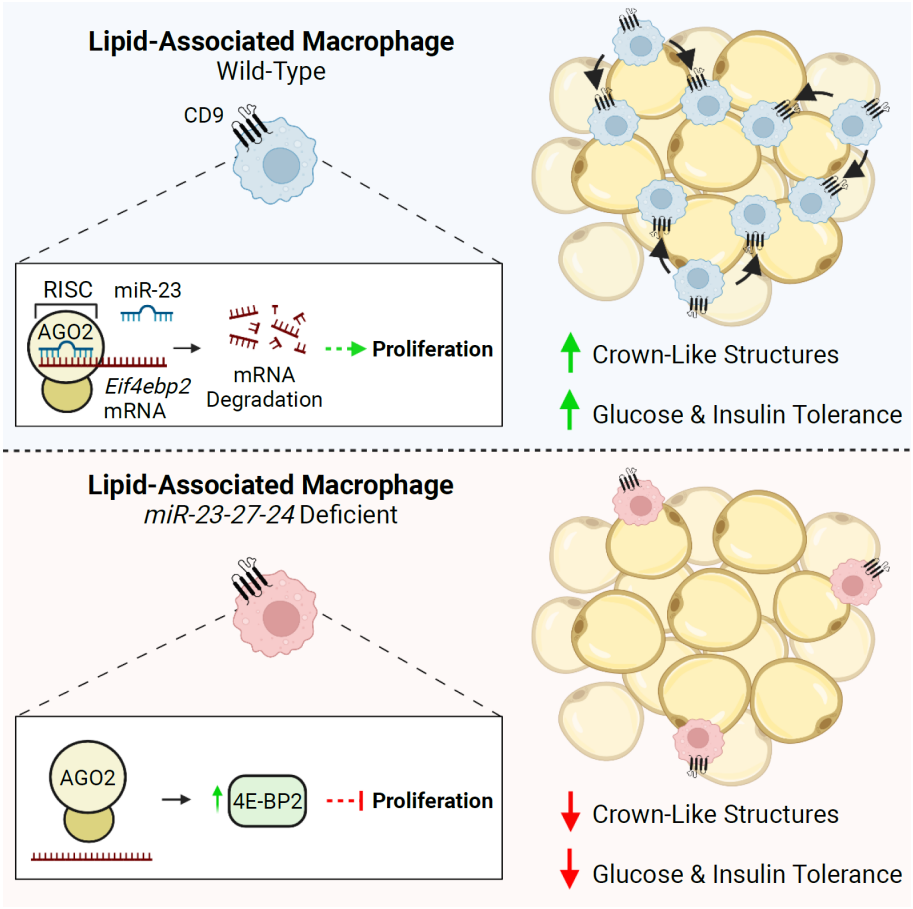

Figure 4.1. Proposed Model for Chapter 3: miR-23 Suppresses *Eif4ebp2* to Promote Lipid-Associated Macrophage Proliferation in Obese Adipose Tissue

4.2. Introduction

Discovery of $CD9^{+}Trem2^{+}$ LAMs has led to a newfound appreciation that cells of the immune system support adipose tissue function in obesity by mediating tissue-level lipid homeostasis. Historically, monocyte recruitment, proliferation, prolonged survival, and reduced egress have all been linked to encouraging ATM accrual in obese adipose tissue. Recent lineage tracing studies indicate LAMs are monocytic in origin and the

temporal accrual of LAMs in obese adipose tissue over the course of high-fat diet (HFD) feeding is a product of monocyte recruitment into inflamed tissue. Nevertheless, complementary mechanisms driving LAM accrual in obese adipose tissue and how they overlap with those that promote pathological ATM accumulation remains an open area of investigation. Our studies in **Chapter 3** identified an additional cellular mechanism contributing LAM accretion in obese adipose tissue. Here, we discovered that miR-*23-27-24* deficiency in myeloid cells selectively impaired LAM proliferation, without notable influence on apoptosis, necrosis, and monocyte production or recruitment.

Non-coding miRNAs are essential regulators of macrophage function[1–3] and their unique functional properties allow them to fine-tune complex gene networks that govern specific functional programs to control immune responses by regulating tens to hundreds of target genes. Following incorporation into Argonaute 2 (Ago2) within the RNA-induced silencing complex (RISC), the selected miRNA "guides" the RISC to target mRNA by annealing to miRNA response elements (MRE) typically located within the 3' untranslated region (UTR). The 5' end of miRNA contains a 2-8 nt seed sequence that is critical for nucleating miRNAs to its cognate MRE on target mRNA. The consequent messenger ribonucleoprotein complex formed concentrate to cytoplasmic foci called P bodies, where most miRNAs promote mRNA deadenylation, decapping, and exonuclease-mediated degradation. Taken with the understanding that miRNAs regulate a network of genes to regulate specific cellular processes, we hypothesized that miRNAs from the *miR-23-27-24* clusters could directly repress macrophage proliferation by targeting multiple target genes considered to suppress proliferation. Therefore, the focus of **Chapter 4** is to identify candidate targets genes that negatively regulate proliferation in obese ATMs and

to test which members of the *miR-23-27-24* clusters directly regulate the expression of these critical transcripts.

4.3. Materials & Methods

Animals and Diets

All animal studies were performed after obtaining approval from the Vanderbilt Institutional Animal Care and Use Committee. C57BL/6 ES cells were targeted using constructs generated as a resource for the conditional deletion of miRNA clusters as described[4] to produce chimeric mice with a conditionally mutant allele of the miRNA cluster containing miR-23a, miR-27a, and miR-24-2 (the *Mirc11* cluster). These chimeras were crossed to *Rosa26-Flp* mice (*Gt(ROSA)26Sortm1(FLP1)Dym*; 009086, the Jackson Laboratory) to delete the selection cassette. Mice previously generated with a conditionally mutant allele containing miR-23b, miR-27b and miR-24-1 (the *Mirc22* cluster)[5] were backcrossed for 10 generations to C57BL/6J mice (000664, the Jackson Laboratory). These two lines were intercrossed, and the progeny crossed to *Lyz2*^{Cre} mice (*B6.129P2-Lyz2*$^{tm1(cre)Ifo}$*/J*; 004781, the Jackson Laboratory) to generate mice with myeloid cells lacking expression of *Mirc11* and *Mirc22* clusters in myeloid cells (MyelΔ). For the diet-induced obesity model, 7–9-week-old male or female *Mirc11*$^{fl/fl}$*Mirc22*$^{fl/fl}$ and *Mirc11*$^{fl/fl}$*Mirc22*$^{fl/fl}$*Lyz2*^{Cre} mice were fed a high-fat diet (HFD, 60% kcal fat; Research Diets) for 20+ weeks. Body weight and food intake were recorded weekly. Body composition measurements, collection of fasting blood samples, and intraperitoneal

glucose and insulin tolerance tests were performed before or during HFD feeding. All other analyses were performed after the mice were euthanized.

Bone Marrow-Derived Macrophage Cultures

Primary bone marrow-derived macrophages (BMDMs) were prepared by culturing bone marrow of mice in RPMI-1640 media supplemented with 20% L929-conditioned medium, 10% FBS, gentamicin, glutamine, HEPES, non-essential amino acids, and penicillin-streptomycin for 7+ days. Media was changed on Day 1, then every three days of culture. To plate for experiments, BMDMs were detached from the flask using cold PBS containing 0.5 - 5 mM EDTA and plated into tissue culture plates at a concentration of 1 x 10^6 cells/mL.

To metabolically activate BMDMs, BMDMs were cultured in supplemented DMEM media containing 25 mM glucose, 10 nM insulin (Novolin), and 150-250 μM palmitic acid (MP Biomedicals) conjugated to BSA (Research Products International) for 24 h – 48 h. BMDMs in the control group were cultured in supplemented RPMI-1640 medium (11 mM glucose) containing BSA alone. Conditions were adapted from Kratz et al.[6].

Bulk RNA Sequencing

F4/80-selected ATMs from perigonadal fat pads were homogenized with TRIzol® Reagent (Life Technologies). Large RNA (> 200 nt) was isolated using the RNeasy Mini Kit (Qiagen) and submitted to the Vanderbilt Technologies for Advanced Genomics Core for sequencing on the NovaSeq 6000 (Illumina). Data were processed on the Vanderbilt computing cluster (ACCRE) using the lab's RNA-seq pipeline (https://github.com/parkdj1/RNASeq-Pipeline). Briefly, FastQC was used to evaluate data

quality, adaptors were trimmed using Cutadapt, and alignment with quantification was performed using Salmon. Primary will be submitted to GEO at or before the time of publication and can be made available to reviewers on request. Downstream analysis included differential expression (DESeq2) and gene set enrichment (www.broadinstitute.org/gsea). IDs of the following GSEA gene sets were used to identify candidate target transcripts: GO:0070373, GO:0008285, GO:0043409, GO:1904262, GO:0009890, GO:0097696, R-HSA-5675221.

Electroporation

One to two million BMDMs from the indicated genotype resuspended in 100 µL Buffer R were mixed with 500 nM miRNA mimic (miRIDIAN) or 100 nM siRNA (siGENOME), then electroporated using the Neon Transfection System (Thermo-Fisher) at pulse code (10 ms x 3 pulses) using 100 uL Neon tips (Thermo-Fisher) at 1500 V. Following electroporation, cells were slowly pipetted into wells of tissue culture plates containing prewarmed supplemented RPMI-1640 medium containing 20% L929 conditioned media. Cells incubated in media for 24-48h, then were subjected to metabolic activation.

Locked Nucleic Acid Treatments

BMDMs were plated into tissue culture plates (1 x 10^6 cells/mL) and allowed to rest overnight. Media was replaced the next day, and cells were treated with 50 nM of the indicated locked nucleic acid inhibitor (miRCURY LNA miRNA Power Inhibitors). Cells incubated with inhibitors for 24h, then subjected to metabolic activation.

miRNA and mRNA Quantification via RT-qPCR

TRIzol® Reagent (Life Technologies) was used to extract and purify RNA from tissues and cultured cells. Small RNA (< 200 nt) of F4/80-selected adipose tissue macrophages from perigonadal fat pads was isolated using the RNeasy Mini Kit (Qiagen). For miRNA quantitation, the Mir-X miRNA First-Strand Synthesis Kit (Takara) was used for cDNA synthesis. For mRNA quantitation, the SuperScript™ IV First-Strand Synthesis System Kit (Invitrogen) was used for cDNA synthesis. Real-time PCR of cDNA was performed on a CFX96 Real-Time PCR Detection System (BioRad) located at the Vanderbilt Cell & Developmental Biology Equipment Resource Core using FastStart Universal SYBR Green master mix (Roche). Expression of the indicated genes was normalized to β-actin (*Actb*) using the $2^{-\Delta\Delta Ct}$ method.

Palmitic Acid-BSA Preparation

Palmitic acid (MP Biomedical) was dissolved in Molecular Biology Grade Ethanol (Fisher BioReagents) by alternating between heating at 70ºC and vortexing to produce a 1M palmitic acid solution. Immediately afterward, the dissolved palmitic acid was conjugated to BSA by gently mixing and heating (70ºC) 40 uL of the 1 M palmitic acid solution with 960 uL of a 10% BSA in HEPES (Gibco) solution for 20 – 30 min, creating a 40 mM palmitic acid-BSA solution. Before cell culture treatment, the 40 mM palmitic acid-BSA solution was shaken at 50ºC for 20 min prior to dispensing into a tube containing supplemented DMEM media which was then incubated with cells. 10% BSA in HEPES solution was used as the vehicle control.

Puromycin Incorporation Assay

Puromycin (10 μg/mL; InvivoGen) was added to BMDMs 15 min before harvest. Cells were then washed with ice-cold PBS twice, and protein was collected and processed for Western blotting. A “no puromycin” treatment group served as a negative control.

RNA-Argonaute 2 Immunoprecipitation

Primary or immortalized BMDMs[7] were cultured in 150 mm tissue culture plates until they reached 100% confluence. Following indicated treatments, ribonucleoprotein complexes were crosslinked with 300 mJ/cm^2 UV (wavelength 254 nm). To isolate RNAs complexed with Argonaute 2 (AGO2), we first conjugated 5 μg of anti-AGO2 (Wako; clone 2D4) to 50 μL of protein G Dynabeads (Invitrogen; 10004D) by incubating both at room temperature for 1 h while rotating. Beads were then collected using the DynaMag-2 magnet (Invitrogen; 12321D) and washed 3x with lysis buffer. After which, cell lysate from crosslinked cells incubated with anti-AGO2 conjugated beads for 2 h at 4^{o}C while rotating. Beads were washed 3x with high-salt buffer (50 mM Tris-HCl pH 7.4, 1 M NaCl, 1 mM EDTA, 1% NP-40, 0.1% SDS, 0.5% sodium deoxycholate), then 3x with wash buffer (20 mM Tris-HCl pH 7.4, 10 mM MgCl, 0.2% Tween). Proteins were then digested with proteinase K to release AGO2-associated RNA. TRIzol LS Reagent (Life Technologies) was used to isolate RNA, then treated with DNase to remove contaminating genomic DNA. cDNA synthesis and qPCR of cDNA were carried out as described above. Prior to proteinase K digestion, a small fraction of beads was collected and used to confirm successful pull-down of AGO2. Pull-down with mouse IgG1κ isotype control (Invitrogen) served as a negative control.

Stromal Vascular Fraction Isolation and Flow Cytometric Analysis

The stromal vascular fraction (SVF) from perigonadal fat pads were isolated following collagenase digestion and differential centrifugation as previously described[8]. Adipose tissue (AT) myeloid cells were characterized via flow cytometry using the following anti-mouse antibodies [BioLegend, eBioscience, BD Pharmingen, Tonbo]: PE-Cy7 F4/80; FITC Ly6G; PE Siglec F; APC and V450 CD9; V450 CD9; APC CD64; FITC and PerCP-Cy5.5 CD64; FITC CD11c; PE CD163; PE-Cy7 CD206; BV421 CCR2; FITC Ly6C; PE-Cy7 TCRβ. Dead cells were identified with e780 viability dye (ThermoFisher).

For Ki67 staining, cells were first stained with surface antigen fluorescent antibodies, then were fixed and permeabilized using the Foxp3 / Transcription Factor Staining Buffer Set (ThermoFisher). Afterward, intracellular staining was performed using either PE anti-Ki67 or PE IgG1, κ isotype control from the PE Mouse Anti-Ki67 Set (BD Biosciences) according to the manufacturer's instructions. % $Ki67^+$ cells were calculated by subtracting % PE^+ cells stained with isotype control from % PE^+ cells stained with anti-Ki67 [% PE^+ (anti-Ki67) - % PE^+ (isotype)]. For Annexin V and 7-AAD staining, SVF cells were stained using reagents from the FITC Annexin V Apoptosis Detection Kit with 7-AAD (TONBO) as described by manufacturers. All flow cytometry was performed on an 8-color FACSCANTO II flow cytometer (BD Biosciences) provided by the Division of Molecular Pathogenesis. FlowJo was used to process data.

Western Blotting

Cells were lysed in Pierce™ Ripa buffer (ThermoFischer) supplemented with a Halt™ protease and phosphatase inhibitor cocktail (ThermoFischer) on ice. Lysed cells were scraped off tissue culture plates, and lysates were cleared by centrifugation at 4ºC at 12,000 x g for 15 min. Protein concentrations were quantified with the Pierce™ BCA

Protein Assay Kit (ThermoFischer), and equal amounts of protein (20-30 ug) were loaded on BoltTM 4-12% Bis-Tris Plus precast gels for SDS-PAGE. Proteins were transferred onto nitrocellulose membranes with a tank blotting system (Invitrogen), blocked with 5% milk in TBS-T for 30min – 1h after transfer, then incubated with antibodies specific for the following proteins of interest overnight: 4E-BP2 (2845), β-Actin (8457), GAPDH (5174), puromycin (MABE343), and BHLHE40/DEC-1 (17895). Anti-4E-BP2, anti-β-Actin, and anti-GAPDH antibodies were from Cell Signaling Technology. Anti-puromycin antibody (clone 12D10) was from Millipore. Anti-BHLHE40/DEC-1 was from Proteintech. Following overnight incubation with primary antibodies, the membrane was washed with TBS-T, then incubated with HRP-conjugated goat anti-rabbit or anti-mouse secondary antibodies (ThermoFisher) for 1h. Blots were imaged using an AI600 Imager (GE Healthcare) housed at the Vanderbilt Cell & Developmental Biology Equipment Resource Core. Images and quantifications were obtained using ImageJ software.

Statistical Analyses

Statistics were done on experiments with 3+ biological replicates or independent experiments as outlined in figure legends. Analyses were performed using R (www.r-project.org) and GraphPad Prism8 (GraphPad Software, Version 8.02). *P* values of less than 0.05 were considered significant.

4.4. Results

The miR-23-27-24 Clusters Enhance the Expression of Multiple Genes Involved in the Negative Regulation of Cell Proliferation

Because miRNAs attenuate the expression of networks of genes, we set out to identify candidate target mRNA transcripts regulated by these miRNAs in ATMs. We bead-selected F4/80$^+$ ATMs from male fl/fl and MyelΔ mice after 20 weeks of HFD and performed bulk RNA sequencing (RNA-seq). Differential expression analysis identified multiple genes that were selectively regulated in ATMs with deletion of the *miR-23-27-24* clusters (**Figure 4.2A, Tables A.1-2**). Consistent with the proposed function of CD9$^+$Trem2$^+$ macrophages in phagocytosis[9] and within the central nervous system[10], pathway analysis identified lysosome, phagosome and microglial gene signatures as downregulated in MyelΔ ATMs (**Figure 4.2B**). To further test whether myeloid-specific deletion of these miRNA clusters leads to reduced LAMs, we performed gene set enrichment analysis of our data with a list of genes generated from published single-cell RNA-seq data comparing LAMs to lean ATMs[9]. We found that ATMs from obese fl/fl mice were significantly enriched in this gene signature compared to ATMs from MyelΔ mice (**Figure 4.2C**). Finally, consistent with our previous data, we did not detect global changes in the expression of M2-like macrophage genes, though *Mrc1* and *Retnla* were slightly increased in MyelΔ ATMs (**Figure 4.2D**). We also did not detect differences in gene signatures for inflammation or apoptosis between groups (**Figure 4.2E**); however, we did detect an increased a leukocyte proliferation signature in fl/fl ATMs (**Figure 4.2E**).

Given that we observed a proliferation defect in *miR-23-27-24*-deficient BMDMs cultured in MMe conditions, we also performed RNA-seq in these cells (**Figure 4.3A, Tables B.1-2**). In these cell culture conditions, we found similar differentially regulated

pathways in MyelΔ macrophages when compared with fl/fl controls (**Figure 4.3B**). There was an overall strong concordance between differentially expressed genes within both data sets that highlighted lysosome, phagosome and microglia-like pathways (**Figure 4.3C-D**). Gene set enrichment analysis also showed an enrichment in a LAM-like transcriptional profile in control fl/fl BMDMs in MMe conditions and no changes in inflammatory or apoptotic gene signatures (**Figure 4.3E**). Together, this RNA-seq data support our previous findings that loss of miR-23, miR-24 and miR-27 expression leads to selective reduction of LAMs in obese adipose tissue and that *miR-23-27-24*-deficient BMDMs cultured in MMe conditions share similar transcriptional changes.

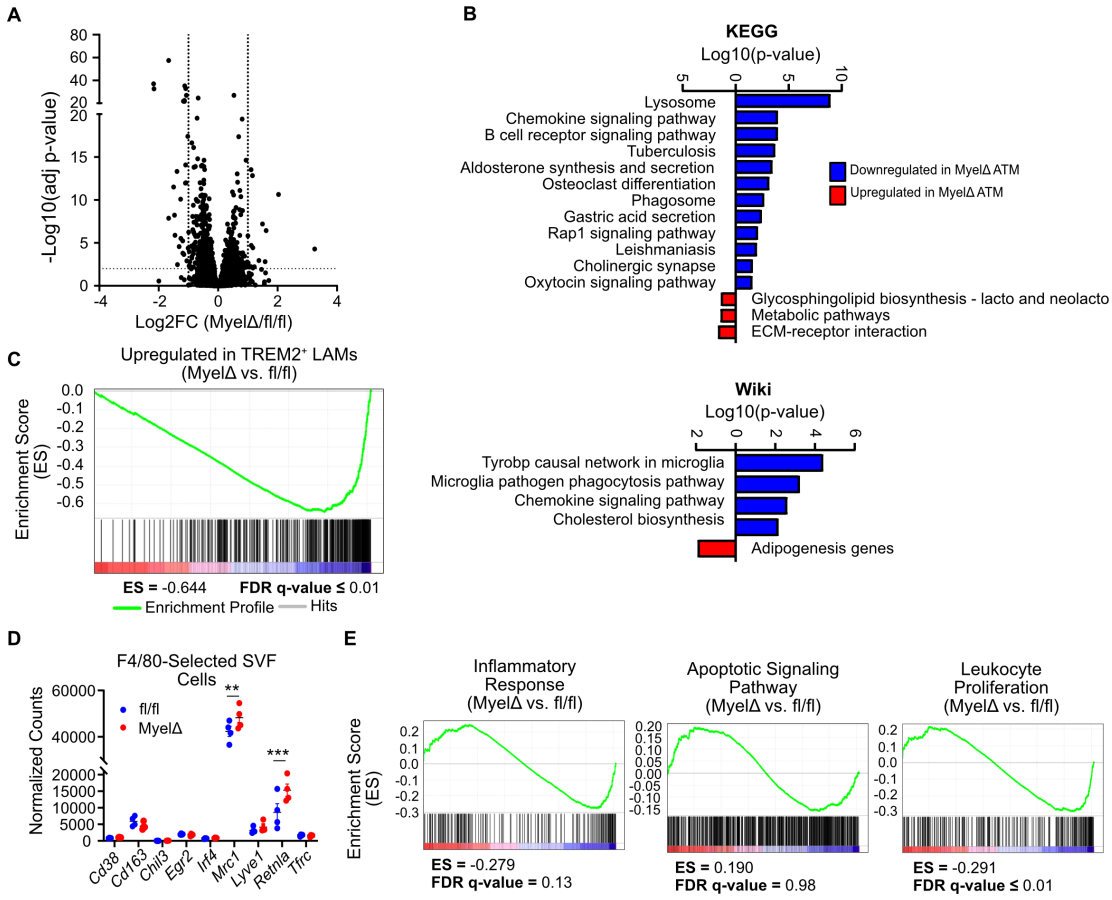

Figure 4.2. Myeloid-Specific Deletion of the *miR-23-27-24* Clusters Attenuates Expression of Genes Associated with Trem2⁺ LAMs and Proliferation in Obese ATMs. (**A**) Volcano plot representing transcriptomic changes between F4/80-selected cells from the stromal vascular fraction (SVF) of obese fl/fl and MyelΔ eWAT (basemean > 100). (**B**) KEGG and Wiki pathway analysis of RNA sequencing (RNA-seq) data. (**C**) Gene set enrichment analysis (GSEA) of RNA-seq data set for genes upregulated in LAMs compared to lean ATMs. (**D**) DESeq2 normalized counts of indicated M2-like macrophage genes were quantified (two-way ANOVA with Sidák's multiple comparison test) (**E**) GSEA of RNA-seq data sets for inflammation, proliferation, and apoptosis. GSEA were plotted with the enrichment curve and rank order location of each gene in the indicated gene set from most upregulated to most downregulated (left to right) in knockout MyelΔ ATMs compared to fl/fl ATMs. Each dot represents one male mouse after HFD feeding. ±S.E.M. **, p<0.01; ***, p<0.001.

Because mRNA decay is the predominant mechanism for miRNA-mediated gene silencing, we first tested whether loss of the clusters resulted in elevated expression of predicted mRNA targets in our RNA-seq data. Cumulative distribution frequency plots

showed a statistically significant global upregulation (right shift) of predicted high confidence 8mer target mRNAs in MyelΔ versus fl/fl ATMs for miR-23, miR-24, and miR-27 (**Figure 4.4A**) as well as MyelΔ versus fl/fl MMe BMDMs (**Figure 4.3F**). We observed no change in global expression of predicted target mRNAs of miR-21 and miR-223, two unrelated miRNAs which have previously demonstrated important roles in macrophage biology[11] (**Figure 4.4A & 4.3F**). Together, these data demonstrate that loss of *miR-23-27-24* specifically upregulates numerous predicted target genes regulated by this cluster but not predicted targets of other miRNAs in MMe BMDMs and obese ATMs.

Next, to generate a list of candidate target mRNAs regulated by the three miRNAs encoded in the *miR-23-27-24* clusters, we leveraged our RNA-seq data set comparing fl/fl and MyelΔ obese ATMs. Candidate target genes were selected based on the following criteria: 1) the 3'UTR of the mRNA contained complementary sequences(s) to the 5' seed sequence of miR-23, miR-24 and/or miR-27 and 2) the transcript was differentially upregulated (adjp value≤0.05) in obese MyelΔ ATMs. Using these criteria, we identified 78, 42, and 76 candidate target genes for miR-23, miR-24, and miR-27, respectively (**Figure 4.4B, Table C.1**)**.** Finally, since loss of the *miR-23-27-24* clusters selectively reduced LAM proliferation (**Figure 3.3A-C**), we hypothesized that these miRNAs would be specifically important for suppressing the expression of negative regulators of cell proliferation. Therefore, we compared the list of candidate targets with gene sets annotated to negatively regulate cell proliferation and biosynthetic processes or signaling pathways involved in cell proliferation. We identified the following candidate genes through this approach: *Dusp5*, *Eif4ebp2*, *Sesn2*, *Socs6*, *Spry1*, and *Tmem127* (**Figure 4.4C**).

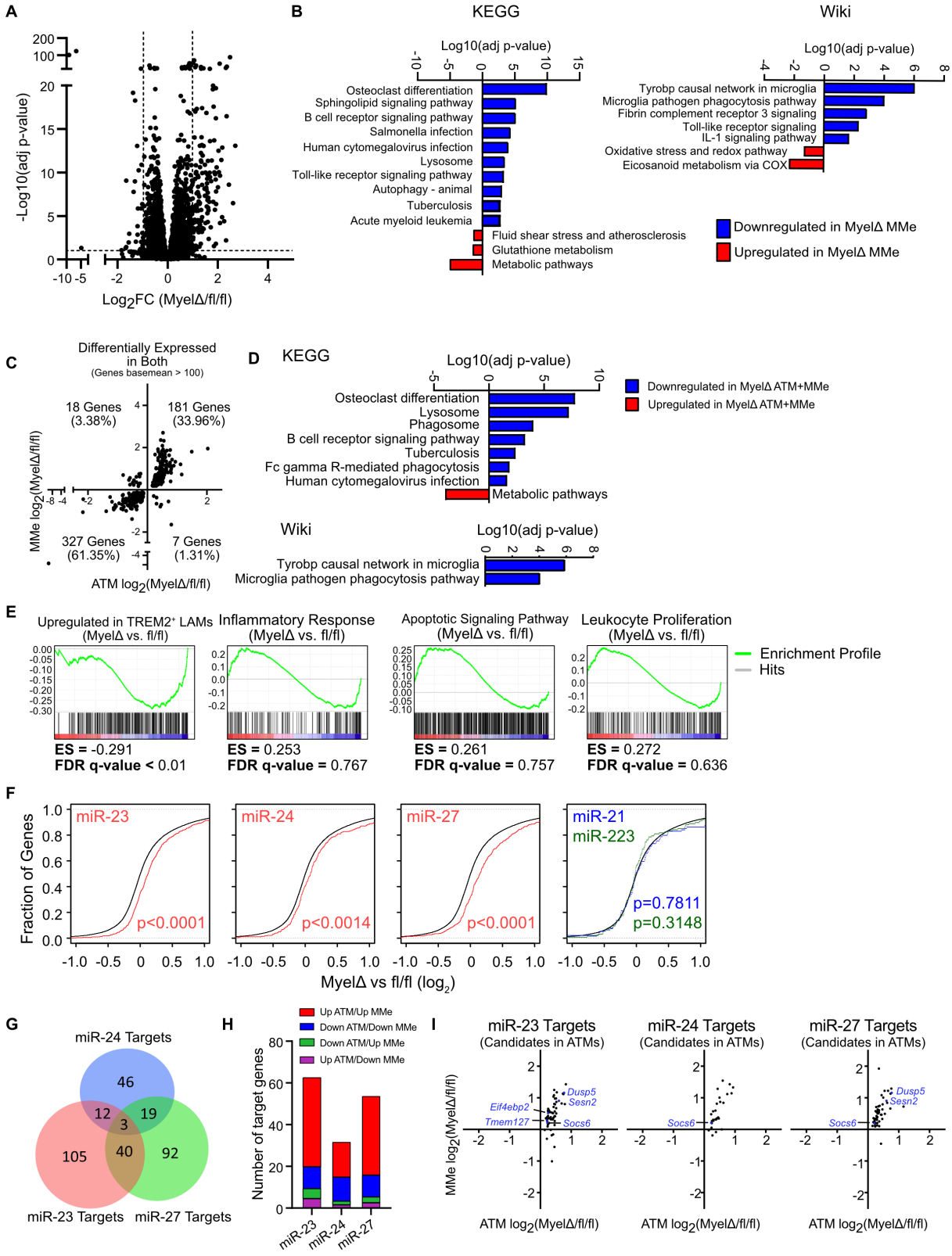

Figure 4.3 (Continued on next page).

Figure 4.3. The *miR-23-27-24* Clusters Transcriptionally Regulate Shared Pathways and Predicted Targets in Metabolically Activated Macrophages and Obese ATMs. (**A**) Volcano plot representing transcriptomic changes between fl/fl and MyelΔ metabolically activated (MMe) BMDMs (basemean > 100). (**B**) KEGG and Wiki pathway analysis of RNA sequencing (RNA-seq) data. (**C**) Log_2(MyelΔ/fl/fl) of differentially expressed genes in both F4/80-selected ATMs and MMe BMDMs were plotted (basemean>100; adjp value≤0.05). (**D**) KEGG and Wiki pathway analysis of genes significantly upregulated or downregulated in both MyelΔ ATMs and MMe BMDMs. (**E**) Gene set enrichment analysis (GSEA) of RNA-seq data from MMe BMDMs for genes upregulated in LAMs compared to lean ATMs or involved in inflammation, apoptosis, or leukocyte proliferation. GSEA were plotted with the enrichment curve and rank order location of each gene in the indicated gene set from most upregulated to most downregulated (left to right) in knockout MyelΔ MMe BMDMs compared to fl/fl MMe BMDMs. (**F**) Cumulative distribution frequency plots depicting global mRNA expression by RNA-seq as log_2(MyelΔ/fl/fl) in MMe BMDMs plotted against the cumulative fraction of all genes (black), miR-23/24/or/27 8mer targets (red), miR-21 targets (blue), or miR-223 targets (green) (Kolmogorov-Smirnov test). Target predictions were made using TargetScan. (**G**) Venn diagram depicting number of shared or unique candidate target genes significantly upregulated in MMe BMDMs whose 3'untranslated region (3'UTR) is predicted to be regulated by miR-23, miR-24, and/or miR-27 (basemean>100; adjp value≤0.05). (**H**) Bar graph indicating distribution of shared candidate target genes among differentially expressed in both obese ATMs and MMe BMDMs (basemean>100; adjp value≤0.05). (**I**) Log_2(MyelΔ/fl/fl) of MMe BMDM and obese ATM of predicted target genes from the indicated miRNA significantly upregulated in obese ATMs. Blue dots represent candidate target genes predicted to regulate proliferation in ATMs. *Spry1* not depicted as candidate target gene due to basemean<100 in MMe BMDMs.

In MMe conditions, we also identified numerous predicted targets of miR-23, miR-24 and miR-27 that were significantly upregulated in this data set (**Figure 4.3G**). More than 60% of significantly differentially expressed predicted target transcripts of all three miRNAs were upregulated in both MMe BMDMs and ATMs, with relatively few targets that were upregulated in one cell population but not the other (**Figure 4.3H**). And although gene set enrichment analysis did not show reduction of a leukocyte proliferation gene list in MMe conditions (**Figure 4.3E**), most predicted targets significantly upregulated in MyelΔ ATMs showed concordant upregulation in MyelΔ MMe BMDMs when compared to fl/fl controls, including candidate targets identified as potential regulators of cell

proliferation in ATMs (**Figure 4.3I**). qPCR studies confirmed that MyelΔ MMe BMDMs expressed ~2-4x greater levels of *Dusp5*, *Eif4ebp2*, *Sesn2*, *Socs6*, *Spry1*, and *Tmem127* mRNAs relative to control MMe macrophages (**Figure 4.4D**). Interestingly, there were no significant differences in levels of any of the candidate target transcripts between control and MyelΔ BMDMs under non-stimulating (BSA) conditions (**Figure 4.4D**), indicating that the differential expression of these transcripts was selectively observed during metabolic activation.

Next, we reconstituted individual miRNA expression in MyelΔ MMe BMDMs using miRNA mimics to determine which miRNAs were essential to suppress the expression of each candidate target gene. Transfection of miR-23 in MyelΔ MMe BMDMs significantly reduced *Dusp5*, *Eif4ebp2*, *Socs6*, and *Tmem127* mRNA levels (**Figure 4.4E**). In contrast, reconstituting miR-24 only attenuated the expression of *Eif4ebp2* mRNA, even though it was not predicted to be a target by the TargetScan predication algorithm[12] (**Figure 4.4C&E**). Finally, despite being predicted to target several of these candidate regulators of cell proliferation, miR-27 overexpression had no notable impact on mRNA levels of any of the genes of interest (**Figure 4.4C&E**). Altogether, we identified candidate target transcripts differentially regulated by the *miR-23-27-24* clusters in obese ATMs and obese-like MMe BMDMs that are known regulators of cellular proliferation.

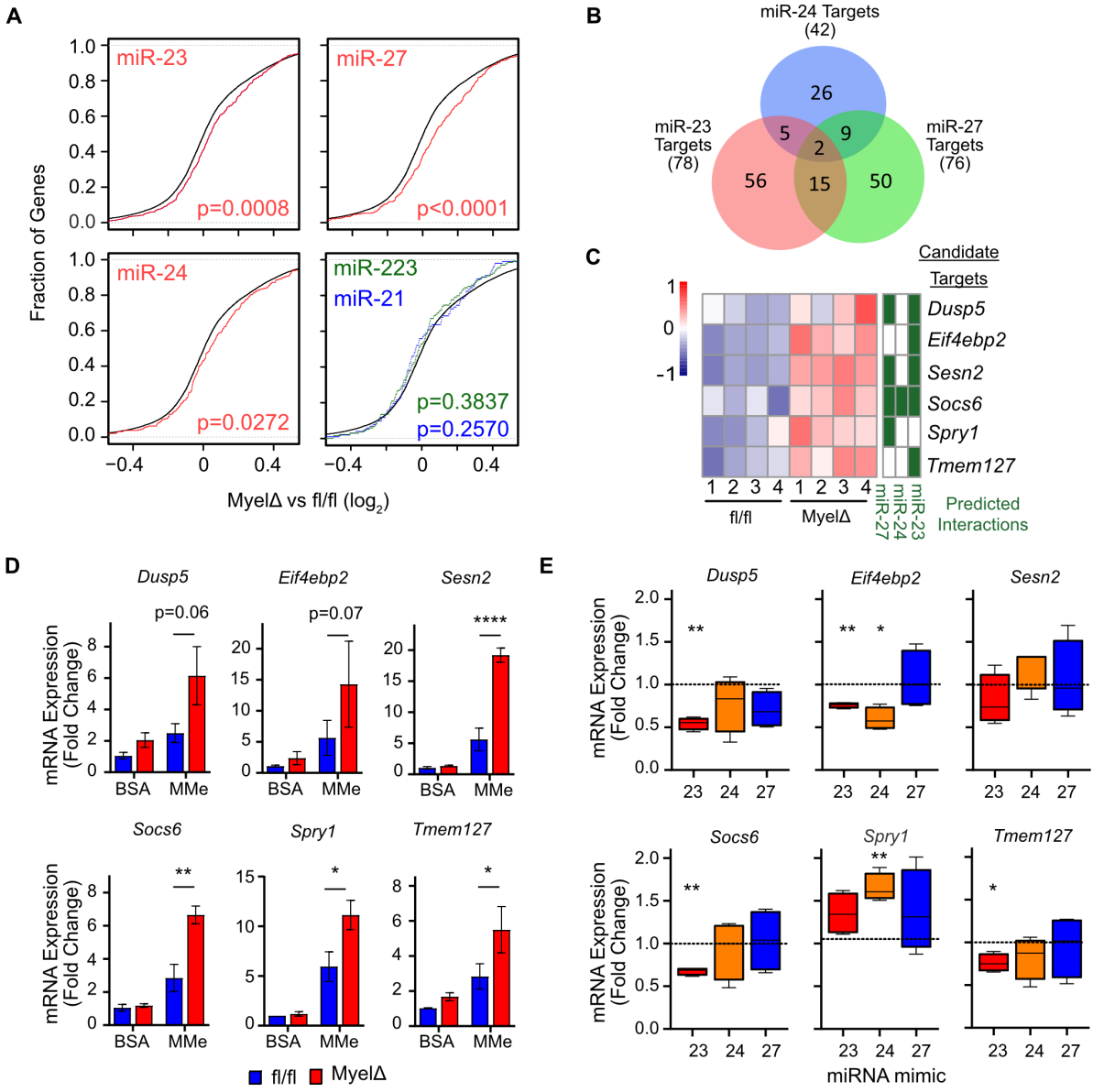

Figure 4.4. The *miR-23-27-24* Clusters Negatively Regulate Multiple Genes Involved in Suppressing Cell Proliferation. (**A**) Cumulative distribution frequency plots depicting global mRNA expression by RNA sequencing as $\log_2$(MyelΔ/fl/fl) plotted against the cumulative fraction of all genes (black), miR-23, miR-24, or miR-27 8mer targets (red), miR-21 targets (blue), or miR-223 targets (green) (Kolmogorov-Smirnov test). Target predictions were made using TargetScan. (**B**) Venn diagram depicting number of shared or unique candidate target genes whose 3'untranslated region (3'UTR) is predicted to be regulated by miR-23, miR-24, and/or miR-27. (**C**) Table and heatmap representing predicted interactions and expression of candidate target genes involved in negatively regulating cell proliferation or proliferative signaling. (**D-E**) mRNA levels of candidate target genes were compared between (**D**) fl/fl and MyelΔ unstimulated (BSA) or metabolically activated (MMe) BMDMs (two-way ANOVA with Šídák's multiple comparisons test) or (**E**) MyelΔ MMe BMDMs transfected with miR-23, miR-24, or miR-27 mimics via RT-qPCR (one-way ANOVA with Dunnett's multiple comparison test). 3-5 biological replicates per group. ±S.E.M. *, p≤0.05; **, p<0.01; ****, p<0.0001.

The miR-23-27-24 Clusters Suppress Eif4ebp2 Expression to Promote Metabolically Activated Macrophage Proliferation

To test which of the candidate target genes might regulate proliferation in macrophages exposed to obese-like conditions, we performed an siRNA screen for the 6 candidate target genes identified by RNA-seq analysis in MyelΔ ATMs from obese eWAT using our MMe cell culture model. We hypothesized that if negative regulation of candidate target genes by the *miR-23-27-24* clusters promotes proliferation, then siRNA-mediated knockdown of these genes would also enhance macrophage proliferation. Among the candidates, only siRNA-mediated knockdown of *Eif4ebp2* increased MMe BMDM proliferation (**Figure 4.5A**). Interestingly, this was also the only candidate target suppressed by miR-23 transfection and by miR-24 transfection (**Figure 4.4E**), the two miRNAs encoded by this cluster that supported proliferation in these macrophages (**Figure 3.3F**). To verify the results of this screen, we tested if knockdown of *Eif4ebp2* could enhance proliferation of primary ATMs from obese adipose tissue. Consistent with our cell culture results, F4/80-selected ATMs from MyelΔ obese eWAT transfected with si*Eif4ebp2* proliferated more *ex vivo* compared to obese ATMs transfected with control siRNA (**Figure 4.5B).** Together, these findings indicate that the negative regulation of *Eif4ebp2* contributes to MMe BMDM and ATM proliferation.

Since miRNAs can affect the expression of target mRNAs directly or indirectly, we next sought to test whether members of the *miR-23-27-24* clusters directly regulate *Eif4ebp2* expression. To do this, we performed immunoprecipitation assays of Argonaute 2 (AGO2), an RNA-binding protein that facilitates miRNA-mRNA engagement to result in post-transcriptional silencing of target transcripts as part of the RNA-induced silencing

complex (RISC)[13]. We detected a significant enrichment of *Eif4ebp2* mRNA after immunoprecipitation of AGO2 (AGO2-IP) in control MMe BMDMs, indicating that AGO2 interacts with *Eif4ebp2* mRNA during metabolic activation (**Figure 4.5C**). Next, we compared the enrichment of *Eif4ebp2* mRNA isolated from primary fl/fl and MyelΔ MMe BMDM lysates following AGO2-IP. Consistent with *Eif4ebp2* mRNA being directly regulated by the clusters, we detected a ~35% reduction in enrichment of *Eif4ebp2* mRNA associated with AGO2 in MyelΔ MMe BMDMs relative to fl/fl MMe BMDMs (**Figure 4.5D**).

Because *Eif4ebp2* mRNA is predicted to be directly regulated by miR-23 (**Figure 4.4C**), but its expression can be reduced by transfection of MMe macrophages with either miR-23 or miR-24 (**Figure 4.4E**), we sought to determine which of these miRNAs directly target *Eif4ebp2* mRNA in macrophages. Depletion of miR-23 lock nucleic acids in immortalized WT BMDMs cultured in MMe conditions reduced *Eif4ebp2* mRNA enrichment in AGO2-IPs by ~20% (**Figure 4.5E**). Contrary to miR-23 inhibition, loss of miR-24 did not reduce enrichment of *Eif4ebp2* mRNA in AGO2-containing complexes (**Figure 4.5E**). These findings indicate that *Eif4ebp2* mRNA is a direct target of miR-23 in macrophages during metabolic activation.

Eif4ebp2 encodes a member of the eukaryotic translation initiation factor 4E binding protein (4E-BP) family. Canonically, 4E-BP2 binds to and sequesters the translation initiation factor eIF4E, repressing translation of eIF4E-sensitive transcripts[14,15]. Upon mTORC1 activation, 4E-BP2 releases eIF4E to initiate cap-dependent translation. Therefore, 4E-BP2 normally restricts anabolism and proliferation within cells. In BMDMs lacking *miR-23-27-24* cluster expression, we observed increased levels of the protein product of *Eif4ebp2* (4E-BP2) in MMe macrophages (**Figure 4.5F**). To test whether this

increased protein expression of 4E-BP2 correlated with an inhibition of protein translation within *miR-23-27-24* cluster deficient cells, we performed a puromycin incorporation assay to measure changes in active protein synthesis. Supporting our hypothesis, we observed a reduction in the generation of nascent polypeptides in MyelΔ MMe BMDMs relative to control MMe BMDMs (**Figure 4.5G**). To test whether the clusters control *Eif4ebp2*-regulated protein synthesis, we quantified protein levels of *Bhlhe40* (DEC-1), which has previously been reported to depend on loss of 4E-BP1/2 translational repression to promote macrophage proliferation[16,17]. siRNA-mediated knockdown of *Eif4ebp2* increased levels of DEC-1 in wild-type MMe BMDMs, supporting that DEC-1 expression is negatively regulated by 4E-BP2 in these cells (**Figure 4.5H**). Furthermore, DEC-1 levels were markedly reduced in MyelΔ MMe BMDMs relative to control MMe BMDMs (**Figure 4.5I**). Overall, these findings support that the *miR-23-27-24* clusters promote protein synthesis during metabolic activation, in part, by relieving inhibition of eIF4E-dependent translation through suppressing *Eif4ebp2* mRNA.

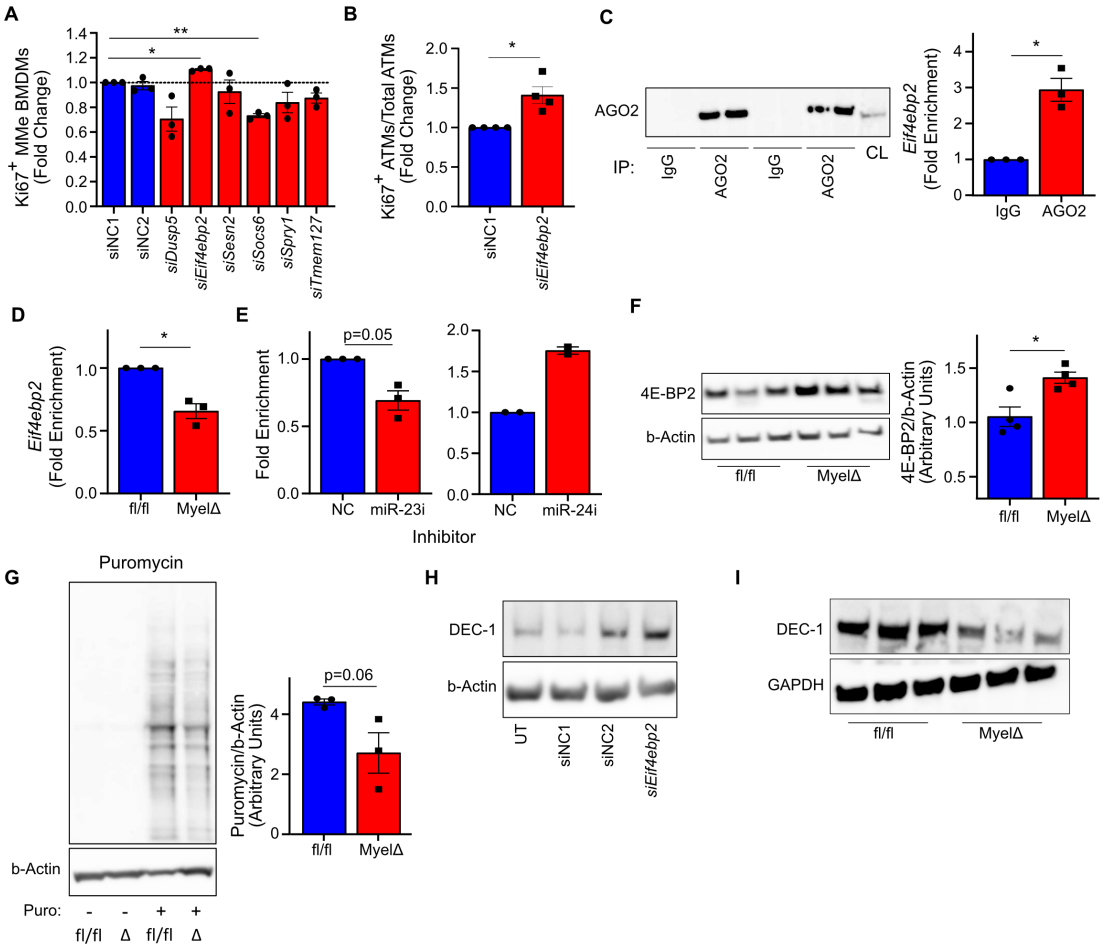

Figure 4.5. *Eif4ebp2* is a Direct Target of miR-23 and Suppresses Macrophage Proliferation. (**A**) Relative changes in Ki67⁺ MyelΔ metabolically activated (MMe) BMDMs following treatment with the indicated siRNA (one-way ANOVA with Dunnett's multiple comparisons test). (**B**) Relative changes in Ki67⁺ MyelΔ obese ATMs following treatment with the indicated siRNA (one sample t-test). (**C**) Western blot for AGO2 following pull down with IgG-conjugated or anti-AGO2-conjugated dynabeads. Each lane represents a technical replicate. CL: cell lysate. Relative enrichment of *Eif4ebp2* mRNA pulled down from wild type MMe BMDM cell lysate using anti-AGO2 antibodies compared to anti-IgG negative control (one sample t-test). (**D**) Relative enrichment of *Eif4ebp2* mRNA pulled down from cell lysate of fl/fl and MyelΔ MMe BMDMs following AGO2-IP (one sample t-test). (**E**) Relative enrichment of *Eif4ebp2* mRNA pulled down from cell lysate of immortalized BMDMs cultured under metabolically activating conditions and treated with either control, miR-23, or miR-24 LNA inhibitor following AGO2-IP (one sample t-test for miR-23 LNA data). (**F**) Representative blot and quantification (two-tailed t-test) of 4E-BP2 expression in fl/fl and MyelΔ MMe BMDMs (each lane in blot represents technical replicate; 4 biological replicates represented in quantification). (**G**) Puromycin incorporation assay to measure nascent protein synthesis in fl/fl or MyelΔ MMe BMDMs. Quantified are values from 3 independent experiments (two-tailed t-test). (**H-I**) Western blot for DEC-1 was examined between (**H**) MMe BMDMs transfected with the indicated siRNA or (**I**) fl/fl and MyelΔ MMe BMDMs. UT, untransfected; NC, negative control siRNA. Each dot represents sample from one biological replicate. ±S.E.M. *, p≤0.05; **, p<0.01.

4.5. Discussion

We identified the cellular and molecular mechanisms whereby miR-23, miR-24 and miR-27 were required for LAM accumulation in obese adipose tissue. We determined a selective defect in the proliferation of $CD9^+$ LAMs *in vivo* and metabolically activated BMDMs *in vitro* in *miR-23-27-24* deficient cells. Combining *ex vivo* RNA-seq analysis with miRNA-mRNA target interaction prediction algorithms allowed us to identify relevant candidate target genes of the clusters in obese ATMs. Importantly, *miR-23-27-24* deficiency in metabolically activated BMDMs drove similar transcriptomic changes in LAM-associated gene signatures and pathways observed in obese ATMs, with a congruent expression in many candidate target genes identified *in vivo*. Subsequent functional siRNA screening in primary cells and studies of a subset of those targets identified *Eif4ebp2* as a direct target of the clusters whose suppression supports macrophage proliferation. Interestingly, both miR-23 and miR-24 independently suppress proliferation as well as attenuate the expression of this transcript in macrophages. Therefore, two members of this cluster may be acting collaboratively to control a key regulatory node in the gene networks of this cell, highlighting one mechanism of how miRNAs of a cluster may evolve together. Of note, assaying AGO2-containing complexes identified miR-23 as a direct regulator of this transcript but showed that miR-24 is likely to act indirectly through other yet undiscovered targets to regulate this gene.

This work also demonstrates how miRNA-directed pathway discovery can reveal novel genes important for immune cell function in physiology and disease. First, the identification of a requirement for the *miR-23-27-24* clusters selectively in $CD9^+$ ATMs

highlights a subset-specific requirements for regulatory function that can be used to query deep mechanisms of immune cell function and could be leveraged for selective therapeutic intervention. They add to the theory that LAMs contribute to maintaining metabolic health in obese adipose and suggest that the *miR-23-27-24* clusters may exert broader regulation that even single-gene changes in this cell population, given that loss of Trem2 alone does not worsen diet-induced obesity in all studies. Identification of the translational repressor *Eif4ebp2* as a critical target of this miRNA cluster also points to the importance of eIF4E-dependent transcripts and their upstream regulator mTORC1[14,15] in the function of LAMs. Indeed, studies in the central nervous system of a related population $CD9^{+}Trem2^{+}$ microglia in mouse models of Alzheimer's disease have identified mTORC1 as an important downstream mediator of Trem2 signaling, controlling autophagy and metabolism in these cells[18].

4.6. Conclusions

Findings from Chapter 4 indicate that myeloid-specific expression of the *miR-23-27-24* clusters, specifically miR-23, supports the proliferation of LAMs by directly suppressing *Eif4ebp2* to promote translation of transcripts that encourage anabolic metabolism and cell growth. Due to the reported functions of LAMs, we propose that the selective reduction in protective LAMs contributes to worsened glucose metabolism observed in MyelΔ mice on HFD.

4.7. References

1. Wu, X.Q., Dai, Y., Yang, Y., Huang, C., Meng, X.M., Wu, B.M., and Li, J. (2016). Emerging role of microRNAs in regulating macrophage activation and polarization in immune response and inflammation. Immunology. 10.1111/imm.12608.

2. Boucher, A., Klopfenstein, N., Hallas, W.M., Skibbe, J., Appert, A., Jang, S.H., Pulakanti, K., Rao, S., Cowden Dahl, K.D., and Dahl, R. (2021). The miR-23a~27a~24-2 microRNA Cluster Promotes Inflammatory Polarization of Macrophages. J. Immunol. 10.4049/jimmunol.1901277.

3. Androulidaki, A., Iliopoulos, D., Arranz, A., Doxaki, C., Schworer, S., Zacharioudaki, V., Margioris, A.N., Tsichlis, P.N., and Tsatsanis, C. (2009). The Kinase Akt1 Controls Macrophage Response to Lipopolysaccharide by Regulating MicroRNAs. Immunity. 10.1016/j.immuni.2009.06.024.

4. Park, C.Y., Jeker, L.T., Carver-Moore, K., Oh, A., Liu, H.J., Cameron, R., Richards, H., Li, Z., Adler, D., Yoshinaga, Y., et al. (2012). A Resource for the Conditional Ablation of microRNAs in the Mouse. Cell Rep. *1*, 385–391. 10.1016/j.celrep.2012.02.008.

5. Pua, H.H., Steiner, D.F., Patel, S., Gonzalez, J.R., Ortiz-Carpena, J.F., Kageyama, R., Chiou, N.T., Gallman, A., de Kouchkovsky, D., Jeker, L.T., et al. (2016). MicroRNAs 24 and 27 Suppress Allergic Inflammation and Target a Network of Regulators of T Helper 2 Cell-Associated Cytokine Production. Immunity *44*, 821–832. 10.1016/j.immuni.2016.01.003.

6. Kratz, M., Coats, B.R., Hisert, K.B., Hagman, D., Mutskov, V., Peris, E., Schoenfelt, K.Q., Kuzma, J.N., Larson, I., Billing, P.S., et al. (2014). Metabolic dysfunction drives a mechanistically distinct proinflammatory phenotype in adipose tissue macrophages. Cell Metab. 10.1016/j.cmet.2014.08.010.

7. Kiritsy, M.C., Ankley, L.M., Trombley, J., Huizinga, G.P., Lord, A.E., Orning, P., Elling, R., Fitzgerald, K.A., and Olive, A.J. (2021). A genetic screen in macrophages identifies new regulators of ifnγ-inducible mhcii that contribute to t cell activation. Elife *10*. 10.7554/eLife.65110.

8. Orr, J.S., Kennedy, A.J., and Hasty, A.H. (2013). Isolation of Adipose Tissue Immune Cells. J. Vis. Exp. 10.3791/50707.

9. Jaitin, D.A., Adlung, L., Thaiss, C.A., Weiner, A., Li, B., Descamps, H., Lundgren, P., Bleriot, C., Liu, Z., Deczkowska, A., et al. (2019). Lipid-Associated Macrophages Control Metabolic Homeostasis in a Trem2-Dependent Manner. Cell. 10.1016/j.cell.2019.05.054.

10. Ponomarev, E.D., Veremeyko, T., Barteneva, N., Krichevsky, A.M., and Weiner, H.L. (2011). MicroRNA-124 promotes microglia quiescence and suppresses EAE by deactivating macrophages via the C/EBP-α-PU.1 pathway. Nat. Med. 10.1038/nm.2266.

11. Sprenkle, N.T., Serezani, C.H., and Pua, H.H. (2023). MicroRNAs in Macrophages: Regulators of Activation and Function. J. Immunol. *210*, 359–368. 10.4049/jimmunol.2200467.

12. Lewis, B.P., Burge, C.B., and Bartel, D.P. (2005). Conserved Seed Pairing , Often Flanked by Adenosines , Indicates that Thousands of Human Genes are MicroRNA Targets We predict regulatory targets of vertebrate microRNAs. Cell.

13. Gebert, L.F.R., and MacRae, I.J. (2019). Regulation of microRNA function in animals. Nat. Rev. Mol. Cell Biol. 10.1038/s41580-018-0045-7.

14. Richter, J.D., and Sonenberg, N. (2005). Regulation of cap-dependent translation by eIF4E inhibitory proteins. Nature. 10.1038/nature03205.

15. Matsuo, H., Li, H., McGuire, A.M., Mark Fletcher, C., Gingras, A.C., Sonenberg, N., and Wagner, G. (1997). Structure of translation factor eIF4E bound to m7GDP and interaction with 4E-binding protein. Nat. Struct. Biol. *4*, 717–724. 10.1038/nsb0997-717.

16. Jarjour, N.N., Schwarzkopf, E.A., Bradstreet, T.R., Shchukina, I., Lin, C.C., Huang, S.C.C., Lai, C.W., Cook, M.E., Taneja, R., Stappenbeck, T.S., et al. (2019). Bhlhe40 mediates tissue-specific control of macrophage proliferation in homeostasis and type 2 immunity. Nat. Immunol. *20*, 687–700. 10.1038/s41590-019-0382-5.

17. Colina, R., Costa-Mattioli, M., Dowling, R.J.O., Jaramillo, M., Tai, L.H., Breitbach, C.J., Martineau, Y., Larsson, O., Rong, L., Svitkin, Y. V., et al. (2008). Translational control of the innate immune response through IRF-7. Nature *452*, 323–328. 10.1038/nature06730.

18. Carlyle, W.C., Mcclain, J.B., Tzafriri, A.R., Bailey, L., Brett, G., Markham, P.M., Stanley, J.R.L., Edelman, E.R., Sciences, C.B., Technologies, E., et al. (2015). TREM2 maintains microglial metabolic fitness in Alzheimer's disease. Cell *162*, 561–567.

CHAPTER 5

FUTURE DIRECTIONS & OPPORTUNITIES

5.1. General Chapter Overview

The following chapter provides a discussion on future considerations that will extend the scope of this thesis work. These include: 1) testing whether direct miR-23-*Eif4ebp2* mRNA engagement is critical for promoting macrophage proliferation, 2) extending our understanding of how the proposed miRNA-mRNA interactions modulate proliferation, 3) determining if miRNA-based regulation of *Eif4ebp2* regulates lipid-associated macrophage (LAM) proliferation and systemic glucose tolerance *in vivo*, 4) identifying alternative targets of the clusters involved in modulating macrophage proliferation and function, 5) determining how myeloid-specific deletion of the clusters in diet-induced obesity impacts tissue-specific insulin sensitivity, and 6) discussing the potential relevance of our findings to human disease. Through this discussion, I hope to lay the groundwork for future research in the Pua laboratory.

5.2. Test if Direct miR-23-*Eif4ebp2* mRNA Interactions are Required for Proliferation in Cultured Metabolically Activated Macrophages.

Our studies indicate that negative regulation of *Eif4ebp2* expression promotes macrophage proliferation, and that miR-23 directly interacts with *Eif4ebp2* mRNA during metabolic activation (**Chapter 4**). While the finding that siRNA-mediated depletion of *Eif4ebp2* in macrophages deficient of the *miR-23-27-24* clusters demonstrates that suppression of the translational inhibitor contributes to proliferation (**Chapter 4**), we do not discern if direct miR-23-*Eif4ebp2* mRNA engagement is required for this regulation. As a result, additional experiments will be necessary to elucidate the functional role of this interaction.

To this end, the application of oligonucleotides called Target Site Blockers could be used to interrogate if direct regulation of *Eif4ebp2* expression by miR-23 supports macrophage proliferation during metabolic activation. Target Site Blockers are oligonucleotides that outcompete miRNAs for their target sites and can be designed to block specific miRNA-mRNA interactions to prevent recruitment of the RNA-induced silencing complex to target transcripts, consequently obstructing translational inhibition/mRNA decay[1]. Treating wild-type metabolically activated (MMe) macrophages with custom Target Site Blockers to obstruct miR-23-*Eif4ebp2* mRNA binding will provide an opportunity to define a role for this interaction in culture. Based on our studies, we hypothesize that blocking miR-23-*Eif4ebp2* mRNA engagement will increase levels of 4E-BP2, consequently restraining anabolic metabolism and macrophage proliferation.

5.3. Investigate how Negative Regulation of *Eif4ebp2* Expression Promotes Macrophage Proliferation.

Eif4ebp2 encodes a member of the eukaryotic translation initiation factor 4E (eIF4E) binding protein (4E-BP) family 4E-BP2. Canonically, members of the 4E-BP family bind to eIF4E to repress translation initiation on eIF4E-sensitive transcripts[2,3]. Activation of the multiprotein complex mTORC1 in response to growth factor stimulation and amino acid surplus, however, leads to 4E-BP hyperphosphorylation and subsequent disassociation from eIF4E. This event allows for the phosphorylation of eIF4E by Mnk1 and Mnk2 to promote translation of transcripts involved in anabolic metabolism to support biomass synthesis and proliferation[4–8]. Gene set enrichment analysis of our RNA sequencing data from obese fl/fl and MyelΔ adipose tissue macrophages (ATMs) (**Chapter 4**) revealed an enrichment of mTORC1 signaling genes in fl/fl ATMs (**Figure 5.1A**), arguing that *miR-23-27-24*-deficiency disrupts mTORC1 signaling in obese ATMs. Taken together, we hypothesized that negative regulation of *Eif4ebp2* would relieve the suppression of eIF4E to drive mTORC1-dependent proliferation.

Contrary to our hypothesis, however, metabolic activation of MyelΔ bone marrow-derived macrophages (BMDMs) increased levels of phosphorylated eIF4E relative to control (**Figure 5.1B**). Moreover, examination of the phosphorylated/total 4E-BP2 ratio was inconclusive (**Figure 5.1C**). Because we observed reduced nascent polypeptide synthesis in metabolically activated (MMe) MyelΔ BMDMs through our puromycin incorporation studies (**Chapter 4**), these results indicate that regulation of eIF4E-dependent translation may not be critical for the control of global protein synthesis by the clusters. Since our RNA sequencing data on obese ATMs showed a general enrichment in mTORC1 signaling genes in transcripts downregulated in MyelΔ ATMs, we examined

multiple levels of mTORC1 signaling to determine if other convergent or divergent branches of the pathway could be affected.

In brief, engagement of PI3K in response to extracellular cues phosphorylates the 3' hydroxyl group of PI(4,5)P to produce PI(3,4,5)P, thereby providing docking sites for pleckstrin domain-containing signaling mediators such as Akt. Recruitment of Akt to the plasma membrane leads to phosphorylation of Thr308 and Ser473 by PDK1 and mTORC2, respectively, resulting in optimal Akt function[9]. Once activated, Akt suppresses the GTPase activating protein activity of the tuberous sclerosis complex 1/2 heterodimer, allowing RHEB-GTP to stimulate the kinase activity of the multiprotein complex mTORC1[10]. Following mTORC1 activation is a dramatic increase in the translation of target mRNAs through the phosphorylation of ribosomal protein S6 kinase (S6K) and 4E-BP. Regulation of 4E-BP in this manner relieves the inhibition of cap-dependent translation, while phosphorylated S6K phosphorylates ribosomal protein S6 to promote the translation of many enzymes that support cell proliferation and the shift toward glycolytic metabolism[2,11].

Due to their established roles in the mTORC1 signaling pathway, we quantified phosphorylation levels of Akt and ribosomal protein S6 in MMe macrophages treated with locked nucleic acid inhibitors depleting individual members of the clusters to examine activity upstream or downstream of mTORC1, respectively. Flow cytometric analysis did not reveal changes in phosphorylation levels of Ser473 on Akt or Ser235/236 on ribosomal protein S6 between any of the miRNA-depleted groups vs control (**Figure 5.1D**). These preliminary cell culture experiments indicate that acute inhibition of miR-23,

miR-24, or miR-27 expression does not influence mTORC1 signaling during metabolic activation.

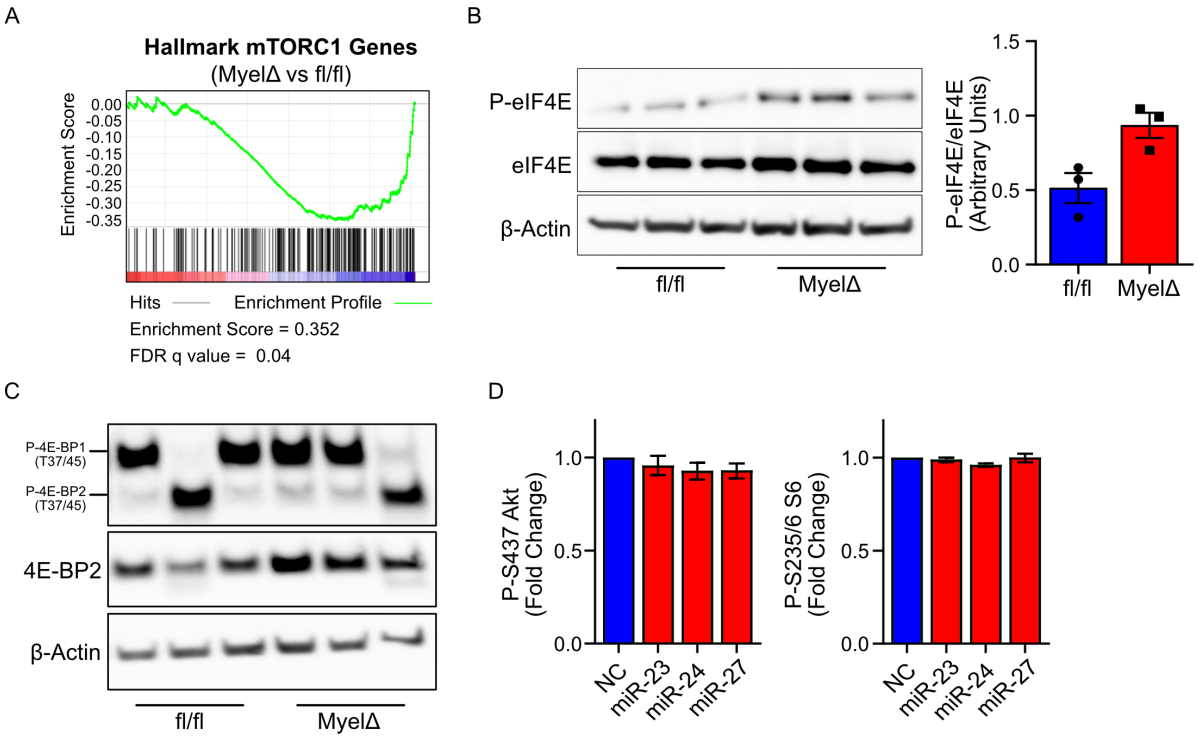

5.1. Loss of the miR-23-27-24 Clusters or Individual Members of the Clusters Does Not Attenuate mTORC1 Signaling in Metabolically Activated Macrophages. (**A**) Gene set enrichment analysis (GSEA) of RNA sequencing data from obese ATMs for genes involved in mTORC1 signaling. GSEA were plotted with the enrichment curve and rank order location of each gene in the indicated gene set from most upregulated to most downregulated (left to right) in knockout MyelΔ obese ATMs compared to fl/fl obese ATMs. (**B-C**) Levels of the indicated proteins were examined through Western blot analysis. Each lane represents one technical replicate. (**B**) Quantitation is consolidation of 3 technical replicates per genotype. (**D**) Flow cytometry was used to quantify levels of the indicated phospho-antigen in metabolically activated BMDMs treated with locked nucleic acid inhibitors against the indicated miRNA for 48h (24h before and 24h after metabolic activation). Data reflects two biological replicates per graph. ±S.E.M.

Observations from our cell culture experiments suggest that regulation of *Eif4ebp2* by miRNAs from the *miR-23-27-24* clusters may influence proliferation independently of

mTORC1 signaling. To determine if mTORC1 signaling is critical for LAM proliferation *in vivo*, we administered rapamycin to control and MyelΔ mice starting at the 15 wk period on high-fat diet (HFD) to determine if pharmacological inhibition of mTOR signaling could attenuate LAM proliferation in obese adipose tissue[12]. LAM signatures are observed 12 wks after the start of HFD feeding and increase in distribution as obesity persists[13]. Though monocyte recruitment signifies a key event for LAM acquisition, our data supports a model where expression of the clusters promote proliferation of differentiated LAMs once in tissue. Based on this, we decided to begin rapamycin treatment within a specific window where LAM proliferation would impact cell numbers the most.

Body weight curves demonstrate no significant differences in body weight gain from the start of HFD feeding to the beginning of rapamycin treatment (0-15 wks HFD feeding) or during the 5 weeks of weekly rapamycin administration (**Figure 5.2A**). While total body weight and cell numbers in collected epididymal white adipose tissue (eWAT) (**Figure 5.2B**) were unchanged after HFD feeding, we found that epididymal fat depots of rapamycin-treated mice weighed significantly more compared to their control counterparts (**Figure 5.2C**). We then immunophenotyped eWAT of vehicle and rapamycin-treated mice on HFD to determine if late-stage disruption of mTOR signaling impaired ATM and LAM accumulation. Rapamycin treatment significantly reduced P-S6 levels in total stromal vascular fraction cells and LAMs by 34% and 38%, respectively, demonstrating the efficiency of the inhibitor (**Figure 5.2D**). When normalized to grams of adipose tissue, we found the total counts of ATMs, LAMs, and proliferative Ki67^{+} LAMs were reduced following rapamycin administration (**Figure 5.2E**). However, since we recovered more adipose tissue in the rapamycin-treated mice, potentially a result of

increased adipocyte hypertrophy/hyperplasia, we could not exclude that normalization in this manner would bias the results. When normalized to total live cells, we detected no differences in % of ATMs between treatment groups (**Figure 5.2F**), which contrasts to our previous HFD studies (**Chapter 2**). Frequency of LAMs relative to total ATMs (**Figure 5.2G**) and proliferative Ki67^{+} LAMs compared to total live cells were also unchanged (**Figure 5.2H**). Altogether, these data indicate that late-stage mTOR signaling may not be required for the regulation of LAM proliferation in obese adipose tissue.

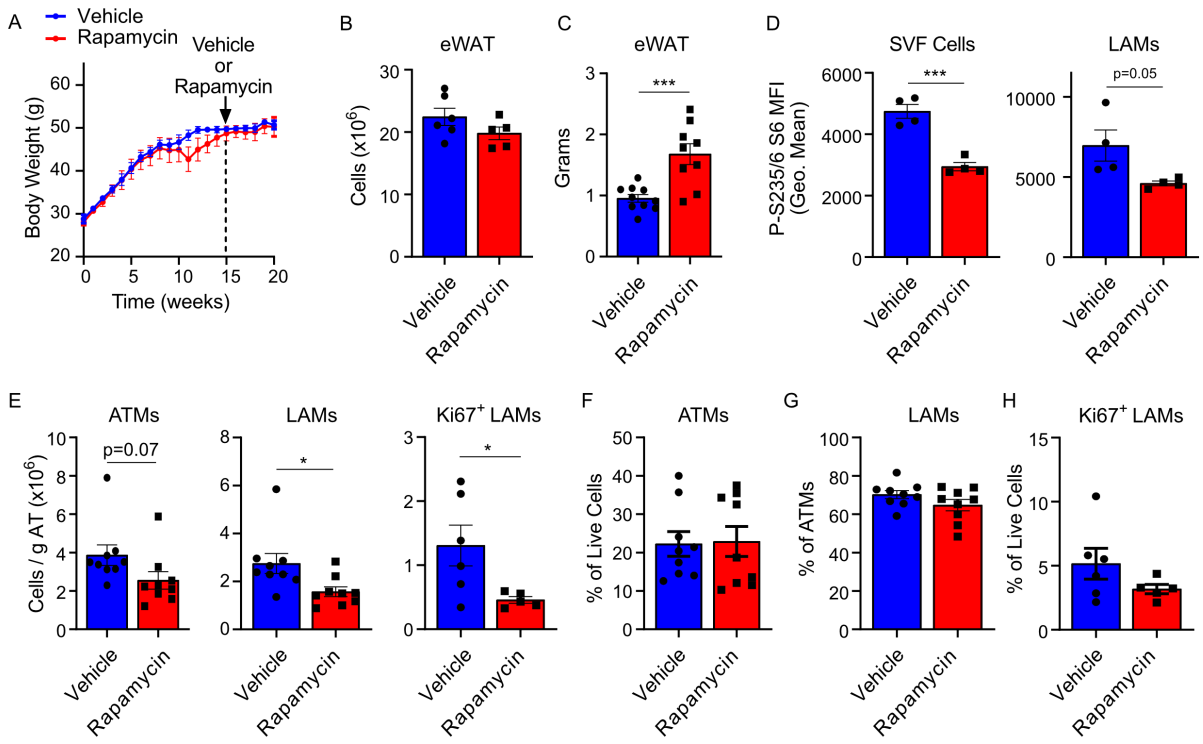

5.2. Late-Stage mTOR Suppression Does Not Attenuate LAM Proliferation in Obese Adipose Tissue. (**A**). Body weight curves of male mice on high-fat diet (HFD) before and after weekly treatment with either vehicle (10% PEG400/8% ethanol combined with equal volume of sterile 10% Tween 80) or rapamycin for 5 weeks starting the 15 week time period (two-way ANOVA with Sidák's multiple comparison test). N=9 per treatment group. (**B**) Total number of live cells from epididymal white adipose tissue (eWAT) (two-tailed t test). (**C**) Total weight of eWAT collected from each treatment group after intervention (two-tailed t-test). (**D**) Quantification of P-Ser235/236 S6 levels in stromal vascular fraction (SVF) cells or LAMs isolated from eWAT via flow cytometry (two-tailed t test). (**E**) The indicated cells were quantified based on normalization to collected eWAT (two-tailed t test). (**F**) % of ATMs relative to total number of live cells, (**G**) % of LAMs relative to total ATMs, or (**H**) % Ki67$^+$ LAMs relative to total live cells were quantified via flow cytometry. (**F-H**) two-tailed t test. Each dot represents one mouse after high-fat diet feeding. ±S.E.M. *, p≤0.05, ***, p<0.001.

Our preliminary data suggest a potential non-canonical mechanism where *Eif4ebp2* regulates cell proliferation independently of its control of eIF4E-dependent translation. Before arriving at this conclusion, however, integration of RNA sequencing

data with ribosome profiling should be used to functionally determine whether genetic/pharmacological targeting of the *miR-23-27-24* clusters or *Eif4ebp2* regulates translational efficiency of global transcripts or a specific class of mTORC1-regulated transcripts containing 5' terminal oligopyrimidine motifs[14,15]. Additional polysome profiling can discern if loss of the clusters or *Eif4ebp2* expression impairs both ribosome and polysome assembly globally or at known eIF4E-regulated transcripts[15]. If no differences are discovered, this will engender exciting investigation into unknown molecular mechanisms underscoring how *Eif4ebp2* regulates macrophage proliferation.

5.4. Determine if *miR-23-27-24* Cluster's Regulation of *Eif4ebp2* Modulates LAM Accrual and Glucose Tolerance in a Diet-Induced Obesity Murine Model.

Functional studies provided in **Chapter 4** demonstrate that acute suppression of *Eif4ebp2* in *miR-23-27-24*-deficient MMe macrophages or obese ATMs cultured *ex vivo* augments proliferation. Nevertheless, these findings fall short of uncovering if this regulation is critical for LAM proliferation in obese adipose tissue and conferring protection against glucose and insulin intolerance in a chronic diet-induced obesity model. It is recommended that future studies seeking to address these questions utilize methods that selectively attenuate *Eif4ebp2* expression in ATMs from mice containing a myeloid-specific deletion of the *miR-23-27-24* clusters to determine if silencing *Eif4ebp2* in these mice can rescue LAM proliferation and glucose regulation.

One method to target tissue-resident macrophages that is gaining increasing attention is the use of glucan-encapsulated siRNA particles (GeRPs)[16–20]. Here, custom siRNAs are encapsulated in micrometer-sized glucan-shells extracted from Saccharomyces cerevisiae composed of mainly 1,3-D-glucan, a ligand for Dectin-1 and other receptors expressed by macrophages, to produce GeRPs. Administration of GeRPs to mice on HFD has led to successful gene knockdowns in select macrophage populations with minimal undesired targeting[17,18,20]. Biodistribution of these particles appears to depend on the route of administration, as GeRPs injected intraperitoneally have been reported to be primarily taken up by ATMs in eWAT[17] while GeRPs injected intravenously appear to be internalized by liver macrophages[16,18]. Therefore, experiments incorporating the following treatments groups would determine whether negative regulation of *Eif4ebp2* in *miR-23-27-24*-deficient ATMs could rescue LAM proliferation and systemic glucose-handling *in vivo*: 1) HFD fl/fl mice + negative control siRNA GeRP, 2) HFD fl/fl mice + *Eif4ebp2* siRNA GeRP, 3) HFD MyelΔ mice + negative control siRNA GeRP, 4) HFD MyelΔ mice + *Eif4ebp2* siRNA GeRP (20 wks HFD feeding and weekly intraperitoneal GeRP injections).

Alternatively, the application of CRISPR-Cas9 genome editing can be used to target *Eif4ebp2* expression. Crossing *Mirc11*$^{fl/fl}$ *Mirc22*$^{fl/fl}$ *Lyz2*^{Cre} mice with Cre-regulated Cas9 knockin mice[21] for multiple generations will produce *Mirc11*$^{fl/fl}$ *Mirc22*$^{fl/fl}$ *Lyz2*^{Cre} mice expressing the enzyme Cas9, an RNA-guided endonuclease that cleaves foreign nucleic acids bearing sequence complementary to the single-guide RNA (sgRNA), in myeloid cells[22]. Bone marrow transplant experiments transferring *Mirc11*$^{fl/fl}$ *Mirc22*$^{fl/fl}$ *Lyz2*^{Cre} Cas9^{+} bone marrow transduced with *Eif4ebp2-directed* sgRNA *ex vivo* to irradiated wild-

type recipient mice would produce mice containing a myeloid-specific deficiency of the clusters and a hematopoietic deficiency of *Eif4ebp2*. Conducting diet-induced obesity studies with recipient mice containing *Mirc11*$^{fl/fl}$ *Mirc22*$^{fl/fl}$ *Lyz2*^{Cre} Cas9^{+} bone marrow transduced with either control sgRNA or *Eif4ebp2*-directed sgRNA would enable investigators to determine if suppression of *Eif4ebp2* by the clusters rescues LAM proliferation and systemic glucose and insulin tolerance in this model. Because this approach will impact macrophages residing in multiple tissues in addition to adipose tissue, there will be an opportunity to study this regulation in other insulin-sensitive metabolic organs such as the liver. Nevertheless, this understanding will need to be considered when making conclusions about this interaction on the observed metabolic phenotype.

5.5. Identification of Additional Targets Involved in Metabolically Activated Macrophage Proliferation and Function.

Although we identified *Eif4ebp2* as a target gene important for ATM proliferation, there are likely other critical miRNA-mRNA interactions among the 163 significantly regulated predicted targets in our RNA sequencing data set (**Chapter 4**). miRNAs almost always act to inhibit multiple critical target genes to exert a biological effect. Indeed, it remains possible that *Dusp5*[23], *Sesn2*[24], *Socs6*[25], *Spry1*[26], and *Tmem127*[27], may be critical for the *in vivo* function of LAMs despite not affecting *in vitro* proliferation in metabolically activating conditions. Moreover, due to the nature of miRNAs, we anticipate

that in addition to regulating cellular proliferation, target genes inhibited by the *miR-23-27-24* clusters may coordinate additional cell-autonomous changes in aspects of ATM biology that dictate macrophage function in systemic metabolic homeostasis and obesity. Therefore, testing additional functions for miR-23, miR-24 and miR-27 within ATMs may be needed to identify unique characteristics of cell subsets within this tissue.

Functional siRNA screens utilizing miRNA-deficient immune cells represent an invaluable *in vitro* tool to study how negative regulation of candidate target genes modulates select cellular functions[28–30]. Our own investigation utilized this method to test how candidate target genes identified in obese ATMs linked to restraining proliferation, proliferative signaling, and anabolic metabolism regulate macrophage proliferation during metabolic activation *in vitro* and *ex vivo* using F4/80-selected obese ATMs deficient of the clusters (**Chapter 4**). Because these genes were identified by cross-referencing our ATM candidate target list to curated gene set enrichment analysis gene sets that seemed to be relevant to our proliferation phenotype, we may be missing additional candidate targets whose suppression by the clusters promote macrophage proliferation. Therefore, I propose consolidating a list of 15-20 candidate target genes based on the following criteria to test for critical regulators of metabolically-induced macrophage proliferation using an siRNA rescue screen for proliferation (see **Chapter 4**): 1) identified as a candidate target gene (basemean >100 in RNA sequencing data) in both obese ATMs and MMe macrophages (**Chapter 4**) and 2) ranked based on mRNA expression in ATMs.

Because loss of the clusters downregulates a network of genes found to be upregulated in $CD9^{+}Trem2^{+}$ LAMs relative to lean ATMs or associated with the “lysosome” and “phagosome” in both obese ATMs and MMe macrophages (**Chapter 4**),

I hypothesize that the clusters also promote the phagocytotic program of LAMs, potentially promoting their homeostatic function in obese adipose tissue in addition to their accrual (**Chapter 4** and [13]). Like how we screened for candidate targets involved in regulating proliferation, an siRNA rescue screen can be utilized against select candidate target genes identified through cross-referencing to relevant gene set enrichment analysis gene sets and/or the aforementioned criteria using *in vitro* phagocytosis assays as a functional read-out.

5.6. Determine how Expression of the Clusters in Myeloid Cells Regulates Tissue-Specific Insulin Sensitivity in Diet-Induced Obesity Model.

Metabolic studies described in **Chapter 2** demonstrate that myeloid-specific deletion of the *miR-23-27-24* clusters aggravated glucose and insulin intolerance after 20 wks of HFD feeding. Because MyelΔ mice on HFD weighed less compared to control mice at the time of tolerance testing, the confounding issue that increased body weight could drive the observed phenotype was not applicable to our studies. While our findings are suggestive of an augmented insulin resistance phenotype, they do not discern the specific metabolic tissues driving the observed metabolic phenotype in response to conditional deletion of the *miR-23-27-24* clusters.

To address this gap in knowledge, I propose establishing a collaboration the Mouse Metabolic Phenotyping Center at Vanderbilt University to carry out hyperinsulinemic-euglycemic clamps using fl/fl and MyelΔ mice on HFD. This procedure is considered the “gold standard” for assessing insulin action *in vivo*[31]. Not only do

hyperinsulinemic-euglycemic clamps enable for comparison of glucose infusion rates to gage alterations in whole-body insulin action[31], but the administration of isotopic 2[^{14}C]deoxyglucose and [3-^{3}H]glucose during the assessment reveals differences in tissue-specific glucose uptake (e.g. adipose tissue, liver, muscle, pancreas,…etc.) or the ability of insulin to suppress endogenous glucose appearance, a marker of hepatic glucose production, respectively[31,32]. As a complementary approach, I propose performing *in vivo* insulin injections in fasted obese fl/fl and MyelΔ mice, then examining phosphorylated Ser437/Thr308 Akt levels from whole cell lysates of different insulin-sensitive tissues (e.g. adipose tissue and liver) to examine differences in downstream insulin signaling between genotypes.

While our data does not support differences in insulin production between groups, I propose collaborating with the Mouse Metabolic Phenotyping Center to conduct hyperglycemic clamps on a separate cohort of mice as a complementary approach. This procedure functions to assess the insulin secretory capacity of pancreatic β-cells in response to hyperglycemia to determine if the observed difference in glucose tolerance is due to changes in pancreatic function[31]. This procedure will provide a comprehensive control testing whether the glucose-handling defects observed in MyelΔ mice on HFD is dependent on altered insulin production in response to glucose levels.

5.7. Relevance to Human Disease

miRNAs play a major role in a wide range of macrophage-driven processes and dysregulated expression or activity of select miRNAs has been linked to human diseases[34]. In regards to the *miR-23-27-24* clusters, the 5' seed sequences of miR-23a/b, miR-24, and miR-27a/b are conserved from mice to humans and their differential expression under pathological conditions implicates their involvement in human disease outcomes, including those involved in multiple types of cancer and cardiovascular diseases (https://www.mirbase.org/ and reviewed in [33]). Relevant to our studies, single cell-RNA sequencing maps the presence of LAMs and the Trem2 pathway in visceral adipose tissue from the omental fat depot of obese subjects, indicating that the induction of the LAM program is also conserved from mouse to human obesity[13]. Due to the conservation of these two entities and relationship between the clusters and LAM accrual observed in our studies, I hypothesize that the *miR-23-27-24* clusters also contribute to regulating either LAM accumulation and/or induction of the LAM program in human obese adipose tissue.

In collaboration with Dr. John Koethe and Dr. Celestine Wanjalla here at Vanderbilt University, we have isolated small RNAs from abdominal adipose tissue from obese patients and performed qPCR for miR-23, miR-24, and miR-27 in a proof-of-concept experiment to determine if there is a correlation between expression of the clusters and body mass. Preliminary observations uncovered a negative correlation between miR-23a, miR-23b, and miR-24 levels and body mass index (**Figure 5.3**). This human data suggests that levels of these miRNAs are reduced in response to increased adiposity, potentially hinting at a protective role for these mediators. However, the relationship between miRNAs from our clusters and LAMs in human obesity requires a more in-depth

investigation. In particular, the *miR-23-27-24* clusters are expressed both in immune cells and numerous other cell types. Therefore, we cannot be sure that this correlation in total adipose tissue is specific to macrophages. To answer that important question will require cell sorting and/or spatial tissue analysis. In addition, it would be valuable to have a study powered to analyze men and women separately. Nevertheless, I believe the laboratory will be excited to pursue these research questions in future studies to delineate how the clusters modulate immune cell behavior and adipose tissue function in human disease.

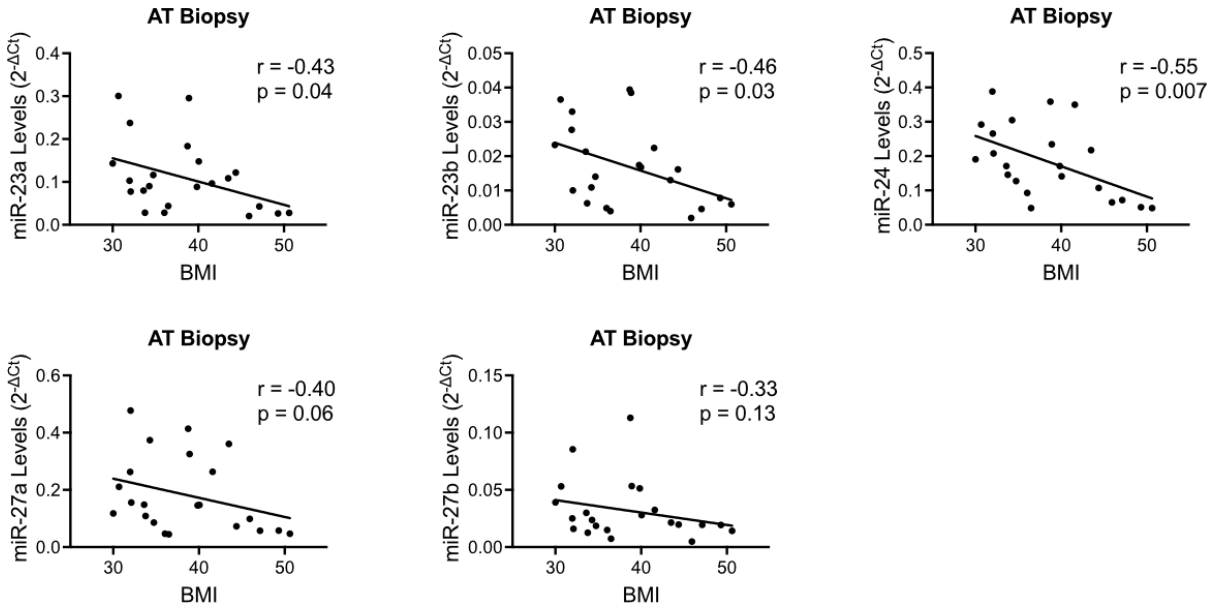

5.3. Levels of miR-23a, miR-23b, and miR-24 in Abdominal Subcutaneous Adipose Tissue are Inversely Correlated with Body Mass Index. Spearman correlation analysis between levels of the indicated miRNA in abdominal adipose tissue and recorded body mass indexes of biopsied patients. N=15 females and N=7 males. r = correlation coefficient. Each dot represents one biopsied patient.

5.8. Author Summary

Communication between immunological and metabolic systems is pivotal for mediating organismal nutrient homeostasis. Therefore, it is no surprise that dysregulation in either entity during chronic obesity predisposes individuals to acquiring complex metabolic disorders. Great focus has been placed on identifying molecular nodes to therapeutically alleviate macrophage-driven “metaflammation” that aggravates systemic insulin resistance. Independent of sterile tissue inflammation, recent discovery of $CD9^+$ $Trem2^+$ LAMs has fueled a new appreciation that cells of the immune system support adipose tissue function in obesity by mediating tissue-level lipid homeostasis. Findings from this study provide molecular details underlying LAM accrual in obese adipose tissue and implicates LAM proliferation in conferring protection against obesity-induced glucose intolerance. Accordingly, we propose a novel pathway which can be exploited by the application of miRNA-based therapeutics to modulate the innate immune cell compartment of obese adipose tissue to improve metabolic function. Furthermore, identification of target genes and downstream gene networks regulated by the miR-23-27-24 clusters will uncover additional avenues to pharmacologically regulate the immune system to treat obesity-associated metabolic complications.

5.9. References

1. Sonneville, F., Ruffin, M., Coraux, C., Rousselet, N., Le Rouzic, P., Blouquit-Laye, S., Corvol, H., and Tabary, O. (2017). MicroRNA-9 downregulates the ANO1 chloride channel and contributes to cystic fibrosis lung pathology. Nat. Commun. 10.1038/s41467-017-00813-z.
2. Richter, J.D., and Sonenberg, N. (2005). Regulation of cap-dependent translation

by eIF4E inhibitory proteins. Nature. 10.1038/nature03205.

3. Matsuo, H., Li, H., McGuire, A.M., Mark Fletcher, C., Gingras, A.C., Sonenberg, N., and Wagner, G. (1997). Structure of translation factor eIF4E bound to m7GDP and interaction with 4E-binding protein. Nat. Struct. Biol. *4*, 717–724. 10.1038/nsb0997-717.

4. Pyronnet, S. (2000). Phosphorylation of the cap-binding protein eIF4E by the MAPK-activated protein kinase Mnk1. Biochem. Pharmacol. *60*, 1237–1243. 10.1016/S0006-2952(00)00429-9.

5. Müller, D., Lasfargues, C., El Khawand, S., Alard, A., Schneider, R.J., Bousquet, C., Pyronnet, S., and Martineau, Y. (2013). 4E-BP restrains eIF4E phosphorylation. Translation *1*, e25819. 10.4161/trla.25819.

6. Jefferies, H.B.J., Reinhard, C., Kozma, S.C., and Thomas, G. (1994). Rapamycin selectively represses translation of the “polypyrimidine tract” mRNA family. Proc. Natl. Acad. Sci. U. S. A. *91*, 4441–4445. 10.1073/pnas.91.10.4441.

7. Ben-Sahra, I., and Manning, B.D. (2017). mTORC1 signaling and the metabolic control of cell growth. Curr. Opin. Cell Biol. *45*, 72–82. 10.1016/j.ceb.2017.02.012.

8. Bianchini, A., Loiarro, M., Bielli, P., Busà, R., Paronetto, M.P., Loreni, F., Geremia, R., and Sette, C. (2008). Phosphorylation of eIF4E by MNKs supports protein synthesis, cell cycle progression and proliferation in prostate cancer cells. Carcinogenesis *29*, 2279–2288. 10.1093/carcin/bgn221.

9. Manning, B.D., and Toker, A. (2017). AKT/PKB Signaling: Navigating the Network. Cell. 10.1016/j.cell.2017.04.001.

10. Inoki, K., Li, Y., Zhu, T., Wu, J., and Guan, K.L. (2002). TSC2 is phosphorylated and inhibited by Akt and suppresses mTOR signalling. Nat. Cell Biol. *4*, 648–657. 10.1038/ncb839.

11. Jones, R.G., and Pearce, E.J. (2017). MenTORing Immunity: mTOR Signaling in the Development and Function of Tissue-Resident Immune Cells. Immunity. 10.1016/j.immuni.2017.04.028.

12. Lamming, D.W. (2016). Inhibition of the mechanistic target of rapamycin (mTOR)–Rapamycin and beyond. Cold Spring Harb. Perspect. Med. *6*. 10.1101/cshperspect.a025924.

13. Jaitin, D.A., Adlung, L., Thaiss, C.A., Weiner, A., Li, B., Descamps, H., Lundgren, P., Bleriot, C., Liu, Z., Deczkowska, A., et al. (2019). Lipid-Associated Macrophages Control Metabolic Homeostasis in a Trem2-Dependent Manner. Cell. 10.1016/j.cell.2019.05.054.

14. Hong, S., Freeberg, M.A., Han, T., Kamath, A., Yao, Y., Fukuda, T., Suzuki, T., Kim, J.K., and Inoki, K. (2017). LARP1 functions as a molecular switch for mTORC1-mediated translation of an essential class of mRNAs. Elife *6*. 10.7554/eLife.25237.

15. Su, X., Yu, Y., Zhong, Y., Giannopoulou, E.G., Hu, X., Liu, H., Cross, J.R., Rätsch, G., Rice, C.M., and Ivashkiv, L.B. (2015). Interferon-γ regulates cellular metabolism and mRNA translation to potentiate macrophage activation. Nat. Immunol. *16*, 838–849. 10.1038/ni.3205.

16. Tencerova, M., Aouadi, M., Vangala, P., Nicoloro, S.M., Yawe, J.C., Cohen, J.L., Shen, Y., Garcia-Menendez, L., Pedersen, D.J., Gallagher-Dorval, K., et al. (2015). Activated Kupffer cells inhibit insulin sensitivity in obese mice. FASEB J. 10.1096/fj.15-270496.

17. Aouadi, M., Tencerova, M., Vangala, P., Yawe, J.C., Nicoloro, S.M., Amano, S.U., Cohen, J.L., and Czech, M.P. (2013). Gene silencing in adipose tissue macrophages regulates whole-body metabolism in obese mice. Proc. Natl. Acad. Sci. U. S. A. *110*, 8278–8283. 10.1073/pnas.1300492110.

18. Morgantini, C., Jager, J., Li, X., Levi, L., Azzimato, V., Sulen, A., Barreby, E., Xu, C., Tencerova, M., Näslund, E., et al. (2019). Liver macrophages regulate systemic metabolism through non-inflammatory factors. Nat. Metab. 10.1038/s42255-019-0044-9.

19. Barreby, E., Sulen, A., and Aouadi, M. (2019). Glucan-encapsulated siRNA particles (GeRPs) for specific gene silencing in adipose tissue macrophages. Methods Mol. Biol. *1951*, 49–57. 10.1007/978-1-4939-9130-3_4.

20. Aouadi, M., Tesz, G.J., Nicoloro, S.M., Wang, M., Chouinard, M., Soto, E., Ostroff, G.R., and Czech, M.P. (2009). Orally delivered siRNA targeting macrophage Map4k4 suppresses systemic inflammation. Nature *458*, 1180–1184. 10.1038/nature07774.

21. Platt, R.J., Chen, S., Zhou, Y., Yim, M.J., Swiech, L., Kempton, H.R., Dahlman, J.E., Parnas, O., Eisenhaure, T.M., Jovanovic, M., et al. (2014). CRISPR-Cas9 knockin mice for genome editing and cancer modeling. Cell *159*, 440–455. 10.1016/j.cell.2014.09.014.

22. Pyle, A.M., and Christianson, D.W. (2019). CRISPR-Cas Enzymes. Methods Enzymol. *616*, 1–433.

23. Grasset, M.-F., Gobert-Gosse, S., Mouchiroud, G., and Bourette, R.P. (2010). Macrophage differentiation of myeloid progenitor cells in response to M-CSF is regulated by the dual-specificity phosphatase DUSP5. J. Leukoc. Biol. *87*, 127–135. 10.1189/jlb.0309151.

24. Lee, J.H., Budanov, A. V., Talukdar, S., Park, E.J., Park, H.L., Park, H.W., Bandyopadhyay, G., Li, N., Aghajan, M., Jang, I., et al. (2012). Maintenance of metabolic homeostasis by Sestrin2 and Sestrin3. Cell Metab. *16*, 311–321. 10.1016/j.cmet.2012.08.004.

25. Bayle, J., Letard, S., Frank, R., Dubreuil, P., and De Sepulveda, P. (2004). Suppressor of Cytokine Signaling 6 Associates with KIT and Regulates KIT Receptor Signaling. J. Biol. Chem. *279*, 12249–12259. 10.1074/jbc.M313381200.

26. Hanafusa, H., Torii, S., Yasunaga, T., and Nishida, E. (2002). Sprouty1 and Sprouty2 provide a control mechanism for the Ras/MAPK signalling pathway. Nat. Cell Biol. *4*, 850–858. 10.1038/ncb867.

27. Kim, E., Ilagan, J.O., Liang, Y., Daubner, G.M., Stanley, C., Ramakrishnan, A., Li, Y., Chung, Y.R., Micol, J., Murphy, M., et al. (2010). Germline mutations in TMEM127 confer susceptibility to pheochromocytoma. Nat. Genet. *42*, 229–233.

28. Steiner, D.F., Thomas, M.F., Hu, J.K., Yang, Z., Babiarz, J.E., Allen, C.D.C., Matloubian, M., Blelloch, R., and Ansel, K.M. (2011). MicroRNA-29 Regulates T-Box Transcription Factors and Interferon-γ Production in Helper T Cells. Immunity. 10.1016/j.immuni.2011.07.009.

29. Pua, H.H., Steiner, D.F., Patel, S., Gonzalez, J.R., Ortiz-Carpena, J.F., Kageyama, R., Chiou, N.T., Gallman, A., de Kouchkovsky, D., Jeker, L.T., et al. (2016). MicroRNAs 24 and 27 Suppress Allergic Inflammation and Target a Network of Regulators of T Helper 2 Cell-Associated Cytokine Production. Immunity *44*, 821–832. 10.1016/j.immuni.2016.01.003.

30. Wigton, E.J., Mikami, Y., McMonigle, R.J., Castellanos, C.A., Wade-Vallance, A.K., Zhou, S.K., Kageyama, R., Litterman, A., Roy, S., Kitamura, D., et al. (2021). MicroRNA-directed pathway discovery elucidates an miR-221/222–mediated regulatory circuit in class switch recombination. J. Exp. Med. *218*. 10.1084/jem.20201422.

31. Ayala, J.E., Samuel, V.T., Morton, G.J., Obici, S., Croniger, C.M., Shulman, G.I., Wasserman, D.H., and McGuinness, O.P. (2010). Standard operating procedures for describing and performing metabolic tests of glucose homeostasis in mice. Dis. Model. Mech. 10.1242/dmm.006239.

32. Ayala, J.E., Bracy, D.P., Malabanan, C., James, F.D., Ansari, T., Fueger, P.T., McGuinness, O.P., and Wasserman, D.H. (2011). Hyperinsulinemic-euglycemic clamps in conscious, unrestrained mice. J. Vis. Exp. 10.3791/3188.

33. Chhabra, R., Dubey, R., and Saini, N. (2010). Cooperative and individualistic functions of the microRNAs in the miR-23a~27a~24-2 cluster and its implication in human diseases. Mol. Cancer *9*. 10.1186/1476-4598-9-232.

34. Sprenkle, N.T., Serezani, C.H., and Pua, H.H. (2023). MicroRNAs in Macrophages: Regulators of Activation and Function. J. Immunol. *210*, 359–368. 10.4049/jimmunol.2200467.

APPENDIX A

RNA SEQUENCING ANALYSIS: OBESE ADIPOSE TISSUE MACROPHAGES

A.1. Normalized Gene Counts from RNA Sequencing Analysis of Control (fl/fl) and *miR-23-27-24* Cluster Knockout (MyelΔ) Obese Adipose Tissue Macrophages. Extension of RNA sequencing data set detailed in Chapter 4 Figure 1.

Table S1-Normalized gene counts ATM.xlsx

A.2. DESeq2 Analysis of Obese Adipose Tissue Macrophages (fl/fl vs MyelΔ) RNA Sequencing Data Set. Extension of RNA sequencing data set detailed in Chapter 4 Figure 1.

Table S2-DESeq2 analysis ATM.xlsx

APPENDIX B

RNA SEQUENCING ANALYSIS: METABOLICALLY ACTIVATED MACROPHAGES

B.1. Normalized Gene Counts from RNA Sequencing Analysis of Control (fl/fl) and *miR-23-27-24* Cluster Knockout (MyelΔ) MMe Bone Marrow-Derived Macrophages. Extension of RNA sequencing data set detailed in Chapter 4 Figure 2.

Table S3-Normalized gene counts MMe.xlsx

B.2. DESeq2 Analysis of MMe Bone Marrow-Derived Macrophages (fl/fl vs MyelΔ) RNA Sequencing Data Set. Extension of RNA sequencing data set detailed in Chapter 4 Figure 2.

Table S4-DEseq2 analysis MMe.xlsx

APPENDIX C

CANDIDATE TARGET TRANSCRIPTS

C.1. Candidate targets from fl/fl and MyelΔ obese Adipose Tissue Macrophages and MMe Bone Marrow-Derived Macrophages. Extension of RNA sequencing data set detailed in Chapter 4 Figures 1 and 2.

Table S5-Candidate Targets.xlsx

APPENDIX D

RNA SEQUENCING ANALYSIS: NETRIN-1 PATHWAY IN OBESE ADIPOSE TISSUE MACROPHAGES

A.

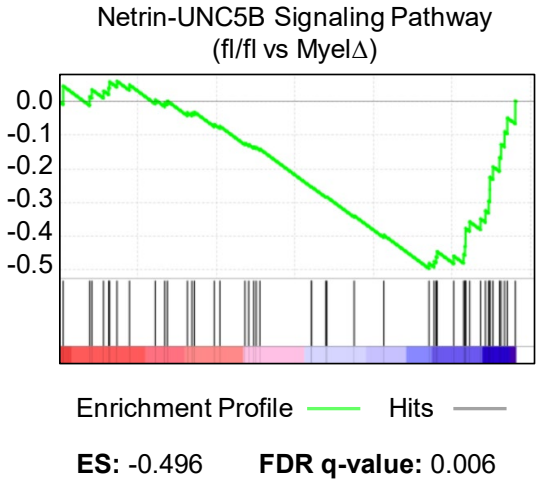

B.

Gene Symbol	Log_2FC (KO / fl/fl)	Adjusted P Value
Adora2b	0.7261	1.35E-06
Ntn1	0.35996	0.02365
Ntn4	0.44499	0.01940
Unc5a	0.35341	0.09977
Unc5b	0.30453	0.30034

D.1. RNA Sequencing Analysis: Netrin-1 Pathway in Obese Adipose Tissue Macrophages. (**A**) Gene set enrichment analysis (GSEA) of RNA-seq data set for genes in netrin-1-UNC5B signaling pathway. GSEA was plotted with the enrichment curve and rank order location of each gene in the indicated gene set from most downregulated to most upregulated (left to right) in knockout MyelΔ ATMs compared to fl/fl ATMs. (**B**) Log_2(MyelΔ / fl/fl) values of the indicated transcripts were quantified via RNA sequencing. Extension of RNA sequencing data set detailed in Chapter 4 Figure 1.